



National Library
of Canada

Bibliothèque nationale
du Canada

Canadian Theses Service Service des thèses canadiennes

Ottawa, Canada
K1A 0N4

NOTICE

The quality of this microform is heavily dependent upon the quality of the original thesis submitted for microfilming. Every effort has been made to ensure the highest quality of reproduction possible.

If pages are missing, contact the university which granted the degree.

Some pages may have indistinct print especially if the original pages were typed with a poor typewriter ribbon or if the university sent us an inferior photocopy.

Reproduction in full or in part of this microform is governed by the Canadian Copyright Act, R.S.C. 1970, c. C-30, and subsequent amendments.

AVIS

La qualité de cette microforme dépend grandement de la qualité de la thèse soumise au microfilmage. Nous avons tout fait pour assurer une qualité supérieure de reproduction.

S'il manque des pages, veuillez communiquer avec l'université qui a conféré le grade.

La qualité d'impression de certaines pages peut laisser à désirer, surtout si les pages originales ont été dactylographiées à l'aide d'un ruban usé ou si l'université nous a fait parvenir une photocopie de qualité inférieure.

La reproduction, même partielle, de cette microforme est soumise à la Loi canadienne sur le droit d'auteur, SRC 1970, c. C-30, et ses amendements subséquents.

UNIVERSITY OF ALBERTA

MICROSTRUCTURES OF SELECTED PODZOLIC SOILS FROM ALBERTA:
GENESIS AND MINERAL TRANSFORMATION

BY

Joselito Modancia Arocena



A THESIS

SUBMITTED TO THE FACULTY OF GRADUATE STUDIES AND RESEARCH
IN PARTIAL FULFILLMENT OF THE REQUIREMENTS FOR THE
DEGREE OF DOCTOR OF PHILOSOPHY
IN
SOIL GENESIS AND CLASSIFICATION

DEPARTMENT OF SOIL SCIENCE

EDMONTON, ALBERTA

SPRING, 1991



National Library
of Canada

Bibliothèque nationale
du Canada

Canadian Theses Service Service des thèses canadiennes

Ottawa, Canada
K1A 0N4

The author has granted an irrevocable non-exclusive licence allowing the National Library of Canada to reproduce, loan, distribute or sell copies of his/her thesis by any means and in any form or format, making this thesis available to interested persons.

The author retains ownership of the copyright in his/her thesis. Neither the thesis nor substantial extracts from it may be printed or otherwise reproduced without his/her permission.

L'auteur a accordé une licence irrévocable et non exclusive permettant à la Bibliothèque nationale du Canada de reproduire, prêter, distribuer ou vendre des copies de sa thèse de quelque manière et sous quelque forme que ce soit pour mettre des exemplaires de cette thèse à la disposition des personnes intéressées.

L'auteur conserve la propriété du droit d'auteur qui protège sa thèse. Ni la thèse ni des extraits substantiels de celle-ci ne doivent être imprimés ou autrement reproduits sans son autorisation.

ISBN 0-315-66812-1

Canada

UNIVERSITY OF ALBERTA

RELEASE FORM

NAME OF AUTHOR: **Joselito Modancia Arocena**

TITLE OF THESIS: **Microstructures of Selected Podzolic Soils from Alberta:
Genesis and Mineral Transformation**

DEGREE: **Doctor of Philosophy**

YEAR THIS DEGREE GRANTED: **Spring 1991**

PERMISSION IS HEREBY GRANTED TO THE UNIVERSITY OF ALBERTA LIBRARY TO REPRODUCE SINGLE COPIES OF THIS THESIS AND TO LEND OR SELL SUCH COPIES FOR PRIVATE, SCHOLARLY OR SCIENTIFIC RESEARCH PURPOSES ONLY.

THE AUTHOR RESERVES ALL OTHER PUBLICATION AND OTHER RIGHTS IN ASSOCIATION WITH THE COPYRIGHT IN THE THESIS, AND EXCEPT AS HEREINBEFORE PROVIDED NEITHER THE THESIS NOR ANY SUBSTANTIAL PORTION THEREOF MAY BE PRINTED OR OTHERWISE REPRODUCED IN ANY MATERIAL FORM WHATEVER WITHOUT THE AUTHOR'S PRIOR WRITTEN PERMISSION.




Permanent Address:

**5 Bonifacio Street
Liliw, Laguna
PHILIPPINES**


Date: 9/25/1991

UNIVERSITY OF ALBERTA
FACULTY OF GRADUATE STUDIES AND RESEARCH

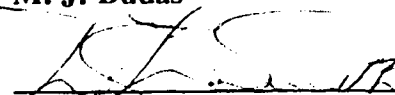
THE UNDERSIGNED CERTIFY THEY HAVE READ, AND RECOMMEND TO THE FACULTY OF GRADUATE STUDIES AND RESEARCH FOR ACCEPTANCE, A THESIS ENTITLED **Microstructures of Selected Podzolic Soils from Alberta: Genesis and Mineral Transformation** SUBMITTED BY **Joselito Modancia Arocena** IN PARTIAL FULFILLMENT OF THE REQUIREMENTS FOR THE DEGREE OF **Doctor of Philosophy** IN **Soil Genesis and Classification**.




S. Pawluk, Supervisor



M. J. Dudas



D. G. W. Smith (Geology)



D. J. Pluth



R. Protz, external examiner

Date: 20 Apr 1991

to my mothers

inay ASYANG

and mama ETANG

ABSTRACT

Three Podzolic soils from the foothills of the Canadian Rockies were investigated through routine physical, chemical and mineralogical analyses, thin section observations under light and electron microscopes, lysimeter and immiscible displacement and *in situ* X-ray microdiffraction to evaluate the formation of the podzolic B horizon. Microstructures range from single grain in the Ae horizon to pellicular and bridge-grain in the matrix and nodules of the Bf horizon and correspond to the chlamydic sequence of microstructural development. The basic components are (a) coarse - quartz and feldspars; (b) fine - phyllosilicates mainly hydroxy interlayered vermiculite (HIV), kaolinite, vermiculite, and chlorite; Fe-oxides and organic matter. The related distribution pattern (RDP) of the coarse and fine components is monic (uncoated coarse grains) in the Ae and C horizons; chitonic (coated coarse grains) in the matrix of Bf horizons and porphyric (coarse grains embedded in fine materials) in the indurated nodules of Bf horizons.

Lysimeter leachates are devoid of major cations and anions, oxalic acid and lignin-containing organic components after passing through the Bf horizon. Colloidal components include globules of ferrihydrite, phyllosilicates, imogolite and opaline materials, Chrysophycean stomatocysts, fulvic and humic acids, quartz and strongly etched feldspar. Eluviation processes include redox reactions, lessivage and podzolization. Infrared analyses indicate that immobilization of imogolite, organic and organo-metallic complexes in the Bf horizon occur in the type A OH functional group of goethite nodules. These Fe-rich nodules occupy as much as 50% of the total area in the thin sections of the Bf horizon. Accumulation of phyllosilicates seems to start in cracks and pits and along the network of fungal hyphae around coarser materials such as quartz and feldspar.

The nature of selected minerals within each of the microstructure showed the importance of microenvironment(s) in mineral transformation. Occurrence of euhedral gypsum crystals is very localized in locations with porphyric RDP in the Bf horizon. Vermiculitization of chlorite and mica is the major transformation of phyllosilicates and leads to the formation of HIV. The degree of HIV formation associated with different microfabrics follows the order: monic < porphyric < chitonic. The extent of Al for Fe substitution in goethite (mole% Al) is measured with the use of the *in situ* X-ray microdiffraction technique and is found to be < 10 (low) in monic RDP; 10-15 (medium) in chitonic RDP and > 15 (high) in porphyric RDP. The "low" and "medium" goethites are believed to be the inherited phase while the "high" is conceived to be pedogenic in origin. The difference in the extent of biological activity in the various RDPs is assumed to be in part, at least, responsible for the observed variations in the nature of minerals.

ACKNOWLEDGEMENT

I wish to express my thanks to a lot of people whose names may not be in print but their assistance during sampling to editing have been indispensable to the completion of this work. They are unsung!

My earnest appreciation goes to Dr. S. Pawluk, my supervisor, for the independence accorded to me; for his views notably about the natural occurrence and organization of soil components; for his punctual comments on every draft of the manuscript despite his myriad chores at the Dean's Office, NSERC, Soil Science Society of America Journal, *Geoderma etc.*, it really made me comprehend the essence of effective time management.

I also acknowledge the meaningful criticisms of Drs. M. J. Dudas, D. G. W. Smith and D. J. Pluth who served as members of the committee and Dr. R. Protz of the University of Guelph not only for serving as the external examiner but also for helpful suggestions to improve the manuscript.

My sincere gratitude is likewise extended to the following: M. Abley for his expertise on thin section preparation and endless tutorials on "chip-driven" machines; P. Yee for valuable help in the laboratory; G. Braybrook of Entomology SEM laboratory for those candid shots of mica and fungal hyphae; P. Geib for his answers to queries on cartographic/photographic matters; T. Messier, Dr. J. J. Miller, A. Gajdostik, B. Xing, C. Kohut, S. Luther, M. Rutherford, J. Warren; the FOP especially when it stands for "Friday of Pilsen"; and the ladies in the 4th: Maisie, Marilyn and Sandy for making life in the Department easier and livelier. Gratitude is also due to Dr. G. A. Spiers for selfless sharing of ideas and knowledge particularly about the network of analysts and equipment around the campus (and the country).

Appreciation is also endowed to the great Filipino tandems of Irma and Allan, Ecel and Dodong, Linda and Oca, Alice and Les, Andrea and Mike, Clarita and Butch and to Gene for the social company, encouragement and moral supports.

I am indebted to the Natural Science and Engineering Research Council of Canada for providing the financial support through a research grant to Dr. S. Pawluk and to the Department, particularly Dr. J. Robertson, the chair, for the opportunity to work as graduate assistant.

Lastly, my wholehearted gratitude goes to *Jô* for her LOVE and to *Pong* and *Butsukoy* whose innocent sounding question, "*Tatay (Dad), when are you going to finish?*", mustered me to strive harder and have this dissertation completed.

4.3. Nature and transformation of minerals	
4.3.1. Introduction	77
4.3.2. Results and discussion	77
4.3.2.1. Minerals and their distribution within the sola.	77
4.3.2.2. Vermiculitization and the fate of mica and chlorite	84
4.3.2.3. Composition of the natural solutions.	96
4.3.2.4. Aluminum for Iron substitution in goethite	103
4.3.3. Summary	107
CHAPTER 5 : SYNTHESIS: Genesis and Taxonomy of the pedons	
5.1. Introduction	108
5.2. Genesis of the Alberta Podzols.	108
5.3. Taxonomy of the pedons	112
CHAPTER 6 : BIBLIOGRAPHY .	114
CHAPTER 7 : APPENDICES	
7.1. Distribution of different sand fractions in Podzolic soils from Alberta..	127
7.2. X-ray diffractograms fine and coarse clays in Podzolic soils from Alberta..	129
7.3. X-ray diffractograms of fine silt fractions in Podzolic soils from Alberta..	136
7.4. X-ray diffractograms of sand fractions in Podzolic soils from Alberta..	140
7.5. Definition of Spodic materials (ICOMOD, 1990).	144

LIST OF TABLES

Table 2.6-1. Compiled mean (standard deviation) soil solution chemistry (mg L^{-1}), pH and EC (dS/m) of Ae and Bh _s horizon extracted by immiscible displacement and lysimeter.	13
Table 4.1.1a. Field morphology of pedon 1.	26
Table 4.1.1b. Field morphology of pedon 2.	27
Table 4.1.1c. Field morphology of pedon 3.	28
Table 4.1-2. Selected properties of Podzolic soils from Alberta.	30
Table 4.1-3. Cation exchange capacity, exchangeable cations and acidity of Podzolic soils from Alberta.	31
Table 4.1-4. Cation exchange capacities determined at pH 4.5 and 7.0 of some Podzolic soils from Alberta.	32
Table 4.1-5. Na-pyrophosphate (p), NH_4 -oxalate(o) and Dithionite-citrate-bicarbonate (d) extractable Fe, Al and Si in some Podzolic soils of Alberta.	34
Table 4.1-6. Abridged micromorphology of Podzolic soils from Alberta.	36
Table 4.1-7. Selected statistical parameters for the size of Fe-rich nodules in Podzolic soils from Alberta.	41
Table 4.1-8. Total C, H and N from leachates collected in pedon 1, Fall 1988.	47
Table 4.1-9. Fe, Al and Si extracted from hydroxy-interlayered vermicullite by six successive extractions with citrate-dithionite (cd) at 100 °C and three extractions with citrate-dithionite-bicarbonate (d) at 75 °C	50
Table 4.2-1. Field morphology of the Bf horizon of some Podzolic soils of Alberta.	62
Table 4.2-2. Color, pH, bulk density, total Carbon, and particle size distribution of selected nodules from Podzolic soils of Alberta.	63
Table 4.2-3. Na-pyrophosphate(p), NH_4 -oxalate (o) and dithionite-citrate-bicarbonate (d) extractable Fe, and Al from nodule and soil matrix (Bf) of Podzolic soils from Alberta.	64

Table 4.2-4a. Abridged micromorphology of Bf horizon of Podzolic soils from Alberta.	65
Table 4.2-4b. Abridged micromorphology of nodules from Podzolic soils of Alberta.	66
Table 4.2-5. Amounts of Fe, Al, and Si extracted by six successive citrate-dithionite treatments from clay samples of nodules from Podzolic soils of Alberta.	72
Table 4.3-1. Distribution of minerals in Podzolic soils from Alberta.	79
Table 4.3-2. Allophane content and extractable Fe, Al and Si in clays of Podzolic soil from Alberta.	80
Table 4.3-3. Distribution of chlorite and mica in different soil separates of Podzolic soils from Alberta.	91
Table 4.3-4. Charge density of vermiculite, amounts of Al, Fe and Mg and the ratio of Mg:Fe:Al extracted by citrate-dithionite in clay fraction from Podzolic soils of Alberta.	95
Table 4.3-5. Calculated (-log) activities for the different ionic species of the natural solutions based on analytical concentrations. Calculations was done using SOLMINEQ-PC (Kharaka <i>et al.</i> , 1988) at 25 °C and 1 atm.	99
Table 4.3-6. Calculated saturation indices of natural solutions with respect to selected carbonates and gypsum in Podzolic soils from Alberta.	100
Table 4.3-7. Calculated saturation indices of natural solutions with respect to selected Fe oxides in Podzolic soils from Alberta.	101
Table 4.3-8. Calculated saturation indices of natural solutions with respect gibbsite and imogolite in Podzolic soils from Alberta.	102
Table 4.3-9. Calculated saturation indices of natural solutions with respect to selected phyllosilicates in Podzolic soils from Alberta.	103

LIST OF FIGURES

Figure 3.1-1.	Location and topography of the study areas.	18
Figure 3.1-2.	Mean monthly temperature and precipitation recorded at the meteorological stations closest to (A) pedons 1 and 2 at Entrance station and to (B) pedon 3 at Grande Prairie station. (sources: Dumanski <i>et al.</i> , 1972; Twardy and Corns, 1980).	19
Figure 4.1-1.	Microstructures of Podzolic soils from Alberta (a) Ae (b) Bf matrix (c) Bf nodule (d) matrix-nodule interphase (e) C horizon.	33
Figure 4.1-2.	<i>In situ</i> Laue photographs of selected pedological features. (A) reddish coating of 2:1 phyllosilicates (B) isotropic infillings composed of 2:1 phyllosilicates and goethite (C) whitish coatings around coarse components composed of materials amorphous to X-rays (D) nodules composed of goethite and 2:1 phyllosilicates.	39
Figure 4.1-3.	Pedological coating around a root fragment (A and B) micrographs showing the layered morphology and (C) its EDS spectrum indicating the predominance of Al and the small amounts of Fe, Si and P.	40
Figure 4.1-4.	Class size distribution of Fe-rich nodules in the different horizons of Podzolic soils from Alberta.	42
Figure 4.1-5.	Enlarged portion of the infra red spectrum of goethite nodules adsorption of ring C-H at around 1275 cm^{-1} , symmetric COO^- at 1410 cm^{-1} and assymmetric COO^- at 1490 cm^{-1} onto the surface of goethite.	42
Figure 4.1-6.	Micrographs of pedological features of biological origin (A) polymorphic organic matter where the plant structures are still recognizable (B) tissue residue plant roots (C) remnants of decomposed spruce needle from the Ae horizon (D) network of fungal hyphae in the Bf horizon (E) <i>Oribatid</i> droppings in the parenchymatic tissues of plants in the LF layer (F) discrete granular units of <i>Collembola</i> and <i>Enchytraeidea</i> excrements composed of mixture of organic and inorganic materials.	43
Figure 4.1-7.	Micrographs of the different types of siliceous Chrysophycean stomatocysts observed in the leachates from Ae horizon. (A) smooth, non-ornamented and high collared stomatocyst (B) ornamented type of stomatocyst (C and D) smooth, non-ornamented and low-collared stomatocysts	45

Figure 4.1-8.	Micrographs of allogenic pseudo-sand fraction from the C horizon showing the (A) oriented phyllosilicates (argillans) along the voids composed of Fe, Al, Si, P and K as indicated by the (B) EDS spectrum of the argillans	46
Figure 4.1-9.	Amounts of selected mobile chemical components and E4/E6 ratio in lysimeter leachates of Podzolic soils from Alberta. The "podzolic signature" is indicated by the enrichment of the chemical components in the Ae horizon and their depletion in the Bf horizons.	48
Figure 4.1-10.	Infra red spectra of lysimeter leachates from LFH, Ae and Bf horizons. The absorption bands at 1225-1265 and 1410 cm^{-1} in the LFH and Ae horizons are absent in the Bf and may indicate the immobilization of lignin and phenol-containing organic compounds.	49
Figure 4.1-11.	Citrate and oxalate content of lysimeter leachates from the different horizons of Podzolic soils.	51
Figure 4.1-12.	Amounts of selected anions in the lysimeter leachates from different horizons of Podzolic soils.	52
Figure 4.1-13.	Micrographs of the colloidal components of the leachates from the Ae horizon. (A and B) phyllosilicates composed predominantly of hydroxy-interlayered vermiculite (C) globules of ferrihydrite (D) etched sand-size feldspar.	53
Figure 4.1-14.	X-ray diffractograms of phyllosilicates from the leachates of Ae horizon of Podzolic soils.	54
Figure 4.1-15.	Infra red spectrum of whitish sediments in the lysimeter of Ae horizon in pedon 1.	56
Figure 4.1-16.	Amounts of Fe and Al in the leachates of the Ae horizon before (Ae) and after (AeL) removal of the leaf litter.	57
Figure 4.2-1.	Class distribution of the different sand fractions in the Bf matrixes and Bf nodules of Podzolic soils from Alberta.	61
Figure 4.2-2.	Micrographs of (A) pellicular microstructure, 1 cm = 420 μm ; (B) pseudo-sand fraction and (C) phyllosilicate in quartz grains from the Bf nodules.	67
Figure 4.2-3.	X-ray diffractograms of selected clays from nodules of Podzolic soils from Alberta (*-citrate treated)	70

Figure 4.2-4.	X-ray behavior of hydroxy interlayered vermiculite in Podzolic soils of Alberta upon ethylene glycol (EG) solvation after dithionite-citrate-bicarbonate (DCB), citrate (C) and citrate-dithionite (CD) treatments.	71
Figure 4.2-5.	Laue photographs of (A) very fine clay (B) Fe nodule and (C) opaque component in the nodule of Podzolic soils from Alberta.	73
Figure 4.2-6.	(A) Micrographs of the coating of quartz grain and (B) its <i>in situ</i> Laue photograph.	74
Figure 4.2-7.	Micrographs of the network of fungal hyphae (A) before and (B and C) after ultrasonic dispersion in the nodules of Podzolic soils from Alberta.	76
Figure 4.3-1.	Scanning electron micrographs of euhedral gypsum crystals from the indurated nodules in Bf horizon of Podzolic soils from Alberta.	78
Figure 4.3-2.	<i>In situ</i> Laue photographs of (A) goethite alone (B) goethite in association with hematite and (C) goethite in association with phyllosilicates.	79
Figure 4.3-3.	The (A) XRD patterns of clay from the Ae horizon under different treatments and (B) relationships between d_{001} spacings and nC in alkylammonium chain.	81
Figure 4.3-4.	The (A) XRD patterns of clay from the C horizon under different treatments and (B) relationships between d_{001} spacings and nC in alkylammonium chain.	82
Figure 4.3-5.	The XRD behavior of hydroxy interlayered vermiculite under different treatments (A) before and (B) after citrate-dithionite treatments.	85
Figure 4.3-6.	XRD diffractograms of chlorite-rich samples from (A) silt and (B) clay fractions of C horizon of Podzolic soils from Alberta.	86
Figure 4.3-7.	Laue photographs of aerogels of very fine clay in the Bf horizon (A) before and (B) after heat treatment at 550 °C.	87
Figure 4.3-8.	Differential XRD of clay fractions from Bf horizons at different regions from (A) 1.6 nm (B) 0.44 nm (C) 0.33 nm (D) 0.26 nm and (E) 0.23 nm.	88

Figure 4.3-9.	Transmission electron micrograph of imogolite from fine clay fractions of Bf horizon of Podzolic soils from Alberta. magnification = 70,000 X	89
Figure 4.3-10.	Differential XRD patterns of clays from Bf horizon at (A) 0.33 and (B) 0.245 nm regions.	90
Figure 4.3-11.	X-ray diffractogram of magnetic fraction of clay from the Ae horizon.	92
Figure 4.3-12.	X-ray diffractograms of the silt fractions from the (A) Ae (B) Bf1 (C) Bf2 (D) C horizons.	93
Figure 4.3-13.	X-ray diffractograms of the clay fractions from the (A) Ae (B) Bf1 (C) Bf2 (D) BC (E) C1 and (F) C2 horizons.	94
Figure 4.3-14.	X-ray diffractograms of vermiculite from Ae horizons (A) before and (B) after hot citrate-dithionite treatments.	97
Figure 4.3-15.	<i>In situ</i> Laue photographs of goethite from the different horizons (A) Ae (B) Bf matrix (C) Bf nodule (D) C horizon of pedon 3.	104
Figure 4.3-16.	Class distribution of the extent of Al for Fe substitution in goethite in pedon 3.	106

Chapter 1

INTRODUCTION

Podzolic soils of Alberta are found mostly along the foothills to the tree line regions of the Canadian Rockies. These soils are developed from Quaternary sands of aeolian or alluvial origin and exhibit morphologies from Luvisolic-like (Smith *et al.*, 1981), Brunisolic-Podzolic intergrades to Orthic Podzol (Dumanski *et al.*, 1972; Pettapiece, 1970; Twardy and Corns, 1980). Earlier studies of these soils indicate an influence of the deposition of Mazama ash (Beke and Pawluk, 1971) and calcareous sand from Brûlé Lake (Dumanski, 1970) in the genetic differentiation of the Podzolic profiles.

Recently, the identification of proto-imogolite sols in a number of Podzols led to the formulation of the inorganic theory for the formation of some podzolic B horizons (Farmer *et al.*, 1980). The proto-imogolite theory, as it became known, contends that Fe, Al and Si migrate from the eluvial horizon as positively charged inorganic proto-imogolite sol. The theory challenges the organic concept, or the movement of Fe and Al as negatively charged chelates (Ponomareva, 1969; De Coninck, 1980; Duchaufour, 1982) as the *de facto* concept of podzolization and thus prompted the re-evaluation of the whole concept of Podzol formation and its classification by the International Commission on the Classification of Spodosols (ICOMOD). Taxonomic experiences show that the classical concept of migration and accumulation of organic matter and Al with or without Fe or "podzolization" (Soil Survey Staff, 1975) is inadequate to explain the formation of "other soils" observed to have distinct Bh/Bf horizons (ICOMOD, 1984) such as soils derived from volcanic ash that contain significant amounts of extractable Fe and Al or high amounts of allogenic Fe-oxides as well as soils with more than 10% clay. Efforts of the ICOMOD to reconcile such soils with the concept of Podzolic soils resulted in the abolition of the amount of Fe and Al extracted by pyrophosphate as a chemical requirement for podzolic B horizon identification (ICOMOD, 1990); the revision has yet to be incorporated in the Canadian System of Soil Classification. The major implication of the change recognizes the observation that the classical processes referred to as "podzolization" are not the only processes responsible for the formation of podzolic B horizons.

The lack of agreement between some podzol morphologies and the previous podzolic criteria implies that pedogenetic processes other than complexation of organic and mineral components are involved in the formation of such morphologies, a logical

assumption because the soil being a natural body is seldom (or never) a product of any single process but a set of various elementary pedogenetic processes (Samoilova, 1986). In fact, prominent researchers of Podzolic soils had identified apart from "podzolization", the migration of aluminosilicates (Anderson *et al.*, 1982; Farmer, 1982) and the intensity of biological activities (De Coninck, 1980) as being responsible for various Bh/Bf morphologies. Stoner and Ugolini (1988) advanced evidence from soil solution studies that episodic heavy rainstorms account for most of the movement of organo-metallic complexes in the Arctic region and are responsible for the occurrence of inverse Bf/Bh morphology. The process is referred to as threshold-controlled sub-surface leaching episodes. Studies such as the latter, represent the current focus of research in pedology, termed dynamic pedology (Singer *et al.*, 1977; Ugolini *et al.*, 1987). The approach emphasizes the dynamic nature of the soil as a basis for better understanding the complexities of soil formation. Usually, lysimeter leachates are used to monitor changes with time to the constitution and properties of the soil solution and colloidal components extracted from specific soil horizon(s). Equilibrium studies of soil solution by immiscible displacement have also been employed to study soil dynamics.

The soil is not only a dynamic but also an anisotropic natural body and therefore requires a spatial *in situ* approach to measure its properties. Properties obtained by *in situ* investigation have recently been recognized as one of the most important factors in predicting the behavior of soils whether for genetic, agronomic, or environmental purposes, especially by modelers and simulators. McGill and Myers (1987) stated that in the dynamics of soil and fertilizer N, soil architecture is a major but neglected factor. Similarly, Samoilova (1986) stated that it is the spatial organization of the elementary pedogenetic processes that is responsible for the characteristic structure of the soil profile. These microsites may differ in chemical and physical constituents but may behave similarly and are thus referred to as functionally homogeneous units and it is this function of the units that dictates the behavior of soils. One of the best ways to study and understand soil anisotropy is through an investigation of the soil organization and microsites by techniques of soil micromorphology. The importance of micromorphology in soil zoological studies, paleopedology, archaeology, sedimentology, and in pollution studies had been recently stated (McGill and Spence, 1985; Kooistra, 1990). The view is echoed by Wilding (1990) who stated further that the architecture of the soil can be appreciated only in microfabrics.

The unique bio-climatic attributes of Alberta Podzols offer an excellent opportunity to assess the dynamics of organic matter decomposition, mineral

weathering and authigenesis, translocation and accumulation and the development of microstructure in relation to the genesis of cold Podzolic soils. Moreover, earlier studies of these soils were focused on "macro" and general physical and chemical characterization that provide a paucity of information about their microenvironments. In-depth investigation of the microstructure combined with the dynamic aspects will further enlighten the understanding of cold Podzolic soils.

The principal objectives of this inquiry deal with the formation of Podzolic soils in the mountain regions of Alberta. Specific objectives are:

1. to provide physical and chemical characterization of the soils,
2. to characterize the nature of minerals with emphasis on the phyllosilicates and their transformations in relation to soil genesis,
3. to evaluate the nature, distribution and formation of Fe-oxide minerals,
4. to evaluate the nature and determine the mechanism for the development of microstructure and
5. to monitor soil dynamics through the determination of the chemistry of soil solutions and the nature of colloidal components migrating through the major horizons, particularly the Ae and Bf horizons.

Chapter 2

REVIEW OF LITERATURE

2.1. Taxonomic history of Podzolic soils

Originally, it is in the description of Podzols where Dokuchaev and his students first used the A-B-C horizon nomenclature with vertical subdivisions designated numerically by 1,2,3 and so on, where the suffix 2 denoted the maximum expression of the horizon, *e.g.*, the designation A2 connotes a horizon of maximum eluviation. The nomenclature was later adapted by the Europeans and established that in between the A and the C horizons is the layer of accumulation designated as the B horizon. The concept of B became that of the illuvial horizon (Soil Survey Staff, 1960); thus B2 was recognized as a subsurface horizon of maximum illuviation. In this system however, no distinction was made on the basis of nature of the illuvial materials (*e.g.*, sesquioxides vs. organic matter vs silicate clays) and this was one of its shortcomings.

As soil classification progressed with advances in instrumentation and methodologies such as X-ray diffraction and spectroscopy, different types of B horizons were distinguished on the basis of the genesis of the illuvial material. Lower case letters were used to describe the nature of the transported materials *e.g.*, crystalline clays that moved without destruction through physical processes in the B horizon were designated Bt and within the classification system used throughout the world separate classes within the taxonomic system were established for such soils as for example Gray Wooded (Canada), Gray Brown Podzolic (USA), Sod Podzolic (USSR) and Brown Forest (Europe).

The classification of Podzols likewise was purified to include only B horizons with amorphous constituents, primarily sesquioxides (Bf), sesquioxides and humus (Bhf) and humus (Bh) accumulated from more intense chemical weathering. The B horizons of Podzols were designated as Bh, Bf, Bhf in Canada; Bs (Bir), Bh, Bsh (Bhir) in USA (Guthrie and Witty, 1982); Bs, Bh in Europe (*e.g.*, Germany and Belgium).

In most of these classification systems, Podzols are recognized on the basis of morphology alone. The presence of an illuvial accumulation of organic matter and Al with or without Fe is normally sufficient for the pedon to be classified or named podzol(ic); *e.g.*, Belgian system of soil classification (De Coninck *et al.*, 1986).

The FAO-UNESCO Soil Map of the World (FAO-UNESCO, 1988), Canadian System of Soil Classification (CSSC, 1978) and Soil Taxonomy (Soil Survey Staff, 1975) differ from the foregoing in that they use the ratio of Al and Fe extractable by

pyrophosphate (Alp and Fep) to clay as being ≥ 0.2 along with other chemical criteria to augment (and confirm) the field identification of a podzolic horizon. These criteria have proven inadequate to accommodate certain soils with well-developed Bh/Bf morphology especially soils having $> 10\%$ clay (Lietzke and McGuire, 1987). This problem prompted the creation of the International Committee on the Classification of Spodosols (ICOMOD) sometime in the mid-80s with a task of reassessing both the morphological and chemical criteria of Spodosols (ICOMOD, 1984). Spodosol is a soil order in Soil Taxonomy (Soil Survey Staff, 1975) more or less equivalent to Podzolic in the Canadian system. As a result, the criteria have been revised and now include properties such as chroma, presence of an albic horizon, humic color, KOH extractable Al, and exclude former requirements such as soil depth in cold areas and indices of accumulation. Excerpts of the latest chemical criteria (ICOMOD, 1990) are given below and the complete definition is in appendix 7.5.

- a. $Feo \text{ in } B > 2X Feo \text{ in } E, A \text{ or } Ap;$
 - b. $(Al_o + Fe_o)/2 \text{ in } B > 2x (Al_o + Fe_o)/2 \text{ in } E, A \text{ or } Ap;$
 - c. $ODOE \text{ in } B = 0.25 \text{ and } > 2.5X ODOE \text{ in } E, A \text{ or } Ap$
- where, o is NH_4 -oxalate, pH 2.5 extract
ODOE is optical density of oxalate extract

The recent chemical criteria abandoned the use of Fe and Al extractable by pyrophosphate because of the uncertainty of the nature of metals extracted. Still, lacking from the revisions, are parameters that take into account processes other than podzolization. Friability and compactness of the illuvial B horizon merit some attention for they reflect the degree of biological activity responsible for certain types of podzolic morphology (De Coninck, 1980). The amount of oxalate-soluble silica is a good measure of allophane (Farmer, 1984) related to the inorganic transport of Al, Si and Fe in Podzols.

2.2. Macromorphology

Typical Podzolic soils have four distinct horizons. At the surface is the organic horizon which consists of partially decomposed and undecomposed organic litter. It is dark coloured, usually less than 20 cm thick and plant roots are prolific. It has an abrupt boundary to the underlying light colored and eluviated Ae horizon. The Ae horizon is composed predominantly of uncoated quartz and feldspar grains, and roots are less abundant. The Ae horizons frequently tongue and interfinger into the underlying Bh/Bf horizons.

Generally, Bh horizons overlie a Bf (Rourke *et al.*, 1988) but inverse Bf/Bh sequences are observed in the central massif of France (Righi and Borot, 1985) and some Arctic Podzols (Stoner and Ugolini, 1988). Bh and Bf layers constitute the podzolic horizon, and have either a very firm or friable consistency. The former connotes a higher degree of faunal activity and the latter reflects an accumulation of organo-metallic complexes (De Coninck, 1980) or cementation by allophanic coatings (Farmer, 1982). Below the podzolic layer is the sandy C horizon.

Accessory layers present in some Podzols include placic horizons, thin (2 to 10 mm thick), reddish to black pans cemented by Fe and/or Mn oxides or by Fe-organic matter complexes usually in hydromorphic conditions (McKeague *et al.*, 1983; Campbell and Schwertmann, 1984). Cementation by allophane and Fe-oxides can also result in the formation of iron pan (Farmer, 1982). Densipan layers (Loveland and Clayden, 1987) are due mainly to the close packing of particles and not to cementation.

2.3. Micromorphology

2.3.1 Organic horizon

Microfabrics of organic horizons are characterized by high porosity and the presence of fresh birefringent cell walls. The related distribution pattern (RDP) is generally mull-phytogenic (monic); plasma separation is trace to absent. Evidence of faunal activity is abundant including hyphae, spores, sclerotia and fecal pellets of mites and Collembola. Mineral grains may be admixed with organics especially in the lower part of the humified layer.

2.3.2 Ae horizon

Two general types of texture-related microfabrics found in Ae horizons are orthogranic RDP typical of loose to moderately packed uncoated sand grains (mainly quartz) with minor amounts of inorganic materials and amorphous organic matter (De Coninck and McKeague, 1985). Milnes and Farmer (1987) termed this type of fabric as quartzogranosoma. In sandy loam to loam Ae horizons, packed granic RDP is formed by unsorted quartz and feldspar grains with plant fragments, equant units of mull-like materials and small rounded units of dark materials of organic origin (Milnes and Farmer, 1987). This fabric is called humo-phyto-mullo-quartzogranosoma; some sections of this type of Ae may exhibit a mull-iunctic fabric or a mull-porphirosoma. Loveland and Clayden (1987) in their examination of hardpan podzol reported that the intrapedal matrix of the Ae horizon has silasepic fabric.

Skeletal grains of quartz and feldspar are strongly etched which indicates a congruent dissolution of the minerals (Farmer *et al.*, 1985). Sesquioxidic pedological features are almost absent (De Coninck and McKeague, 1985; Tongokonov *et al.*, 1987) and speckled amorphous organic matter, wherever present is regarded as a relic feature from previous Bh horizons (De Coninck and McKeague, 1985).

2.3.3. Podzolic B horizon

Friable podzolic B horizons are composed of loose sand grains and aggregates of mineral particles and partly altered plant remains loosely bound by polymorphic organic matter (Righi and De Coninck, 1977; Arousseau, 1983; De Coninck and McKeague, 1985). Fabric is mostly chlamydic with some patches of plectic type RDP. Matrigranic to matrigranoidic RDP is dominant in friable silty podzolic horizons. Intergranular spaces are loosely occupied by isotropic to weakly birefringent, ovoid to irregularly shaped aggregates usually 20-100 μm in diameter and normally contain plant fragments, hyphae, sclerotia and fecal pellets. Skeleton grains are either coated or uncoated with amorphous materials. The friable consistency results from high porosity of granic RDP and from the stabilization of the open structure generated by root penetration through allophanic and fulvate-impregnated cementation of silt and sand grains into porous pellet-like microstructures (Farmer, 1984).

A cemented podzolic horizon generally has plectic to porphyric plasmic fabric due to coatings of organic matter or complexes of organo-mineral composition (De Coninck and McKeague, 1985). In related investigations, Milnes and Farmer (1987) described the fabric to be dominantly quartzic allophaniplectosoma with humi-iunctic sand containing plant roots and root fragments. Plectosoma in some places exhibits multiple boundaries indicating repeated stages of development. Plectosoma has a composition of 29% SiO_2 (Al:Si atomic ratio=2.9) displaced from the ideal imogolite-allophane composition of Al:Si atomic ratio=2. Some parts exhibit porphyric fabric with microgranular gibbsite composing the f-matrix (gibbsiporphyric fabric). With depth, fabric shifts to an intergrade humichlamydic-plectic fabric where the f-matrix is organic matter and clay minerals (Milnes and Farmer, 1987).

Pedological features identified in podzolic horizons are glaeboles, pedotubules, organoferri and channel argillans. Glaeboles have yellow-brown quartzic plectosoma fabric with patches where skeletal grains are completely coated by organic matter and clay (humi-pellichlamydic). Gibbsitic glaeboles crystallize from pre-existing space filling gel with an Al:Si ratio > 6 (Milnes and Farmer, 1987; Righi and De Coninck, 1977). Organo-ferri-argillans result from the dissolution of allophanic material and

subsequent deposition of clays and organic matter. Less than 1% void argillan is reported by Loveland and Clayden (1987) and the presence of humo-ferruginous and ferruginous cutans in fissures and ped surfaces are reported by (Tongokonov *et al.*, 1987).

Cracked monomorphic coatings were recognized by De Coninck as well as other workers (Righi and De Coninck, 1977; Ugolini *et al.*, 1977; De Coninck, 1980; Van Ranst *et al.*, 1980; Flach *et al.*, 1980; De Coninck and Righi, 1983; De Coninck and McKeague, 1985; Ugolini *et al.*, 1987) to be composed of fulvic acids containing either Al only or both Al and Fe and a trace to absence of Si. These coatings appear very discrete as randomly stacked spherical or plate-like bodies (Van Ranst *et al.*, 1980). They are opaque and exhibit a strongly developed angular cracking pattern due to dehydration of the hydrophylic organic or organo-metallic colloids.

2.3.4. Placic horizon

Placic horizons cemented by monomorphic coatings appear dark reddish brown in color, while those cemented mainly by Fe-oxides have paler brown to reddish brown isotropic plasma with little cracking and may show some degree of layering (De Coninck and Righi, 1983). Thin iron pan described by Farmer *et al.* (1985) is composed of aggregated silt grains, cemented by opaque reddish brown deposits with Si:Al:Fe ratio of 1:3.7:3.6. This aggregate is enveloped by a yellow transparent gel with Si:Al:Fe ratio of 1:3.6:0.41 which in turn is locally overlain by a paler gel with Si:Al:Fe ratio of 1:3.3:0.41.

2.4. Nature and transformation of minerals in Podzols

2.4.1. Inherited minerals

Quartz, feldspar, mica (muscovite, biotite and glauconite) are the main inherited minerals in most orthic Podzols (Righi and De Coninck, 1977; McKeague *et al.*, 1983; De Coninck *et al.*, 1987; Loveland and Clayden, 1987), although volcanic glasses dominate in Podzols developed from volcanic ashes (Shoji *et al.*, 1988). The heavy mineral fraction comprises mainly anatase, brookite, epidote, garnet, kyanite, staurolite, tourmaline, zircon and zoisite (Loveland and Clayden, 1987).

Generally, there is a negative accumulation of quartz and feldspar in the Ae horizon due to aggressive disintegrative processes initiated by organic acids from the overlying litter (Righi and De Coninck, 1977; Farmer *et al.*, 1985; Robert and Berthelin, 1986; Tongokonov *et al.*, 1987). The intensive weathering is evident from the etched pits and trenches on quartz and feldspar grains (Tongokonov *et al.*, 1987;

Farmer *et al.*, 1985) and from complete discoloration of amphibole and the virtual absence of chlorite (De Coninck *et al.*, 1987). Resistant biotite are largely oxidized with interlayers still intact and devoid of any components undergoing vermiculitization (Farmer *et al.*, 1985).

Autochthonous clay minerals are mostly mica-smectite mixed layers, kaolinite, Mg-chlorite and transformation products of chlorite weathering (Righi and De Coninck, 1977; De Coninck *et al.*, 1987; Tongokonov *et al.*, 1987). Montmorillonite in some New York Podzols are considered to be inherited from dust deposits (Coen and Arnold, 1972).

2.4.2. Authigenic minerals

Phyllosilicates and oxides largely represent the authigenic group of minerals. Complete dissolution of chlorite and progressive weathering of mica leads to the synthesis of smectites, which are generally Al-rich (McKeague *et al.*, 1983) and incongruent weathering leads to vermiculitization of biotite and chlorite (Farmer *et al.*, 1985; De Coninck *et al.*, 1987). Righi and De Coninck (1977) presented the following generalized stages of chlorite weathering:

stage 1. represents the formation of irregularly interstratified minerals with a vermiculitic layer (HIV)

stage 2. consists of interstratified minerals with some expanding layers

stage 3. consists of expandable or swelling minerals like smectite

Wada *et al.* (1987) reported a chloritized-vermiculite showing no expansion with Mg- or Ca-saturation and glycol solvation nor collapse upon heating of K-saturated sample; it is believed to contain $\text{Al}(\text{OH})_x$ in the interlayer spaces (Coen and Arnold, 1972; Brewer and Pawluk, 1975). Vermiculite-smectite mixed layers were reported by Tongokonov *et al.* (1987). In Podzols, disintegrative processes do not completely coincide with the general stability as proposed in the mineral stability series but depend greatly on particle size (Tongokonov *et al.*, 1987). They propose the following order of stability with respect to weathering initiated by organic acid: clay (smectite < hydromica < chlorite < kaolinite) < fine silt size amphibole and feldspar. If the latter group predominates, potential aggression is "spent" mostly in this group and hydrolysis weakly affects minerals in > 0.1mm fraction.

Allophane and imogolite are reported to be present in Podzols, through IR, electron microscopy and chemical analyses. Their presence is not unique to Podzols from pyroclasts (Tait *et al.*, 1978). Authigenesis of these minerals is related to soil acidity (Wada *et al.*, 1987; Farmer, 1984) since Al^{+3} concentration increases

remarkably with decreasing pH below 4.9 and hardly reacts with Si but forms stable complexes with organics. At pH values above 4.9, hydroxy Al ion concentration increases and preferentially co-precipitates with Si rather than forming stable organic complexes, thus forming imogolite and allophanes. Dissociation of the functional groups of the organics is the main source of acidity (Shoji *et al.*, 1982). Farmer (1984) points to this mechanism as being responsible for the absence of imogolite and allophane in acidic podzolic horizons. He further reported that imogolite and allophane formation is greatly inhibited by competing mechanisms such as high root activity that traps Al and displaced silicic acid, production of hydroxy-Al species, the presence of smectite and vermiculite and the rate of fulvic and humic acid production.

Plant opal is another mineral that forms *in situ*. The formation is traced to the low activity of Al probably due to Al-humus complexation and concentration of Si due to evaporation of soil solution (Shoji *et al.*, 1988). The sources for Si are the weathering of silicates and the decomposition of Si-containing plant materials.

The Al liberated from weathering of primary minerals may end up in the interlayers of 2:1 clays (soil chlorite formation), crystallize to gibbsite (Righi and De Coninck, 1977; Milnes and Farmer, 1987) and/or combine with Si to form imogolite (Farmer, 1982).

The presence of Fe oxide minerals is easily recognized by the reddish brown chroma they impart to the Bf horizon of Podzolic soils. The sensitivity of Fe to variation in redox conditions assures a continuous oxidation/reduction of Fe and Fe minerals and supports the authigenic nature of most Fe oxide and hydroxides in soils.

Goethite is the most common Fe oxide not only in Podzols but also in other soils as well. Goethite is reported to occur widely in Podzols from different geographic regions (Mizota, 1982; Campbell and Schwertmann, 1984; Loveland and Clayden, 1987; Milnes and Farmer, 1987; Shoji *et al.*, 1988).

Lepidocrocite is present in Podzols that have an impeded drainage system (Campbell and Schwertmann, 1984; Kassim *et al.*, 1984; De Coninck *et al.*, 1987; Loveland and Clayden, 1987).

The presence of high amounts of organics is normally expected to suppress the formation of ferrihydrite because of the complexing affinity of organics for Fe, but empirical observations have revealed the wide occurrence of ferrihydrite in Podzols (McIntosh *et al.*, 1983; Kassim *et al.*, 1984; Milnes and Farmer, 1987) and in 2Bsmb horizons of Podzols from volcanic ash (Shoji *et al.*, 1988). This suggests a more complex process of ferrihydrite formation. The presence of ferrihydrite is indicated by the high Fe_o/d ratio in most Bf horizons.

With regard to Fe oxide distribution, maximum accumulation of illuvial Fe oxide occurs in the Bf horizon (Tongokonov *et al.*, 1987).

2.5. Organic components in Podzols

Total carbon content in podzols ranges from as low as 2 in the C horizon to as high as 450 g C·(kg soil)⁻¹ in the organic layer. Usually, there is a second accumulation of C coinciding with the Bh horizon. A typical Podzol reported by McKeague *et al.* (1983) has a Bh containing as high as 100 g organic C·(kg soil)⁻¹ while a Bh horizon in a tropical Podzol has a low value of 2.5 g organic C·(kg soil)⁻¹ (De Coninck, 1980). Buurman and Van Reeuwijk (1984) and Shoji *et al.* (1982) stated that a very rapid turnover of organic C leads to a podzolic morphology without necessarily a second maximum accumulation of organic C in the Bh horizon. Determination of mean residence time (MRT) of C revealed that generally friable podzolic horizons have lower MRT than cemented podzolic horizons which indicates a more rapid organic turnover in the former compared to latter (De Coninck and Righi, 1983).

De Coninck (1980) reported the fulvic (FA) and humic (HA) acid contents of Belgian and Malaysian Bh horizons to range from 243-628 g fulvic acid·(kg C)⁻¹ and 198-543 g humic acid·(kg C)⁻¹. The lower amount of HA and FA extracted from tropical Podzols compared to Podzols in temperate climate is attributed to the presence of a high amount of free Fe that interferes with the extraction (De Coninck, 1980). De Coninck and Righi (1983) reported that the distribution of FA and HA is similar for friable and cemented podzolic horizons. The average composition of soil HA has 562 g C; 47 g H and 355 g O·(kg HA)⁻¹ while FA contains 457 g C; 54 g H and 448 g O·(kg FA)⁻¹ (McKeague *et al.*, 1983).

The major phenolics in the Bh horizons of Podzols are: gallic, *p*-coumaric, gentissic, and protocatechuic acids. Minor components are: salicylic, protobenzoic and syringic acids (Evans, 1980). Among these phenolics, Vance *et al.* (1985, 1986) found that protocatechuic acid contains ortho-dihydroxy functional groups capable of chelating Al and Fe and is believed to be the reason for its accumulation in B horizons of Podzols.

2.6. Soil solution components in Podzols

Soil solution refers to water assumed to be in equilibrium with the mineral phases and includes both the stationary pore water and transient water from the system.

The former is usually extracted by immiscible displacement and the latter through lysimetry.

Lysimeter water provides "solution signatures" (Ugolini *et al.*, 1987) of the dominant process while the latter is proven to be in excellent agreement with long term solubility studies (Kittrick, 1980). Solution signatures of Podzols consist of two components: (a) metals and organic-rich solution from upper horizons and (b) solution devoid of metals and organics from B horizons (Ugolini *et al.*, 1987).

Immiscibly displaced solutions provide input for the evaluation of thermodynamic chemical equilibria of the pedon. Examples of such studies in Podzols were published by Manley *et al.* (1987); Coen and Arnold (1972); Fernandez-Marcos *et al.* (1978); Simmard *et al.* (1988). Persistence and control exerted by mineral phases upon the soil solution chemistry often determines the results from this kind of study.

Table 2.6-1 lists the chemistry of soil solutions from Ae and Bh/Bf horizons of Podzols compiled from the literature. The values reported for lysimeters represent the amounts of constituents moving out of the horizon while values for immiscible displacement represent concentrations of any constituents stationary in that horizon. The general trend shows that pH is slightly lower in the Ae than in the Bh/Bf. Translocation of Fe from the eluvial horizon is evident from the higher Fe content in leachates from the Ae compared to the Bh/Bf horizon (2.71 mg L⁻¹ vs. 0.24 mg L⁻¹). This is a typical example of the "podzolic signature" (Ugolini *et al.*, 1987). A similar trend is observed for the majority of the ions except for Si.

On the other hand, composition of water extracted by immiscible displacement shows an organic and metal rich solution from the upper horizon and a solution devoid of metals and organics in the Bh/Bf. Ugolini *et al.* (1987) quantified a net loss of 0.92 mg Fe L⁻¹ and 0.65 mg Al L⁻¹ from the Ae horizon and a net gain of 1.45 mg Fe L⁻¹ and 0.46 mg Al L⁻¹ in the Bf from a percolating soil solution. Stoner and Ugolini (1988) and Ugolini *et al.* (1988) contended that the simultaneous attenuation of Fe, Al, and Si with organic C in the B horizon strongly suggests the presence of organic ligands and the movement of Al and Fe as organic complexes.

Modifications of the chemistry of the soil solutions can be initiated by vegetation. Ugolini *et al.* (1988) found that the differential cycling of nutrients by Abma and Misi ecosystems in Japan leads to formation of Podzols in the former and Andisols in the latter.

Table 2.6-1. Compiled mean (standard deviation) soil solution chemistry (mg L^{-1}), pH and EC (dS/m) of Ae and Bh/Bf horizons extracted by immiscible displacement and lysimeter.

	Mode of Extraction			
	Immiscible displacement ¹		Lysimeter ²	
	Ae	Bh/Bf	Ae	Bh/Bf
CATIONS				
Si	9.47(4.76)	3.73(1.91)	1.66(1.19)	4.09(2.38)
Al	2.45(1.06)	1.10(0.43)	1.01(1.97)	1.11(1.50)
Fe	2.36(1.97)	0.58(0.35)	2.71(4.41)	0.24(0.33)
Ca	12.90(8.03)	4.28(2.42)	1.74(1.30)	1.06(0.78)
Mg	3.69(1.73)	1.47(0.56)	1.30(0.72)	0.99(0.80)
Na	0.30(0.19)	0.32(0.37)	9.51(11.68)	2.94(2.26)
K	13.17(7.62)	5.32(3.41)	3.51(3.63)	2.38(2.10)
ANIONS				
SO ₄	2.46(0.77)	1.00(0.23)	11.01(8.76)	6.83(5.34)
Cl	13.22(3.31)	8.03(3.27)	14.17(15.02)	2.26(2.45)
NO ₃	0.34(0.51)			
HCO ₃	1.95(1.84)			
PO ₄	0.34(0.13)	0.41(0.05)		
DOC ³	118.00(12)	10.10(7.80)		
pH	4.19(0.20)	4.86(0.39)	4.24(0.34)	4.63(0.41)
EC	1.65(0.49)	0.49(0.22)	0.51(0.32)	0.26(0.06)
pE				
normal		8.45		
extreme oxidation		11.80		
extreme reduction		3.40		

¹ sources: Manley et al. (1987); Chesworth and Macias-Vasquez (1985); Coen and Arnold (1972); David and Driscoll (1983); Simmard et al. (1988)

² sources: Bergvist (1987); Driscoll et al. (1985); Foster and Nicholson (1986); Friesleben and Rasmussen (1986); Dufresne and Hendershot (1986); Hanstchel et al. (1986); Hendershot et al. (1984); Hornung et al. (1986); McDowell and Wood (1984); Nilsson and Bergvist (1983); Nordstrom (1982); Nordstrom and Ball (1986); Rasmussen (1986); Ugolini et al. (1987).

³ DOC-dissolved organic carbon

2.6.1. Mineral phase equilibria in podzolic B horizon

Manley *et al.* (1987) applied the equilibrium diagram of $\text{Al}_2\text{O}_3\text{-SiO}_2\text{-H}_2\text{O}$ system to the chemistry of the soil solution obtained from the Bhs (Bf) horizon. Their results showed that the horizon is supersaturated with respect to kaolinite, gibbsite, allophane, imogolite and halloysite. David and Driscoll (1983) partially agreed with them but not with respect to halloysite and gibbsite, although the latter analyzed lysimeter water while the former used water displaced by CCl_4 . Both authors are in agreement with regards to the undersaturation of the horizon with respect to the solubility of amorphous aluminum trihydroxide. This is likely due to high content of dissolved organic carbon (David and Driscoll, 1983). Montmorillonite is not likely to be stable in the Bhf horizon due to the high amount of Al-hydroxides that prevents chlorite and mica from altering to montmorillonite (Coen and Arnold, 1972). This claim, however, is inconsistent with the empirical observation of vermiculitization of biotite (Farmer *et al.*, 1985) or the transformation of chlorite to swelling minerals (Righi and De Coninck, 1977).

In parallel results obtained using natural waters and computer-simulated conditions, Nordstrom (1982), Nordstrom and Ball (1986) and Arp and Ouimet (1986) showed that some minerals in the $\text{Al}_2\text{O}_3\text{-SO}_4\text{-H}_2\text{O}$ system appear to control the concentrations of Al and SO_4 in the soil solution. Among the minerals are alunite ($\text{KAl}_3(\text{SO}_4)_2(\text{OH})_6$), jurbanite ($\text{AlSO}_4\text{OH}\cdot 5\text{H}_2\text{O}$) and basaluminite ($\text{Al}_4\text{SO}_4(\text{OH})_{10}\cdot 5\text{H}_2\text{O}$). David and Driscoll (1983), however, found that leachates from Bhs horizon of Haplorthods are undersaturated with respect to sulfate minerals.

With regards to less-ordered aluminosilicates, Dahlgren and Ugolini (1989) found that imogolite is undersaturated in the Ae and Bh horizons but is stable in the Bf horizon.

2.7. Transport and accumulation processes of organic matter, Fe and Al in Podzolic soils

Two popular explanations forwarded regarding the fate of Fe, Al and Si released from weathering are the organic or fulvate theory and inorganic or proto-imogolite theory. The fulvate theory supports the migration of these metals through the formation of organo-metallic chelates. The organic compounds are produced by the degradation of organic matter and their mobility is ensured by the presence of functional groups such as carboxyl and hydroxyl groups. These groups are present both in the aliphatic and aromatic organic matter fractions (De Coninck, 1980) which

ensures their hydrophilic characteristics and their ability to chelate metals. The ortho-dihydroxy group in protocatechuic acid is a good example (Vance *et al.*, 1985).

The immobilization of the foregoing mobile organic fraction and chelation occur when the colloids lose their negative charges or in other words when it is rendered hydrophobic. Neutralization occurs by several processes. One example is desiccation which can increase ionic concentration, contraction of the double-layer and consequent expulsion of the water molecules from the particles (De Coninck, 1980).

Other physico-chemical reasons leading to the precipitation of the migrating colloids is the enrichment of the complexed metals in excess of a threshold concentration thereby neutralizing the negative charges necessary for dispersion. Buurman and Van Reeuwijk (1984) estimated a ratio of 4 to 12 between organic C and metals was required to cause the immobilization of mobile organo-metallic complexes. Immobilization can also occur when the mobile colloids encounter regions of high ionic concentration or an acidity different from that of the solution.

Anderson *et al.* (1982) stated that the sesquioxides present in the B horizon can also physically trap the mobile organic and organo-metallic complexes. Collman *et al.* (1987), Kung (1989) and Kung and McBride (1989) stated that chemisorption to the type A OH groups in goethite is responsible for the immobilization of organic matter by sesquioxides. In similar studies, Parfitt *et al.* (1977), Cornell and Schindler (1980) and Jensen (1988) discuss the active role of oxides as absorbing media for benzoates, oxalates, salicylate and other acids.

The processes mentioned above operate simultaneously as exemplified in the Arctic region, where drying in summer can cause migrating colloids to be stranded in the B horizon even if the metal to carbon ratio is 1:1 which is below the ratio required to render colloids non mobile (Stoner and Ugolini, 1988).

The theory of fulvate transport of Al and Fe in Podzols was regarded as the *de facto* process for the development of the B horizon until Farmer and co-workers identified allophanic coatings on skeletal grains of the podzolic B horizon (Farmer *et al.*, 1980; Anderson *et al.*, 1982; Farmer, 1982, 1984; Farmer *et al.*, 1985). These coatings are pale yellow to orange, transparent, strongly fluorescent, isotropic or with weak striated interference color with either layered or gel-like morphology (Farmer *et al.*, 1985; Milnes and Farmer, 1987). The variation in color is due to the different amounts of organic matter (local or illuviated), layered silicates and Fe-oxides mixed with or adsorbed in the allophanes (Farmer *et al.*, 1985).

The findings of Farmer initiated a reassessment of major process(es) in podzolization and forwarded evidence that movement of Al and Si in Podzols is mainly

through the formation of an inorganic $\text{Al}_2\text{O}_3\text{-SiO}_2\text{-H}_2\text{O}$ sol called proto-imogolite sol because it readily converts to imogolite upon heating. Farmer and Fraser (1982) have also synthesized $\text{Al}_2\text{O}_3\text{-Fe}_2\text{O}_3\text{-SiO}_2\text{-H}_2\text{O}$ sols to demonstrate the transport of Fe as inorganic sol. Buurman and Van Reuwijk (1985), however, commented that in the A horizons of Podzols, the formation of a sol will be greatly hampered by organics and maintained that these sols cannot be properly designated as proto-imogolite because of the unlikely substitution of Fe for Al in imogolite.

Farmer (1982) also found that proto-imogolite sol is extremely stable colloiddally and is observed to form from solutions with an Al:Si ratio of about 2 and over a range of 7-35 mg $\text{SiO}_2 \text{ L}^{-1}$ solution.

Deposition of allophane from proto-imogolite sol is likely to occur in lower horizons of higher pH or when the positive charges necessary to maintain dispersion are neutralized by adsorbed anions, or when these positive colloids encounter negatively charged surfaces such as those of smectite, illite or vermiculite (Farmer *et al.*, 1980). Bhf horizons then develop as the migrating organic colloids are precipitated over the previously illuviated inorganic deposits.

In lower sub-horizons of some sandy Podzols of Canada, imogolite is assumed to be the component of pale brown to brown, weakly anisotropic coatings on skeleton grains (Wang and McKeague, 1982; Wang *et al.*, 1986; Wang and Kodama, 1986).

Chapter 3 MATERIALS AND METHODS

3.1. Materials

3.1.1. *The study areas*

Three pedons were selected for the study and their relative location and physiographic positions are given in Fig. 3.1-1. Pedons 1 and 2 are situated in the Wildhay benchland near Hinton, Alberta with approximate locations at $53^{\circ} 46' 24 \pm 15''$ N latitude, $117^{\circ} 37' 37 \pm 30''$ W longitude and $53^{\circ} 44' 21 \pm 15''$ N latitude $117^{\circ} 39' 11 \pm 30''$ W longitude, respectively. Pedon 1 is on a northeast-facing slope with a 7° gradient located 5 km northeast of pedon 2 that is situated on a southeast oriented slope with 9° gradient; they are members of the Blackmud mapping unit, BKM5 (Dumanski *et al.*, 1972). Pedon 3, mapped as the Heart unit, HRT1 (Twardy and Corns, 1980) is located on a 12° gradient west-facing slope on the Alberta plateau benchland along the Forestry Trunk Road with an approximate location at $54^{\circ} 31' 32 \pm 15''$ N latitude and $118^{\circ} 9' 57 \pm 30''$ W longitude.

3.1.2. *Parent materials*

The parent materials are mainly quaternary sandy deposits of alluvial and aeolian origin. Pedons 1 and 2 are developed on non-calcareous Pleistocene alluvial sand deposits of olive brown to grayish brown (2.5Y 4/4-10YR 5/2) color with quartzitic pebbles up to 5 cm in diameter (Roed, 1968; Dumanski *et al.*, 1972). The lithological break in pedon 2 at 76 cm reflects the presence of a calcareous layer, probably loess deposited from the flood plains of the Athabasca River and the shores of Brûlé Lake as reported earlier by Dumanski (1970). The parent material of pedon 3 is mildly acidic aeolian sand with colors ranging from light olive brown to yellowish brown (2.5Y 5/4-2.5Y 4/4) and are believed to originate from the delta near Marlboro and the floodplain deposits of McLeod river (Twardy and Corns, 1980). The dominant phyllosilicates are mica, chlorite and kaolinite.

3.1.3. *Vegetation*

The vegetation at pedons 1 and 2 is dominated by lodgepole pine (*Pinus contorta*) and trembling aspen (*Populus tremuloides*) which provide combined crown cover of approximately 40 and 25% over pedons 1 and 2, respectively; the understory is made up of shrubs mainly Labrador tea (*Ledum groenlandicum*), with *Salix sp.*, *Vaccinium sp.*, *Rosa sp.*, *Arctostaphylos uva-ursi*; herbs, *Selaginella sp.*, *Cornus*

canadensis; and grasses *Elymus sp.*. The forest floor is completely covered with feather moss (*Hylocomium splendens*) and club moss (*Lycopodium complanatum*). Pedon 3 is forested mainly by lodgepole pine with approximately 25% canopy closure; the ground cover is similar to pedons 1 and 2.

3.1.4. Climate

The climate is generally characterized as subhumid and continental with long cold winters and moderately mild summers. The areas are subject to warm chinook winds during winter. The mean annual temperature (MAT) for pedons 1 and 2 recorded at Entrance weather station (Dumanski *et al.*, 1972) is 2.4 °C with July as the warmest month (15 °C) and January the coldest month at -12 °C (Fig. 3.1-2a). The mean annual precipitation is 441 mm and 42% falls in the summer months of June, July and August.

The climatic data for pedon 3 (Fig. 3.1-2b) inferred from the data at Grande Prairie station (Twardy and Corns, 1980) has a MAT of 2.1 °C with July as the warmest month (16 °C) and the coldest month is January with a temperature of -17 °C. The mean annual precipitation is 441 mm and the summer months receive 40% of the total precipitation.

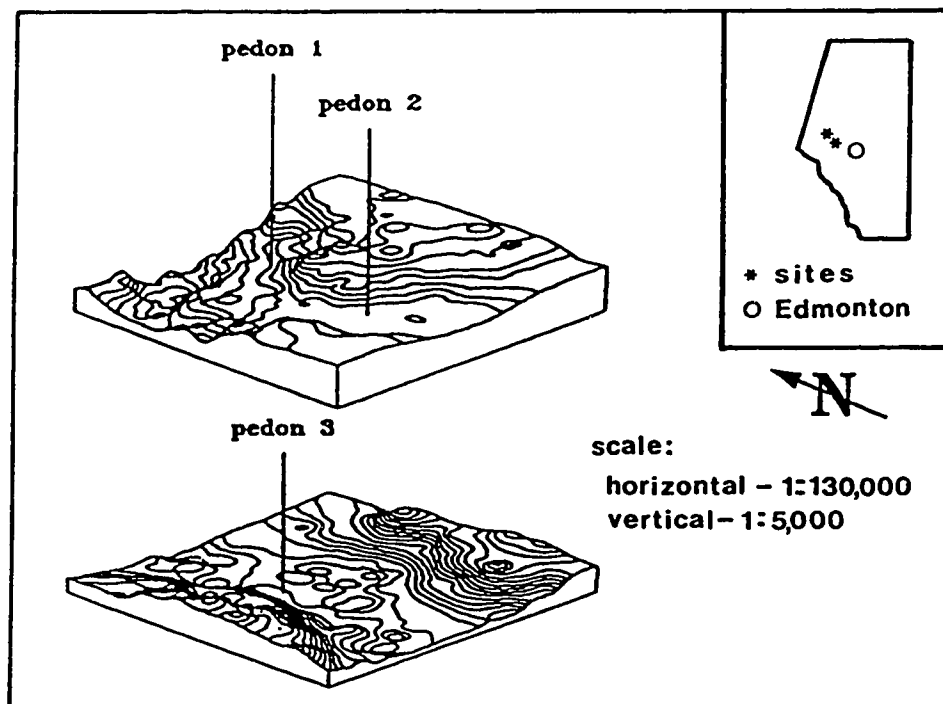


Fig. 3.1-1. Location and topography of the study areas.

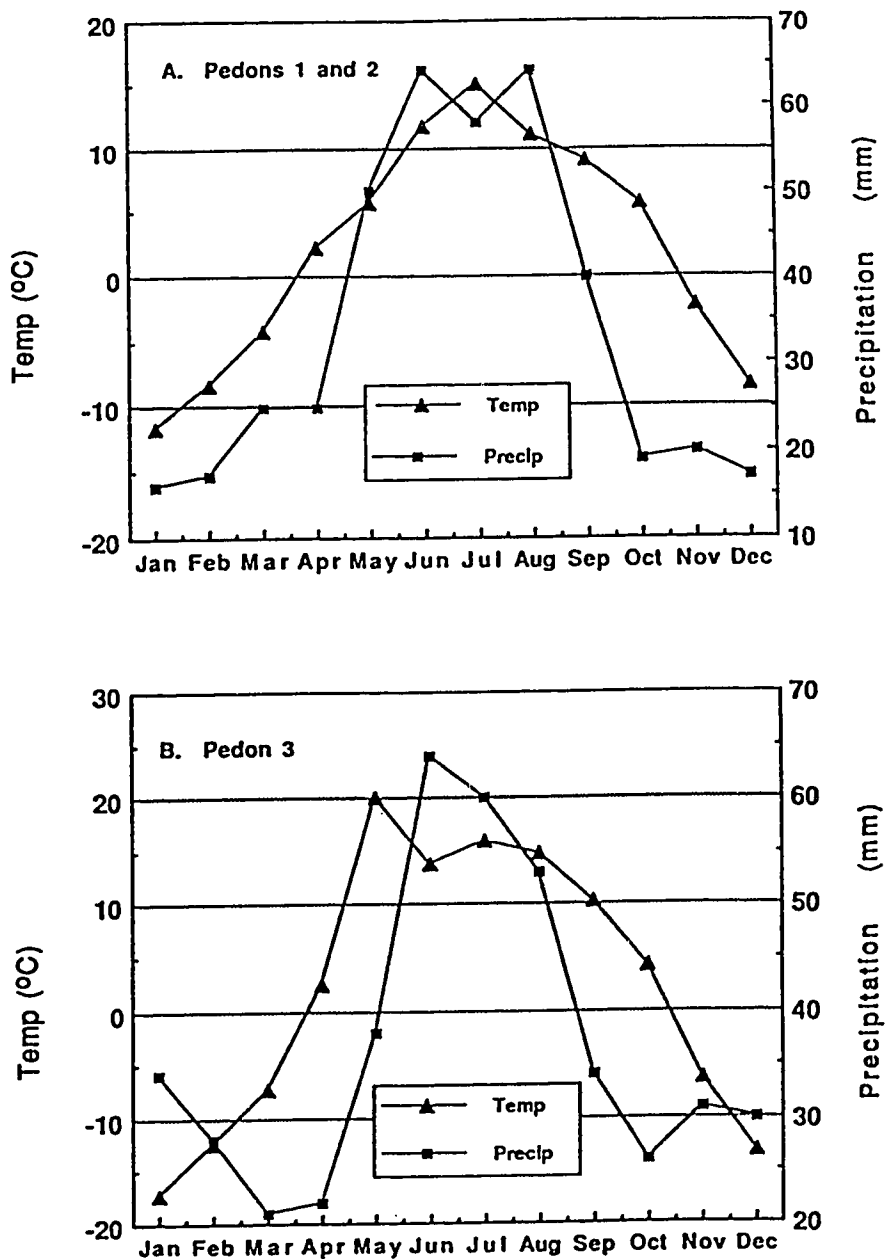


Fig. 3.1-2. Mean monthly temperature and precipitation recorded at the meteorological stations closest to (A) pedons 1 and 2 at Entrance station and to (B) pedon 3 at Grande Prairie station. (sources: Dumanski *et al.*, 1972; Twardy and Corns, 1980)

3.2. Pedon description, sampling and analyses

Pits with dimensions of 1 x 1 x 1 m were dug at each location for detailed profile descriptions. Three soil monoliths measuring 6 x 8 x 24 cm were taken from each pit for the investigation of undisturbed soils. Samples of about 5 kg were collected and subsequently air-dried and passed through a 2 mm sieve for bulk physical and chemical analyses.

3.2.1 Nodules separation

Indurated nodules present in the Bf horizons were separated from the matrix at the time of field sampling primarily on the basis of color and induration. Further separation was conducted in the laboratory by passing the air dried samples through a 2 mm sieve and hand-picking nodules from the retained materials.

Selected nodules were air-dried and subsequently crushed and passed through a 2 mm sieve for physical, chemical and bulk mineralogical analyses; some were retained for microscopy.

3.2.2 Physico-chemical analyses

Particle size analysis was conducted on <2 mm size fine earth fractions of bulk and on nodule samples after ultrasonic dispersion for 6 minutes (3 times for 2 minutes) using a Braun-sonic 1510 sonifier operated at 400 watts. No pre-treatments were applied prior to dispersion. Clay fractions were separated from sand and silt fractions through successive dispersion and sedimentation. The sand fraction was separated from the silt fraction by wet sieving, and further separation to different sand classes was conducted by dry sieving. Bulk density was determined according to the core method using a 7.5 cm diameter core sampler for bulk samples and the paraffin coated clod method for the nodules (McKeague, 1981).

The values for pH (H₂O and CaCl₂) were determined with a Model 10 Corning pH meter using a 1:1 and 1:2 soil:solution ratio, respectively. Total carbon was determined by combustion using a Leco Carbon Determinator model CR 12. The amounts of various forms of free Fe, Al and Si were measured by extracting the fine earth and clay separates of the bulk and nodule samples with dithionite-citrate-bicarbonate, d (Mehra and Jackson, 1960), Na-pyrophosphate, p (McKeague, 1967) and NH₄-oxalate, o (Schwertmann, 1964), and the extracts were analyzed for Fe, Al and Si with an Instrumentation Laboratory model 751 atomic absorption spectrophotometer (AAS).

Cation exchange capacity (CEC) and the amount of extractable cations were determined by extraction with 1N NH_4OAc buffered at pH 7. The CEC was calculated from the measured amount of exchangeable NH_4^+ adsorbed as determined with an auto-analyzer; extractable cations were determined with AAS. The cation exchange capacity at pH 4.5 was also determined to measure the amount of pH-dependent charges using 1N NaOAc buffered at pH 4.5. Cation exchange capacity of the clays were determined following the methods of Alexiades and Jackson (1965). Exchangeable acidity was analyzed by the BaCl_2 -TEA method (Page *et al.*, 1982). Total dissolution for elemental analyses of the different particle separates was conducted according to the microwave digestion procedure proposed by Warren *et al.* (1990).

3.2.3. Mineralogy

Mineral identification was conducted by XRD analyses using a Philips PW1730 X-ray generator operated at 50 kV and 25 mA with $\text{Co-K}\alpha$ radiation; and analyses carried out by step-scanning at $0.05^\circ 2\theta$ intervals every 2 seconds. Untreated clay fractions (fine $<0.8\ \mu\text{m}$ and coarse $>0.8\ \mu\text{m}$) and fine silt ($2\text{-}5\ \mu\text{m}$) samples were Ca^{++} and K^+ saturated. Selected clay samples were extracted with 0.33M Na-citrate (C) and 0.33M Na-citrate-dithionite (CD) solutions and were likewise Ca^{++} saturated. K-saturated clay and fine silt were scanned from $3\text{-}36^\circ 2\theta$ after equilibrating at 0% relative humidity (RH) and from $3\text{-}19^\circ 2\theta$ after equilibrating at 54% RH as well as after heating to 300 and 550 $^\circ\text{C}$. Calcium-saturated clay and silt were likewise scanned from $3\text{-}19^\circ 2\theta$ at 54% RH and from $3\text{-}19^\circ 2\theta$ after glycerol and ethylene glycol solvation. Selected samples were intercalated with $n\text{C} = 6$ to 18 alkylammonium chloride molecules to measure the charge density of expanding 2:1 type phyllosilicates following the method proposed by Lagaly and Weiss (1969) and Olis *et al.* (1990). Vermiculite content of selected clay fractions were determined following the method proposed by Alexiades and Jackson (1965). The coarse clay fraction of the B horizons was also subjected to differential X-ray diffraction (DXRD) following the method outlined by Schulze (1981, 1984). In brief, DXRD patterns were obtained by subtracting the XRD patterns of treated from untreated clay samples. The extractions used were d, p, and o and the diffractions were carried out from $3\text{-}90^\circ 2\theta$ in $0.02^\circ 2\theta$ steps every ten seconds. A Nicolet- FTIR was employed for the infra-red spectrometric analysis of selected fine clay samples.

Mineralogy of the sand and medium and coarse silt fractions was determined by powder diffraction after back-packing in an aluminum sample holder against a filter

paper to minimize preferred orientation. The mounts were scanned from $3-90^{\circ}2\theta$ using the above mentioned equipment and settings.

Iron-containing minerals were concentrated using a modified Frantz isodynamic separator operated over a range of magnetic flux densities from 0.2 to 1.7 tesla. Mineralogy of the separated Fe rich fractions was determined by XRD using the goniometer and a 57.3 mm radius Debye-Scherrer camera, where samples were exposed to Co-K α radiation for a period from 30-60 minutes at 50 kV and 25mA.

3.2.4. Microscopy

Soil monoliths and selected indurated nodules were impregnated with 3M Scotchcast electrical resin and 8 x 5 cm thin sections of 30 μm -thickness were prepared. The sections were described following the terminologies of the proposed international system (Bullock *et al.*, 1985). Cross-descriptions to the conventional system (Brewer, 1976; Brewer and Pawluk, 1975; and Pawluk, 1983) were also conducted when deemed necessary. Micromorphometric analysis of Fe-rich nodules was conducted using a K-Mop Videoplan Image Analysis system under plain, cross polarized and reflected lights.

The sub-microscopic morphology and semi-quantitative chemistry were determined with the aid of a Cambridge Stereoscan 250 scanning electron microscope (SEM) equipped with a Tracor Northern X-ray analyzer. *In situ* mineralogical determinations of selected pedofeatures were conducted by removing part of the thin section containing the features of interest from the glass slide and mounting it on a transmission type Norelco micro-camera equipped with a 50- μm collimator for X-ray microdiffraction.

Removal of the selected feature from the glass slide was achieved by heating the uncovered thin section in distilled water at 80 $^{\circ}\text{C}$ for 10 minutes and peeling the section with the use of a razor blade. The features were either mounted on mylar sheet or on a customized acetate sample holder. The mounted sample was centered on the camera by aligning the sample such that the light from a petrographic microscope passes through the collimator of the camera and impinges directly on the feature of interest.

The camera was attached to a Philips PW 1020 X-ray generator which was operated at 30 kV and 20 mA using fine focus (FF) Co-K α radiation and an Fe-filter. Exposure times varied from 8-12 hours.

3.2.5 *Lysimeter description, installation and leachates collection*

The gravity lysimeters used in this study were made from transparent 0.6 cm thick PVC tubes with a diameter of 10 cm. Undisturbed soil samples were collected inside the tube by attaching a sharp steel cutting edge to one end of the tube. The assembly was forced into the soil by pressing on a steel cap attached to the opposite end of the tube. The tube filled with undisturbed soil was unearthed, the cutting edge and the steel cap were removed and a collecting beaker was assembled at the bottom of the tube completing the lysimeter assembly; the set up was then slid back into the hole. Access to the collected leachates was through Tygon tubing connected to the bottom of the beaker and extended to the soil surface. Collection was done by suction with a hand pump.

The lysimeters were installed beneath the LFH, Ae and Bf horizons from the summer of 1988 in pedon 1 and from the spring of 1989 until the spring of 1990 in pedon 2; no lysimeters were installed in pedon 3. A total of five collections were made from pedon 1 and three from pedon 2. Additional lysimeters were installed beneath the Ae where the LFH layers were removed. The leachates were stored at 4 °C until analyses.

3.2.5.1 *Chemistry of the leachates*

The leachates were analyzed for the content of the following cations Fe, K, Na, Ca, and Mg using AAS. Aluminum was determined colorimetrically using the aluminon method and Si by the blue molybdo-vanado method (Hallmark *et al.*, 1982). Anions such as Cl^- , NO_3^- , SO_4^{2-} and PO_4^{3-} were analyzed with a Dionex high performance ion chromatograph. Carbonates were determined by titration. Solution pH was determined potentiometrically using a model 10 Corning pH meter.

Simple organic acids and sugars were also determined with the Dionex ion chromatograph. The amounts of C, H and N in freeze-dried leachates were determined using a Perkin Elmer 240B CHN Analyzer.

3.2.5.2 *Characterization of the colloidal components*

Colloidal components were separated from the leachate solution by passing the leachates through a 0.2 mm millipore filter. The colloids were then investigated under the SEM for sub microscopic morphology and semi-quantitative chemistry. The leachates were also freeze dried for IR and XRD analyses. Heat treatments at 150, 350, 550 and 750 °C were applied to selected residues from leachates prior to XRD investigation.

3.2.6. Pore water solution and its chemistry

Pore water solutions from the Ae and the Bf horizons of pedons 1 and 2 were obtained by displacement of the soil water by tetrachloroethylene. The initial stage of the exchange was conducted in the field by placing about 20 g of sample into a centrifuge tube containing 20 mL of tetrachloroethylene. The tubes were capped, tightened and brought into the laboratory and centrifuged at 14500 rpm for 30 minutes to complete the displacement. Twelve sub-samples for each horizon were used to collect about 5 mL of pore water. There were three separate collections made for the entire duration of the study. Chemical analyses and methodologies used were similar to those for the lysimeter leachates.

Chapter 4

RESULTS AND DISCUSSION

This is the main part of the thesis and it is divided into three sections that deal with: 4.1. descriptions and genesis of microstructures, 4.2. nature and origin of indurated nodules in the Bf horizons and 4.3. distribution and transformations of minerals. The specific objectives are enumerated in the introduction provided in the beginning of each section.

4.1. Microstructures of Podzols from Alberta

4.1.1. Introduction

Earlier studies of Podzolic soils found in sandy deposits along the foothills to the treeline regions of the Canadian Rockies in Alberta had been limited to general soil surveys and "macro" characterization (Dumanski, 1970; Pettapiece, 1970; Beke and Pawluk, 1971; Dumanski *et al.*, 1972; Twardy and Corns, 1980; Smith *et al.*, 1981). Those studies are quite useful for land and resource inventory but are not sufficient for an understanding of the pedogenetic development of the soils.

Podzolic soil, like any other soils is a natural anisotropic and dynamic body. Soil anisotropy is best studied by investigation of the microstructure through techniques of soil micromorphology (Kooistra, 1990). Dynamic pedology on the other hand is best approached through lysimeter studies (Ugolini *et al.*, 1977). As early as the 1930's, the dynamic nature of Podzol formation had been investigated using lysimeter studies (Rode, 1936).

This section discusses the anisotropy and dynamic characteristic of Podzolic soils of Alberta. Specifically, the objective of this section is to investigate the composition, microstructures and mobile components of selected Podzolic soils and evaluate their role in mineral alteration and structural reorganization within the sola.

4.1.2. Results and Discussion

4.1.2.1. Morphological characteristics

Table 4.1-1 lists the field morphology of the three pedons; they have similar horizon sequences consisting of LFH, Ae, Bf1, Bf2, BC and C. The Ae horizons are diagnostic for albic and all the Bf horizons meet the current criteria for a spodic horizon. Indurated nodules ranging in size from a few mm to about 20 cm are found in the upper boundary of the Bf in pedon 3, lower boundary in pedon 2 and randomly in the Bf horizon of pedon 1.

Table 4.1.1a. Field morphology of pedon 1.

Horizon	Depth(cm)	Description
L	10- 5	Undecomposed leaf litter, mosses, lichens
F	5- 0	Dull reddish brown (5YR 3/4 m); semi-decomposed woody tissue; fibrous; rotting logs; charcoal fragments at the lower boundary.
Ae	0-12	Light brownish gray (7.5YR 7/1 m); sand; single grain; loose; many medium and coarse horizontal and few oblique roots; clear wavy boundary with some tongues to underlying Bf horizon; 12-18 cm.
Bf1	12-20	Bright brown (7.5YR 5/6 m); loamy sand to sand; single grain; very friable to loose; few medium and many fine horizontal and oblique roots; random medium nodules (7.5YR 5/6); gradual wavy boundary; 18-23 cm.
Bf2	20-37	Yellowish brown (10YR 5/8 m); sand; very weakly fragmental to single grain; loose to very friable; few fine and very fine vertical and oblique roots; some zone show weak cementation; few rounded stones (0.5-2 cm diameter); gradual wavy boundary.
BC	37-60	Bright yellowish brown (10YR 6/8 m); sand; very weakly fragmental tends to be single grains; loose to very slightly friable; very few fine and very fine oblique roots; few stones (0.5-3 cm diameter); gradual wavy boundary.
C1	60-110	Dull yellow orange (10YR 6/4 m); sand; single grain; loose; many medium and few fine horizontal and oblique roots at the lower boundary; gradual smooth boundary.
C2k	110+	Dull yellowish orange (10YR 5/3-5/4 m); sand; single grain; loose; no roots; clay and silt lenses present; calcareous.

Table 4.1.1b. Field morphology of pedon 2.

Horizon	Depth(cm)	Description
L	10- 5	Undecomposed leaf litter, mosses, lichens.
F	5- 0	Semi-decomposed woody tissue; fibrous.
Ae	0- 9	Light gray (10YR 7/1 m); sand; single grain to weak fine platy structure; loose to slightly friable; many medium and fine horizontal and oblique roots; clear wavy boundary.
Bf1	9-21	Bright brown (7.5YR 5/8 m); sand; very weak granular to single grain; very friable; plentiful medium and very fine horizontal and oblique roots; nodules (5YR 4/6 m) about 0.5 cm diameter are present in the lower 2cm of the horizon; gradual wavy boundary.
Bf2	21-30	Dull yellow orange (10YR 6/4 m) to bright yellowish brown (10YR 6/6 m); sand; single grain; loose to very friable; plentiful fine and very fine horizontal and oblique roots; mottlings (10YR 5/8); gradual wavy boundary.
BC	30-76	Dull yellow orange (10YR 6/4 m) to dull yellow (2.5 Y 6/4 m); sand; single grain; loose; gradual wavy boundary.
IIC1	76-94	Dull yellowish brown (10YR 4/3 m) with reddish brown (5YR 4/6 m) to dark reddish brown (5YR 3/6 m) bands; sand; weak platy; loose; prominent common mottles with color identical to band; clear smooth boundary.
IIC2k	94+	Dull yellowish brown (10YR 4/3 m); clay loam; weak blocky to fragmental massive; slightly sticky and plastic; very few fine random roots; calcareous.

Table 4.1.1c. Field morphology of pedon 3.

Horizon	Depth(cm)	Description
L	10- 5	Undecomposed leaf litter, mosses, lichens.
F	5- 0	Semi-decomposed woody tissue; fibrous.
Ae	0-10	Light yellowish gray (7.5YR 7/2 m); sand; single grain; loose; abundant coarse medium and fine roots; clear wavy boundary.
Bf1	10-20	Bright brown (7.5YR 5/8 m); sand; very weak granular to single grain; very friable; many fine and very fine dominantly horizontal and oblique roots; medium and coarse nodules (5YR 4/8) at upper 2cm; gradual wavy boundary.
Bf2	20-32	Yellowish brown (10YR 5/8 m); sand; single grain to very weakly granular; very friable; many fine and medium vertical and oblique roots; gradual wavy boundary.
BC	32-70	Dull yellowish brown (10YR 5/4 m); sand; single grain to weakly granular; friable; few medium and fine horizontal and vertical roots; common faint mottles (10YR 4/4); gradual wavy boundary.
C1	70-110	Dull yellowish brown (10YR 5/4 m); sand; single grain; loose; no roots; distinct mottles (10YR 4/6); gradual wavy boundary.
C2	110+	Olive brown (2.5 Y 4/4 m); sand; single grain; loose; no roots.

4.1.2.2. *Physical and chemical properties*

All pedons are sandy in texture throughout the sola with the sand content ranging from 640 to 915 g·(kg soil)⁻¹; silt content from 43 to 316 g·(kg soil)⁻¹ and clay content from 15 to 151 g·(kg soil)⁻¹; an exception is the IIC2k horizon of pedon 2 where the amounts for sand, silt and clay are 118, 557 and 325 g·(kg soil)⁻¹, respectively (Table 4.1-2). This coincides with a lithological break at 76 cm depth. Bulk density generally increases from 1.13 to 1.24 Mg m⁻³ in the Ae to 1.26 to 1.41 Mg m⁻³ in the Bf horizons.

Soil reaction shows a similar trend in all pedons with acidic (pH 4.2-4.6) Ae horizons, moderately acidic (pH 5.1-5.9) B horizons and with calcareous C horizons in pedons 1 and 2 and a mildly acidic C2 horizon in pedon 3 (Table 4.1-2). Total organic carbon content is highest in the Ae and Bf1 with values in the range of 4-7 g·(kg soil)⁻¹ in the sola of all the pedons.

Exchangeable cations are dominated by Ca⁺² followed by lesser amounts of Mg⁺², Na⁺ and K⁺ (Table 4.1-3). Cation exchange capacities of the eluvial horizons at pH 7.0 and at soil pH are consistently lower than Bf1 horizons (Table 4.1-4). The Δ CEC values of the Bf horizons are higher (0.94-1.54 cmol_c·(kg soil)⁻¹) than those of Ae (0.41-0.97 cmol_c·(kg soil)⁻¹) and reflect the accumulation of materials with pH dependent charges such as less-ordered alumino-silicates. The exchangeable acidity values are also higher in the Bf than Ae horizons (Table 4.1-3).

The Bf1 horizons generally have the highest amount of extractable Fe, Al and Si in all their forms (Table 4.1-5). Iron complexed with organic matter (Fep) is lower than the Fe present as less-ordered Fe-oxyhydroxides (Feo) as shown by the high Feo/Fed ratios especially in the Ae and Bf horizons. Dithionite citrate bicarbonate extracted up to 15.1, 8.3 and 1.9 g extractable Fe, Al and Si·(kg soil)⁻¹, respectively from Bf horizons; the amounts in the Ae horizons are lower *i.e.*, respectively, 5.6, 1.1 and 0.9 g of extractable Fe, Al and Si·(kg soil)⁻¹. The extractable metals in the C horizons are believed to originate from the presence of detrital Fe-rich nodules and pseudo sand particle.

Table 4.1-2. Selected properties of Podzolic soils from Alberta.

Sample	pH		C (g kg ⁻¹)	N (Mg m ⁻³)	Db (Mg m ⁻³)	Sand	Silt (g kg ⁻¹)	Clay
	H ₂ O	CaCl ₂						
<u>Pedon 1: Eluviated Dystric Brunisol</u>								
Ae	4.2	3.5	3.17	0.14	1.24	872	114	15
Bf1	5.6	4.9	3.96	0.17	1.28	810	166	25
Bf2	5.9	5.0	2.29	0.10	1.47	824	85	92
BC	6.0	5.1	0.73	0.08	1.53	876	77	47
C1	6.1	5.2	0.62	0.09	nd	881	79	40
C2k	8.3	7.0	23.5 ^a	nd	nd	821	136	44
<u>Pedon 2: Orthic Humo-Ferric Podzol</u>								
Ae	4.6	3.8	6.94	0.26	1.18	640	316	44
Bf1	5.7	4.8	6.07	0.37	1.14	681	245	75
Bf2	5.8	4.9	1.57	0.13	1.41	870	68	62
BC	5.6	4.7	1.38	0.11	1.54	879	66	55
IIC1	7.4	6.6	3.80	0.28	nd	623	226	151
IIC2k	8.3	7.5	24.1 ^a	nd	nd	118	557	325
<u>Pedon 3: Orthic Humo-Ferric Podzol</u>								
Ae	4.2	3.5	5.13	0.18	1.13	889	99	13
Bf1	5.1	4.5	5.19	0.21	1.26	879	61	59
Bf2	5.4	4.6	3.79	0.16	nd	915	43	42
BC	5.7	4.8	1.79	0.15	1.40	871	75	55
C1	5.7	4.7	4.25	0.14	nd	882	93	26
C2	5.8	4.9	5.34	0.18	nd	870	95	35

nd - not determined; a - value includes C from carbonates

Table 4.1-3. Cation exchange capacity, exchangeable cations and acidity of Podzolic soils from Alberta.

Sample	Ca ^a	Mg ^a	Na ^a	K ^a	sum ^a	TCEC ^a	Exch ^b Acid	Cation Sat(%)
(cmol _c kg ⁻¹)								
<u>Pedon 1: Eluviated Dystric Brunisol</u>								
Ae	0.50	0.06	0.50	0.05	1.11	2.73	3.32	41
Bf1	0.66	0.06	0.04	0.11	0.87	6.57	2.95	19
Bf2	0.94	0.20	0.05	0.12	1.31	6.53	1.84	20
BC	1.39	0.39	0.44	0.10	2.32	3.70	1.29	62
C1	1.97	0.41	0.36	0.05	2.79	2.91	0.55	96
Ck	nd	0.47	0.44	0.03	nd	2.70	nd	nd
<u>Pedon 2: Orthic Humo-Ferric Podzol</u>								
Ae	1.25	0.18	0.09	0.12	1.64	6.82	4.42	24
Bf1	1.83	0.20	0.12	0.14	2.29	11.40	7.19	20
Bf2	1.46	0.33	0.08	0.09	1.96	5.07	3.50	39
BC	1.50	0.39	0.08	0.01	1.98	4.61	1.11	45
IIC1	nd	1.17	0.11	0.16	nd	8.46	0.74	nd
IIC2k	nd	1.91	0.12	0.21	nd	12.10	nd	nd
<u>Pedon 3: Orthic Humo-Ferric Podzol</u>								
Ae	0.20	0.04	0.10	0.04	0.38	2.25	1.66	18
Bf1	0.16	0.03	0.12	0.07	0.38	8.42	7.74	5
Bf2	0.21	0.07	0.28	0.08	0.64	5.53	2.95	12
BC	0.80	0.18	0.10	0.09	1.17	2.78	1.11	42
C1	0.81	0.15	0.08	0.07	1.11	3.02	nd	37
C2	1.75	0.21	0.08	0.07	2.11	3.71	nd	57

nd - not determined; a - 1N NH₄OAc, pH7.0
b - BaCl₂-TEA, pH 8.2

Table 4.1-4. Cation exchange capacities determined at pH 4.5 and 7.0 of some Podzolic soils from Alberta.

Sample	pH 4.5	pH 7.0 ($\text{cmol}_c \text{ kg}^{-1}$)	Δ CEC
<u>Pedon 1: Eluviated Dystric Brunisol</u>			
Ae	2.33	2.74	0.41
Bf1	3.74	5.32	1.58
Bf2	2.99	3.91	0.92
<u>Pedon 2: Orthic Humo-Ferric Podzol</u>			
Ae	4.49	5.46	0.97
Bf1	7.27	8.21	0.94
Bf2	3.18	3.80	0.62
<u>Pedon 3: Orthic Humo-Ferric Podzol</u>			
Ae	1.86	2.49	0.63
Bf1	5.95	7.33	1.33
Bf2	3.43	3.56	0.13

4.1.2.3. Microstructures

The micromorphology of the Ae horizons is primarily characterized by an apedal single grain type of microstructure with porosity estimated between 20-30% (Tables 4.1-6). The coarse components ($> 50 \mu\text{m}$) consist mainly of quartz including chert and feldspar and are generally bare (Fig. 4.1-1a) but grains thinly coated by the fine materials are occasionally observed in patches. The associated related distribution patterns (RDP) are monic (bare grains) and chitonic (coated grains). Fine materials ($< 50 \mu\text{m}$) wherever present are dominantly phyllosilicates as is evident from the birefringent domains in coatings of the coarse materials and by organic materials present in patches of mosaic speckled zones. The observed microstructure is similar to Ae horizons described for other Podzolic soils (De Coninck and McKeague, 1985; Milnes and Farmer, 1987).

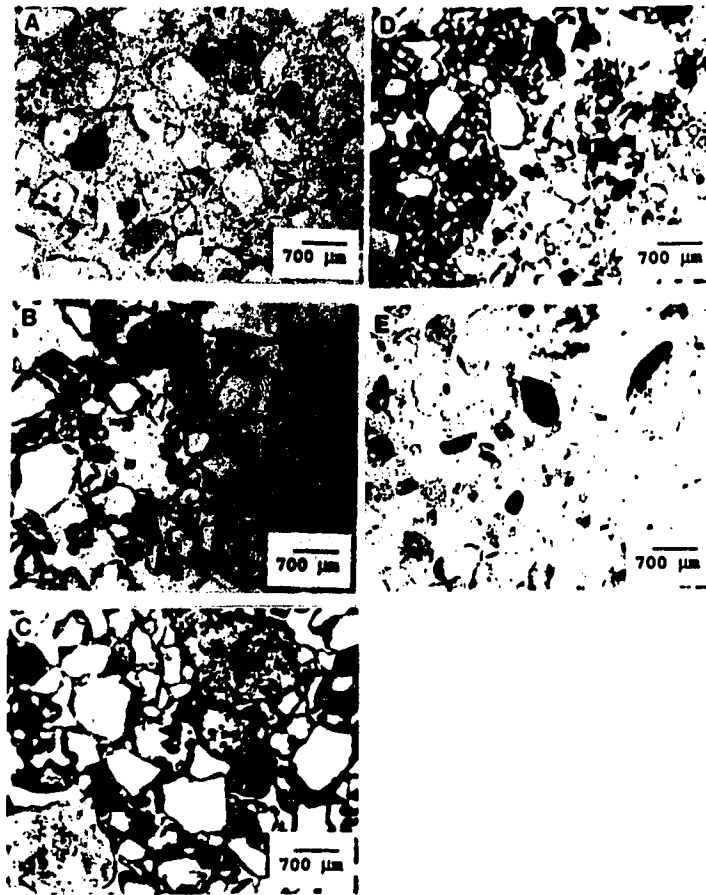


Fig. 4.1-1. The related distribution patterns (RDP) in Podzolic soils from Alberta. (A) monic RDP in the Ae horizons (B) chitonic RDP in the Bf matrix (C) porphyric RDP in the Bf nodule (D) porphyric and chitonic RDPs in the Bf matrix-Bf nodule interphase and (E) monic RDP in the C horizon.

Table 4.1-5. Na-pyrophosphate (p), NH₄-oxalate (o) and Dithionite-citrate-bicarbonate(d), extractable Fe, Al and Si in some Podzolic soils of Alberta.

Sample	Fep	Alp	Sip	Feo	Alo	Sio	Fed	Ald	Sid	Feo/Fed
	(g kg ⁻¹ soil)									
<u>Pedon 1: Eluviated Dystric Brunisol</u>										
Ae	0.2	0.2	0.0	4.8	0.6	0.0	5.6	1.1	1.2	0.90
Bf1	2.3	2.6	0.0	9.0	4.2	0.4	11.9	6.6	1.8	0.76
Bf2	0.9	1.2	0.7	5.0	2.3	1.0	8.2	3.2	2.2	0.62
C1	0.2	0.0	0.0	0.9	0.3	0.1	3.5	0.3	0.5	0.26
<u>Pedon 2: Orthic Humo-ferric Podzol</u>										
Ae	0.4	0.5	0.2	0.5	0.7	0.3	0.6	0.3	0.8	0.86
Bf1	4.4	4.1	0.0	11.5	5.8	0.4	15.1	7.3	1.7	0.76
Bf2	1.4	1.5	0.0	5.6	2.2	0.2	7.9	3.3	1.4	0.71
C1	1.4	0.6	0.2	3.6	1.2	0.4	5.6	0.6	1.3	0.63
<u>Pedon 3: Orthic Humo-ferric Podzol</u>										
Ae	0.2	0.1	0.1	0.7	0.2	0.2	0.9	0.2	0.6	0.83
Bf1	3.3	3.0	0.0	9.6	5.5	0.4	14.3	8.3	1.9	0.67
Bf2	1.7	1.7	0.0	7.0	2.9	0.3	11.2	5.5	1.0	0.63
C1	0.5	0.7	0.4	1.0	1.0	0.5	4.7	0.5	0.9	0.22

The microstructure of Bf horizons is dominated by an apedal pellicular type (porosity=30%) where the coarse components, mainly quartz and feldspar, are coated by fine materials to give a chitonic RDP (Table 4.1-6); patches of bridged grain microstructure have open porphyric RDP (Fig. 4.1-1b). Minor amounts of chlorite, hornblende and zircon are also present as coarse components. The fine materials which are brownish in plain light and speckled under cross polarizers are composed mainly of phyllosilicates, quartz and organic matter. Thick and continuous fine materials accumulate in interspaces between and on surfaces of coarse mineral grains and impart a porphyric RDP (Fig. 4.1-1c). This gives rise to authigenic indurated nodules with sizes ranging from less than a cm to about 20 cm in diameter. The coatings form through accumulation of phyllosilicates, less-ordered alumino-silicates such as imogolite, Fe-oxides and organic matter aided in their aggregation by fungal hyphae. The advanced stage of microstructure development in the nodule as compared to the matrix is shown in Fig. 4.1-1d. The presence of "cracked monomorphic coatings" (De

Coninck, 1980; De Coninck and McKeague, 1985), frequently reported in B horizons of Podzolic soils, were not observed in the present study.

The microstructure of C horizons (Table 4.1-6) is apedal single grain type (porosity=30%) similar to that of the Ae horizons with dominantly monic RDP (Fig. 4.1-1e). Coarse components are dominantly quartz including chert and feldspar and minor amount (5%) of unweathered grains of allogenic chlorites. The fine component is mainly phyllosilicates.

4.1.2.4. *Pedological coatings and infillings*

Coatings of phyllosilicates (argillans) are very thin in the Ae and C horizons but are thick and frequently fill the voids between coarse components in Bf horizons. The coatings exhibit yellow interference colors with wavy extinction patterns under cross-polarizers and *in situ* XRD analyses reveal that they are made up of mainly 2:1 type phyllosilicates (Fig. 4.1-2a). The infillings in voids are mostly isotropic and vary in composition from mixtures of 2:1 phyllosilicates and dispersed goethite (Fig. 4.1-2b) to materials amorphous to X-rays probably composed of less-ordered imogolite, ferrihydrite and organo-metallic complexes. Infillings that show grey to white interference colors are mixture of fine quartz and phyllosilicates (Fig. 4-1-2b).

Coatings observed on the remains of plant materials are Al-rich and amorphous to X-rays. The Al is likely chelated to the organic matter (Fig. 4.1-3). White coatings on a few of the goethite, feldspar and quartz grains have an Al:Si molar ratio of about 1 and with diffuse *in situ* XRD reflections around 0.56 and 0.33 nm indicative for the less-ordered imogolite (Fig. 4.1-2c). Iron-rich coatings are also observed on coarse quartz and feldspar grains.

4.1.2.5. *Fe-rich pedofeatures*

Based on internal morphology, Fe-rich nodules are classified as the typical type; they make up about 27% of the area in the C horizons; 14% in Ae horizons and 50% in the matrix and larger nodules in Bf horizons (Table 4.1-7). The high value for the latter is attributed to a large number of mineral grains completely engulfed by Fe oxides. The number of nodules per cm² of area observed in thin section decreases from 25 in the C to 12 in the Bf and to 3 in the Ae horizon while the mean area (cm²) increases from 0.01 in C to 0.04 in Ae and to 0.06 in Bf horizon. The increase in the number of larger nodules in the Bf horizon is accompanied by a corresponding decrease in the number of smaller nodules in the Ae horizon (Fig. 4.1-4); this suggests a dissolution of nodules in the Ae and reorganization in the Bf horizon.

Table 4.1-6. Abridged micromorphology of Podzolic soils from Alberta.

	Ae	Bf	C
<u>PEDON 1: Eluviated Dystric Brunisol</u>			
<u>Microstructure</u>			
type	apedal (single grain)	apedal (pellicular)	apedal (single grain)
porosity (%)	30	30	30
<u>Basic components</u>			
c/f limit (ratio)	50 μm (5:2)	50 μm (5:3)	50 μm (6:1)
RDP ^a	mainly monic some part chitonic	chitonic	mainly monic
coarse	Qtz ^b +Ct ^c (95) Fd ^d (3), Zr ^e (tr)	Qtz(95), Fd(3) Ch ^{aa} +Zr(2)	Qtz+Ct(90), Fd (2), O ^{ee} +We ^{bb} + Zr+ Ch(5)
fine	all fine material associated to grains as coatings	no fine material (associated to grains as coatings)	occur as part of incomplete coatings on grains
<u>Pedofeatures</u>	typic clay coatings on Qtz/Fd, nodules of Fe-organic complexes	typic clay coatings; impregnative nodules; Fe- nodules	very thin clay coatings on grains; disorthic nodules
<u>Organic</u>	polymorphic	polymorphic	none detected

continued on next page

Table 4.1-6 ... continuation

<u>PEDON 2: Orthic Humo-ferric Podzol</u>			
<u>Microstructure</u>			
type	apedal (bridge grain)	apedal (pellicular)	apedal (single grain)
porosity (%)	20	25-30	30
<u>Basic components</u>			
c/f limit (ratio)	50 μ m (6:2)	50 μ m (5:3)	50 μ m (6:2)
RDP ^a	mainly chitonic some part open porphyric	chitonic with some part open porphyric	mainly monic some part chitonic
coarse	Qtz ^b +Ct ^c (95), Fd ^d (3), Zr ^e (tr)	Qtz (85), Fd (5) Mi ^{cc} (3) Ch ^{aa} , Hb ^{dd} +Zr (2)	Qtz+Ct (92), Fd (5), O ^{ee} +We ^{bb} +Ch+ Zr+ pseudo sand (5)
fine	brownish in PL and mosaic speckled b- fabric; and associated to grains as coatings	brownish in PL and speckled b- fabric	associated to grain as partial coating
<u>Pedofeatures</u>	typic clay coatings on Qtz/Fd, weak impregnative nodules of Fe-organic complexes	typic clay coatings impregnative nodules; Fe- nodules	thin clay coatings on Qtz/Fd
<u>Organic</u>	polymorphic	polymorphic	polymorphic

continued on next page ...

Table 4.1-6... continuation

<u>PEDON 3: Orthic Humo-ferric Podzol</u>			
<u>Microstructure</u>			
type	apedal (single grain with patches of bridged grain)	apedal (pellicular)	apedal (single grain)
porosity (%)	40	30	40
<u>Basic components</u>			
c/f limit (ratio)	50 μm (4:2)	50 μm (5:2)	50 μm (5:1)
RDP ^a	mainly monic some part chitonic	chitonic some part open porphyric	mainly monic some part chitonic
coarse	Qtz ^b +Ct ^c (95), Fd ^d (3), Zr ^e (tr)	Qtz(95), Fd(2) Ch ^{aa} (tr)	Qtz+Ct(90), Fd (2), O ^{ee} (5), pseudo sand
fine	all fine material associated to grains as coatings	brownish in PL and speckled b- fabric	occur as partial coating on Qtz and Fd
<u>Pedofeatures</u>	partial thin clay coatings on Qtz/Fd, impregnative nodules of Fe-organic complexes	typic clay coatings impregnative nodules; Fe nodules	disorthic nodules
<u>Organic</u>	polymorphic	polymorphic	amorphous and opaque occurring as nodule

^a - related distribution pattern; ^b - quartz; ^c - chert;
^d - feldspars; ^e - Zircon; ^{aa} - chlorite; ^{bb} - weathering
minerals; ^{cc} - mica; ^{dd} - hornblende; ^{ee} - opaques; (90) - %

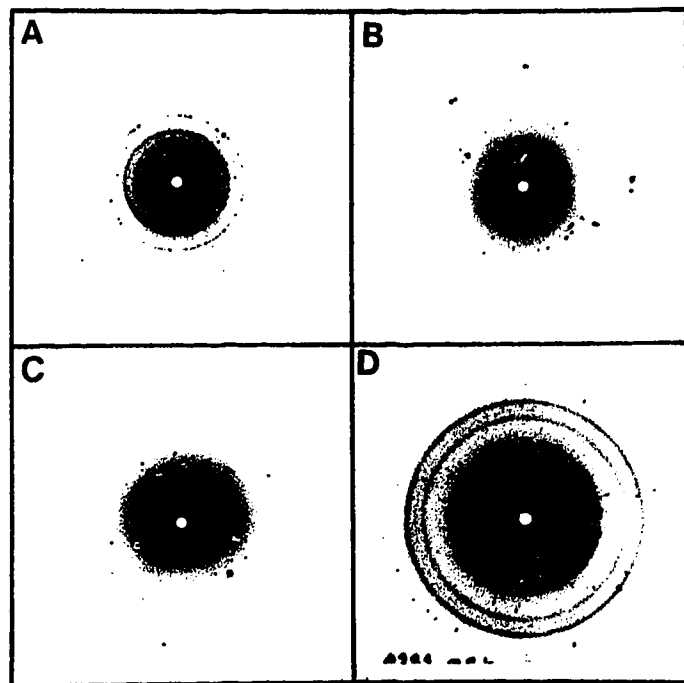


Fig. 4.1-2. *In situ* Laue photographs of selected pedological features. (A) reddish coating of 2:1 phyllosilicates (B) isotropic infillings composed of 2:1 phyllosilicates and goethite (C) whitish coatings around coarse components composed of materials amorphous to X-rays (D) nodules composed of goethite and 2:1 phyllosilicates

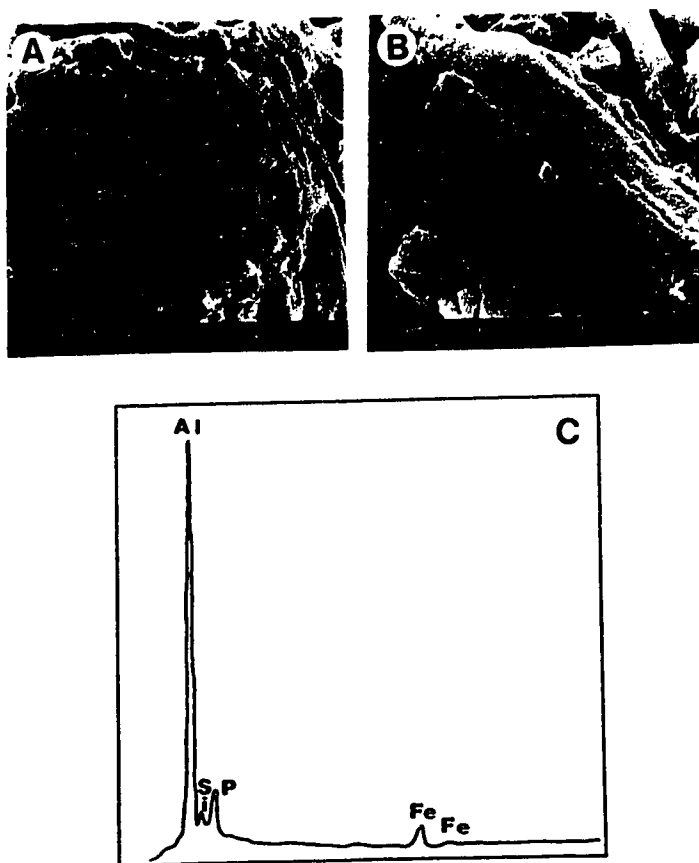


Fig. 4.1-3. Pedological coating around a root fragment (A and B) micrographs showing the layered morphology and (C) its EDS spectrum indicating the predominance of Al and the small amounts of Fe, Si and P.

Table 4.1-7. Selected statistical parameters for the size of Fe-rich nodules in Podzolic soils from Alberta.

	Ae	Bf matrix	Bf nodule	C
Frequency (#/cm ²)	3	12	12	25
Area sampled (cm ²)	10	10	6	10
Range in size (cm ²)	0.003-0.27	0.005-0.56	0.006-0.41	0.002-0.10
Mean size (Std. deviation) (cm ²)	0.04(0.004)	0.05(0.004)	0.06(0.004)	0.01(0.001)
Total Area (cm ²)	1.4	5.8	4.3	2.7

The mineral suite of the Fe-rich nodules is dominated by goethite (Fig. 4.1-2d). Infra-red analyses of the goethite nodules shows absorption bands (wavenumber cm⁻¹) at 1275 for ring C-H, 1410 for symmetric COO⁻ and 1490 for asymmetric COO⁻ (Fig. 4.1-5) which suggests that organic matter is adsorbed onto the surfaces of goethite (Kung, 1989). Infra red absorption bands at 340, 425, 580, 970, 1630 and 3470 cm⁻¹ further suggest an association of imogolite and goethite as well. Aluminum is also a component of the Fe-rich nodules although XRD analysis does not show any evidence for crystalline Al minerals. This suggests that the Al is chelated to organic matter. Quartz is inherent to these nodules.

4.1.2.6. Micromorphological features of biological origin

Organic features are mainly polymorphic composed of different plant materials at various stages of decomposition; some are organ residues where the forms of the original materials can still be recognized (Fig. 4.1-6a); others are tissue residues where no plant structures are discernible (Fig. 4.1-6b). An organ residue of a spruce needle is located in the middle right of Fig. 4.1-6c and on the left are tissue residues showing very dark brown mycelia of mycorrhiza. Intense fungal activity is also evident from the dense mat of hyphae arranged in net-like configuration (Fig. 4.1-6d).

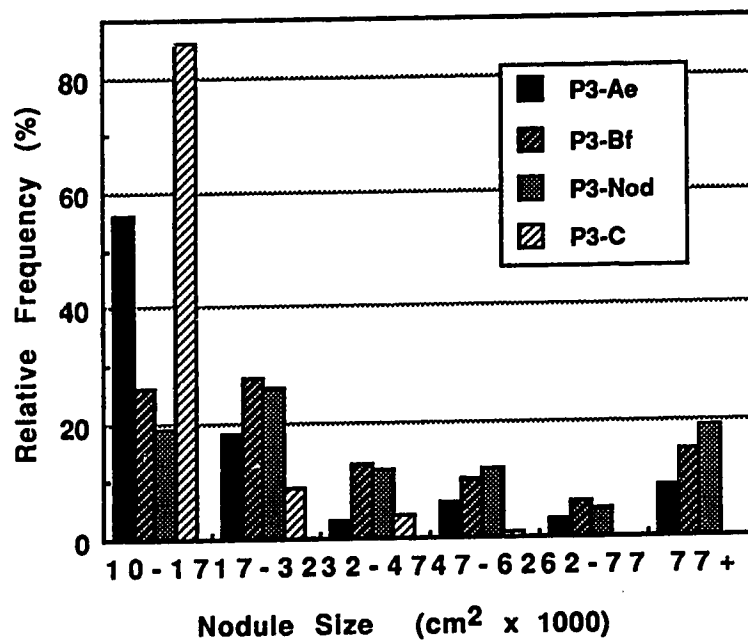


Fig. 4.1-4. Class size distribution of Fe-rich nodules in the different horizons of Podzolic soils from Alberta.

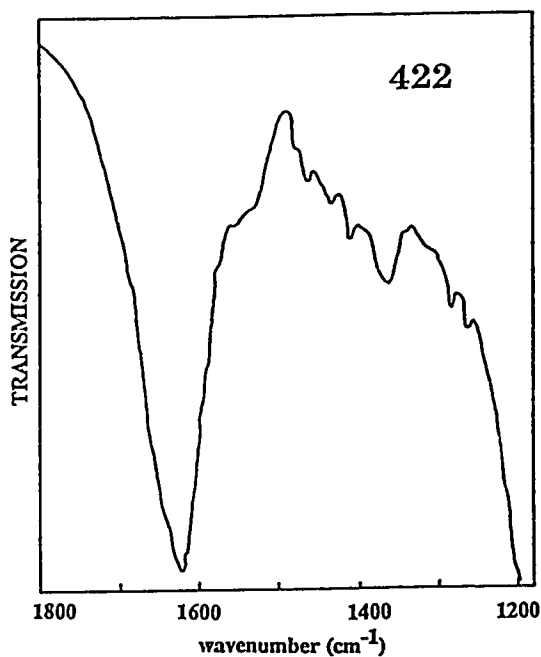


Fig. 4.1-5. Enlarged portion of the infra red spectrum of goethite nodules adsorption of ring C-H at around 1275 cm⁻¹, symmetric COO⁻ at 1410 cm⁻¹ and assymmetric COO⁻ at 1490 cm⁻¹ onto the surface of goethite.

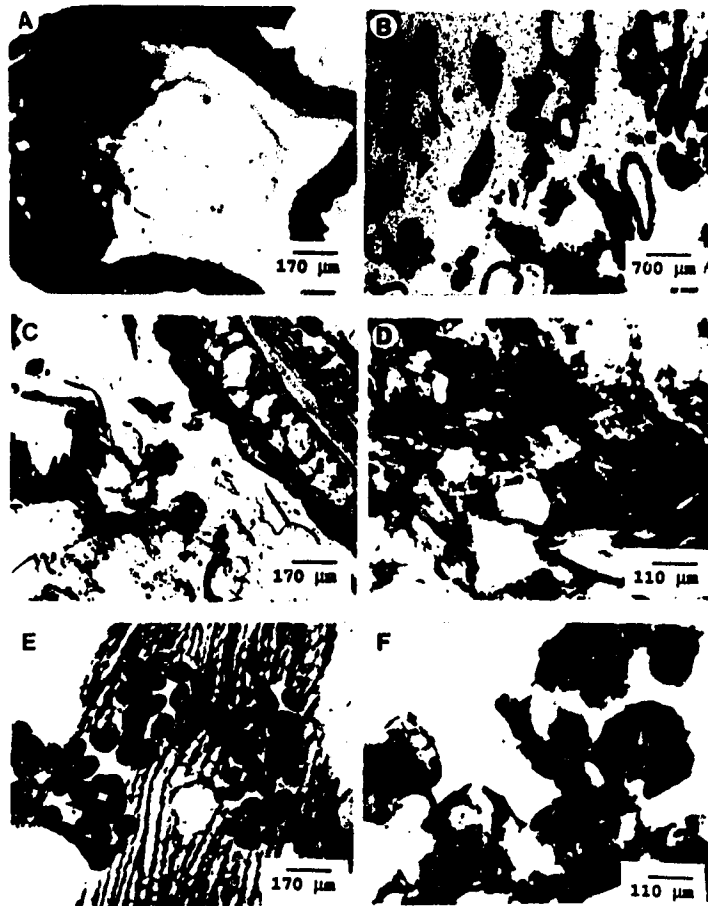


Fig. 4.1-6. Micrographs of pedological features of biological origin (A) polymorphic organic matter where the plant structures are still recognizable (B) tissue residue plant roots (C) remnants of decomposed spruce needle from the Ae horizon (D) network of fungal hyphae in the Bf horizon (E) *Oribatid* droppings in the parenchymatic tissues of plants in the LF layer (F) discrete granular units of *Collembola* and *Enchytraeidea* excrements composed of mixture of organic and inorganic materials.

The presence of other soil fauna is apparent from the observed fecal materials. *Oribatid* mites droppings ($\approx 100 \mu\text{m}$ diameter) often occur as infillings in plant residues (Pawluk, 1985; Babel, 1985) as shown in Fig. 4.1-6e, because they preferentially feed on parenchymatic tissue; but were occasionally observed to be present in places where cell walls were almost completely destroyed. Other fecal material occurs as discrete humigranic units ranging in size from 50-100 μm in diameter (Fig. 4.1-6f); silt size quartz grains are intermixed with a groundmass composed of isotropic organic material characteristic of *Collembola* and *Enchytraeidea* excrements (Pawluk, 1985).

The presence of golden brown algae (Chrysophyceae) is recognized through the identification of spherical siliceous resting spores (stomatocysts) in the leachates collected from the Ae horizons. The spores have a smooth surface about 4.6-5.2 μm diameter with a conical collar about 0.62 μm in height, 1.3 μm at the base and 3.2 μm at the top (Fig. 4.1-7). Chrysophycean algae is a natural colonizer and sensitive indicator of nutrient poor environments (Smol, 1988; Carney and Sandgren, 1983; Duff and Smol, 1988).

4.1.2.7. *Allogenic pedofeatures*

Indurated nodules have been identified as pedofeatures that are inherent in the parent materials. The indurated nodules comprise well oriented argillans around coarse materials (Fig. 4.1-8a) that are of generally larger size and differently packed compared to that of the matrix indicating their disorthic origin (Brewer, 1976). The feature is cemented by organic matter, phyllosilicates and Fe. Iron is identified by the energy dispersive spectrum of the cementing materials (Fig. 4.1-8b). The presence of organic matter is evident from the oxidation of the material upon addition of H_2O_2 . The presence of this unique pedofeature in the C horizons suggests that they maybe remnants of earlier soils which remain as paleofeatures within the sediments that comprise the parent material of the present day soils although a possible sedimentary origin cannot be discounted.

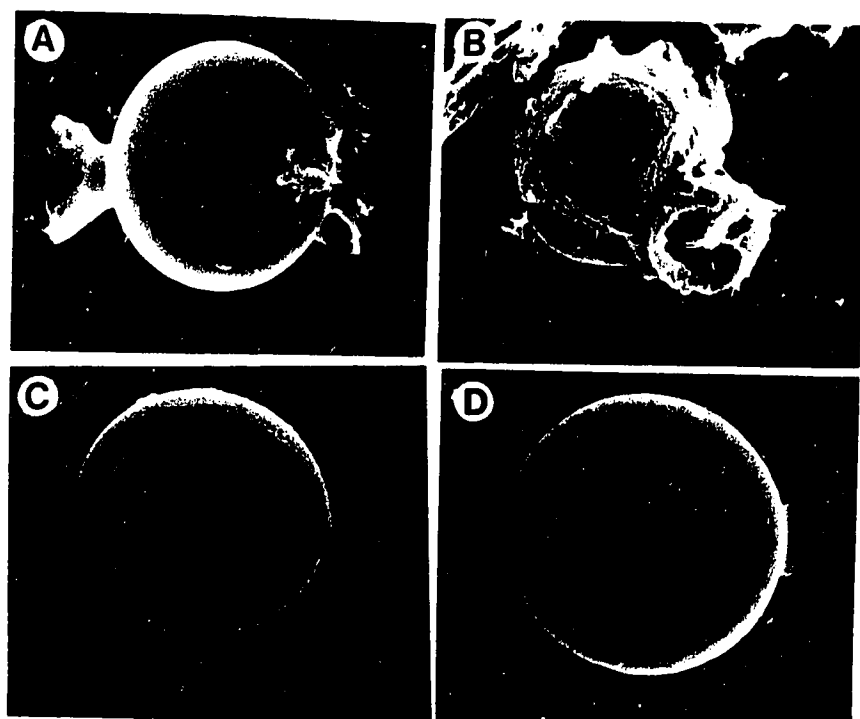


Fig. 4.1-7. Micrographs of the different types of siliceous Chrysophycean stomatocysts observed in the leachates from Ae horizon. (A) smooth, non-ornamented and high collared stomatocyst (B) ornamented type of stomatocyst (C and D) smooth, non-ornamented and low-collared stomatocysts

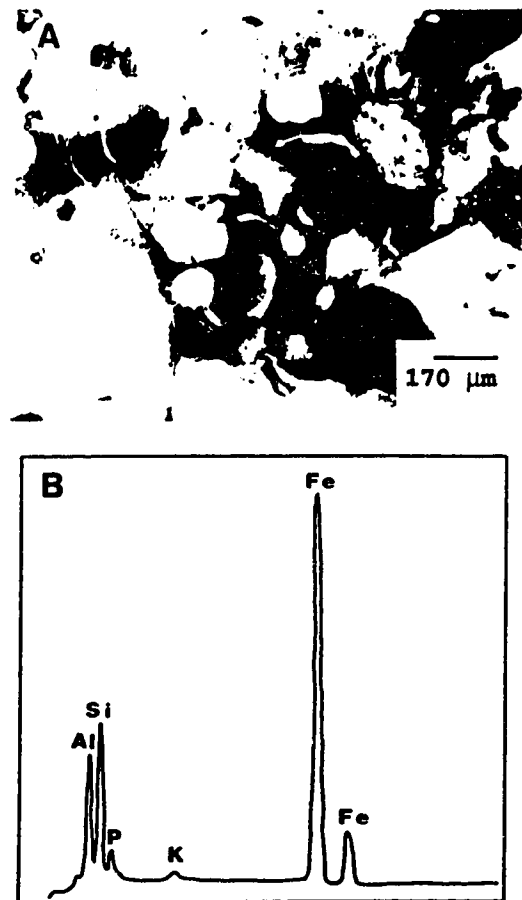


Fig. 4.1-8. Micrographs of allogenic pseudo-sand fraction from the C horizon showing the (A) oriented phyllosilicates (argillans) along the voids composed of Fe, Al, Si, P and K as indicated by the (B) EDS spectrum of the argillans

4.1.2.8. Mobile components

Regardless of season, the amount of Fe, Al, K, Na, Ca and Mg in leachates are enriched from the LFH and Ae horizons as compared to leachates from the Bf horizons (Fig. 4.1-9). Deposition in the Bf horizons reflects the characteristic of a "podzolic signature" as defined by Ugolini *et al.* (1987) and Stoner and Ugolini (1988). The amount of Si in the leachates increases after passing through the Bf horizon and is reported (Farmer, 1982) to reflect the dissolution of deposited imogolite. The decrease in total C and N contents of leachates from the LFH to the Ae and to the Bf horizons suggests that mobile organic materials suffer a similar fate to that of Fe and Al (Table 4.1-8). This is further supported by IR absorption bands of the leachates at 3420 and 1630 (OH water), 2920 and 2860 (assymetric and symmetric stretching of alipathic CH), 2520 (OH carboxyl), 1715 (stretching vibration of C=O), 1600-1650 (aromatic C=C) and 1400 (bending vibrations of δ -OH) cm^{-1} characteristic of fulvic acids (van der Marel and Beutelspacher, 1976). In addition, leachates from the LFH horizons contain lignins as evident from the IR absorption at 1510 (stretching vibration of aromatic C=C), 1225 (stretching vibration of C-O in plane)-1265 (=C-O-C) and 1090 (C-O alcohols) cm^{-1} . Infra red absorption intensities at these band groups were lower in the leachates from the Ae and absent in leachates from the Bf horizons; a similar trend was observed for IR absorption around 1400 cm^{-1} (δ -OH) (Fig. 4.1-10). The decrease in the intensities is believed to reflect the deposition of lignins and phenol-containing organic substances in the Bf horizons.

Table 4.1-8. Total C, H and N from leachates collected in pedon 1, Fall 1988.

	C	H (g kg ⁻¹)	N
LFH	392	40	15
Ae	376	41	17
Bf	239	31	28

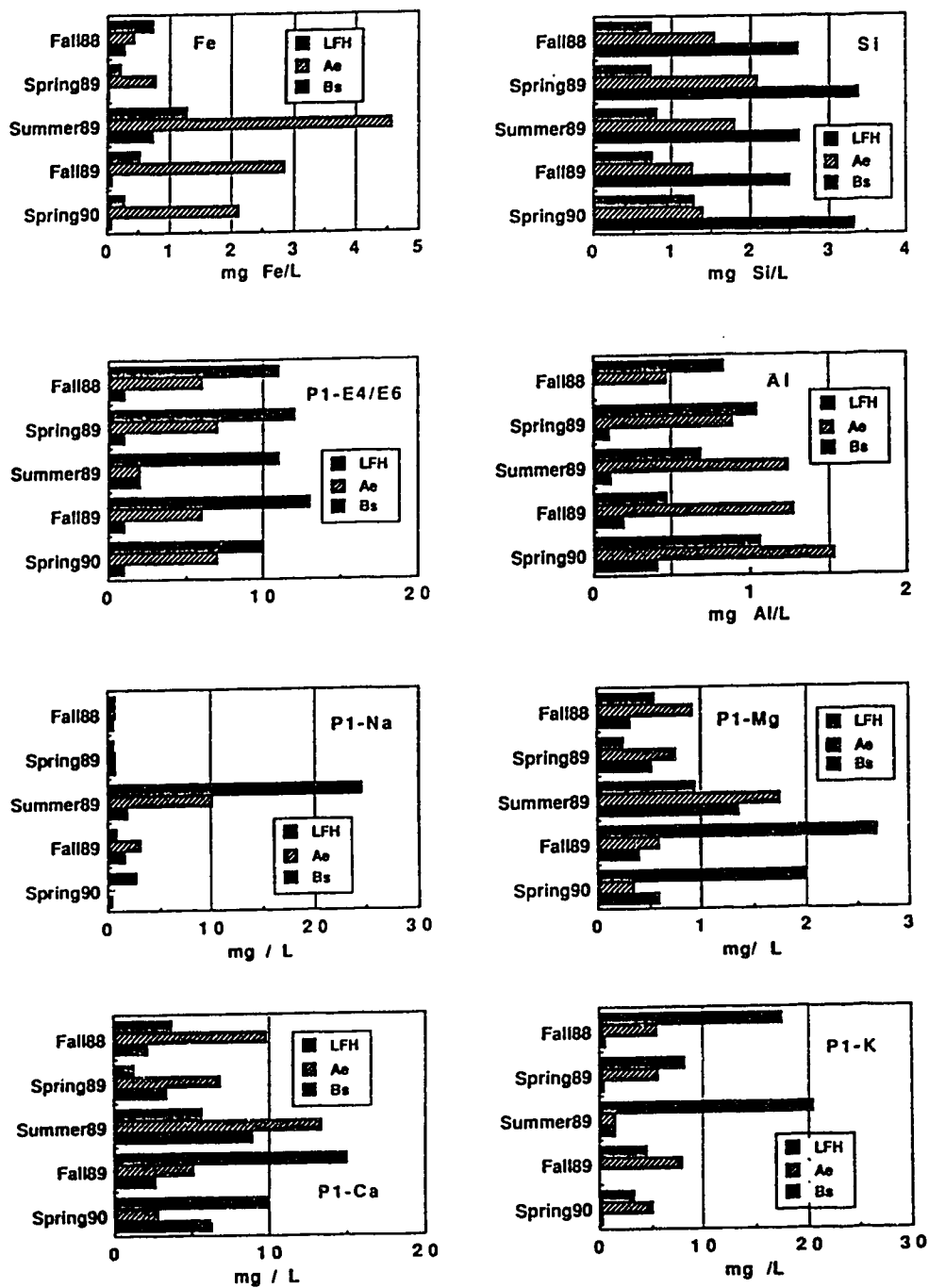


Fig. 4.1-9. Amounts of selected mobile chemical components and E4/E6 ratio in lysimeter leachates of Podzolic soils from Alberta. The "podzolic signature" is indicated by the enrichment of the chemical components in the Ae horizon and their depletion in the Bf horizons.

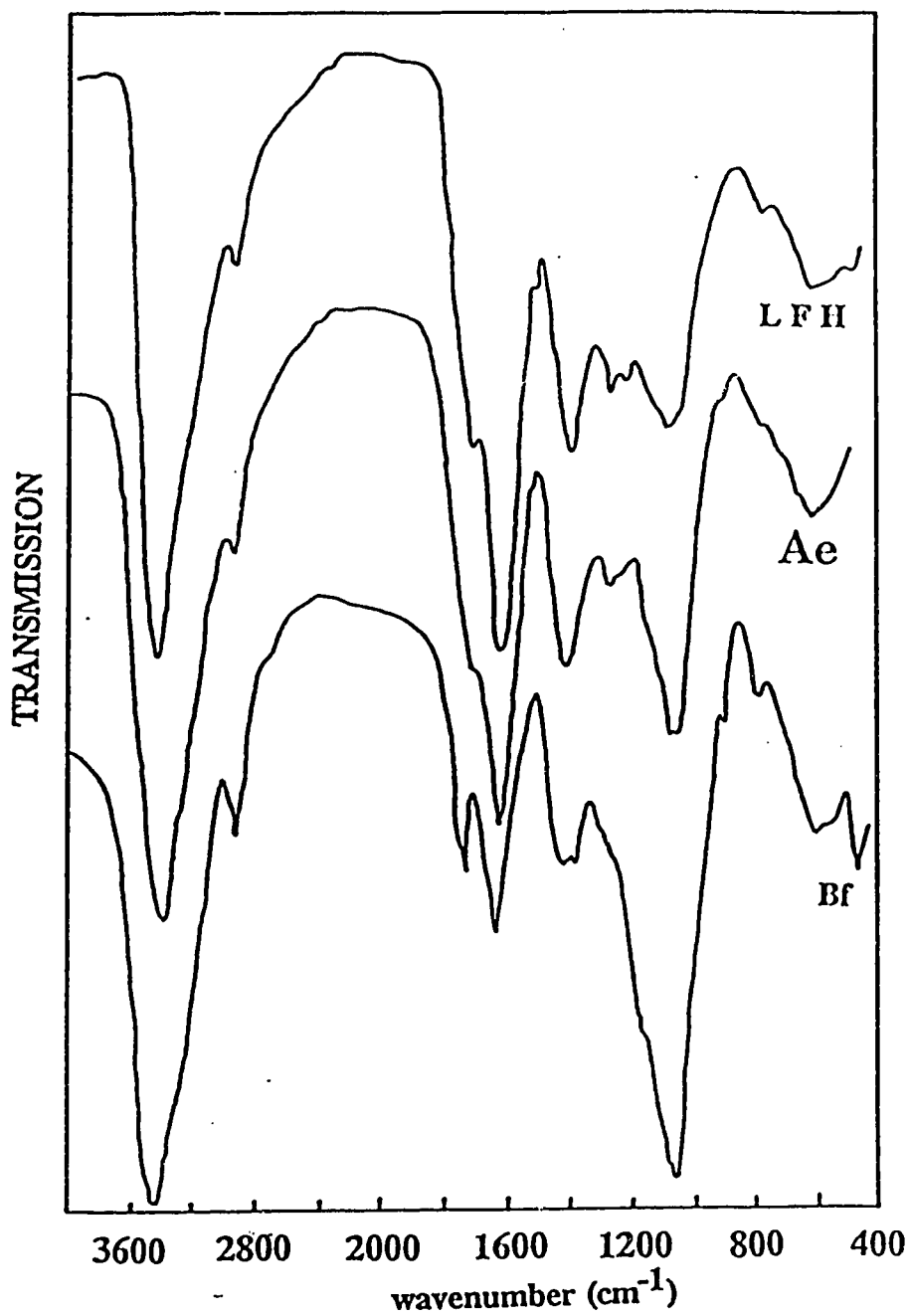


Fig. 4.1-10. Infra red spectra of lysimeter leachates from LFH, Ae and Bf horizons. The absorption bands at 1225-1265 and 1410 cm^{-1} in the LFH and Ae horizons are absent in the Bf and may indicate the immobilization of lignin and phenol-containing organic compounds.

Immobilization of oxalic acid in the Bf horizons is also suggested by its progressive decrease in the leachates from LFH (0.05-0.55 mg L⁻¹) to the Ae (0.13-0.18 mg L⁻¹) and to the Bf horizons (0.02-0.06 mg L⁻¹). Concentration of citric acid shows no definite trend with the following amounts found: 0.02-0.03 mg L⁻¹ in the LFH, 0.04-0.05 mg L⁻¹ in the Ae and 0.04-0.05 mg L⁻¹ in the Bf horizon (Fig. 4.1-11). Ugolini *et al.* (1987) reported that as much as 72% of the organic matter is removed from solution as it passed through the Bf horizon. The amount of PO₄⁻³ and SO₄⁻² decreased while the amount of NO₃⁻ increased after passing the Bf horizons (Fig. 4.1-12).

Powder mounts of freeze-dried components in the leachates show XRD patterns indicative for the presence of feldspar and quartz and SEM observations of feldspar show etched surfaces similar to those reported by Farmer *et al.*

(1985) and presumed to be the result of dissolution action by the organic acids in the eluvial horizon (Fig. 4.1-13d). Mobile crystalline clay components are quartz, mica and vermiculite. Some of the vermiculite appears to be hydroxy interlayered (HIV) as indicated by the failure to expand beyond 1.53 nm upon ethylene glycol solvation and incomplete collapsed to 1.0 nm after 550 °C heat treatment (Fig. 4.1-14).

Table 4.1-9. Fe, Al and Si extracted from hydroxy-interlayered vermiculite from the Bf horizons by six successive extractions with citrate-dithionite (cd) at 100 °C and three extractions with citrate-dithionite-bicarbonate (d) at 75 °C.

sample	Fe		Al		Si	
	cd	d	cd	d	cd	d
	(g kg ⁻¹)					
Pedon 1	12.8	58.2	27.1	55.4	35.3	13.2
Pedon 2	12.1	79.2	15.0	32.9	25.2	12.5
Pedon 3	14.1	118.5	30.3	54.9	32.0	10.5

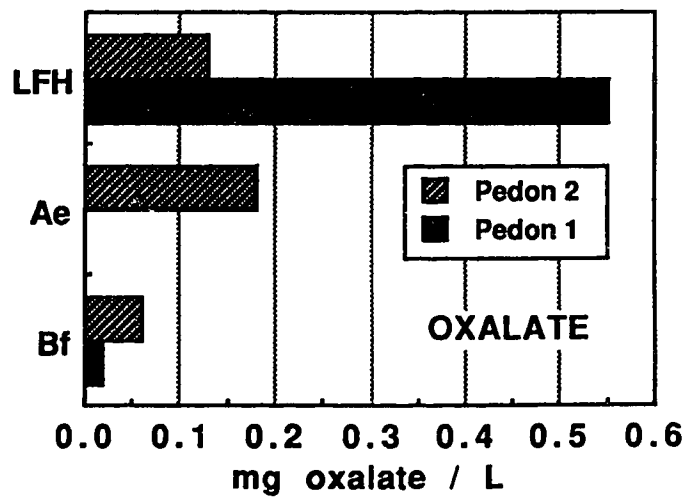
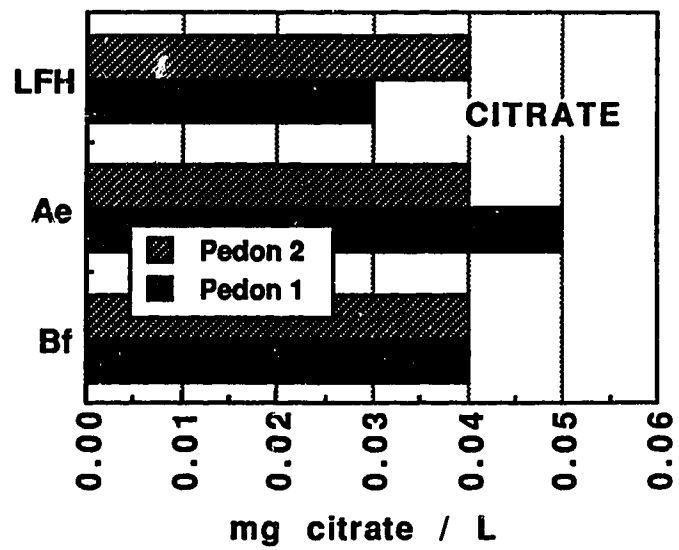


Fig. 4.1-11. Citrate and oxalate content of lysimeter leachates from the different horizons of Podzolic soils.

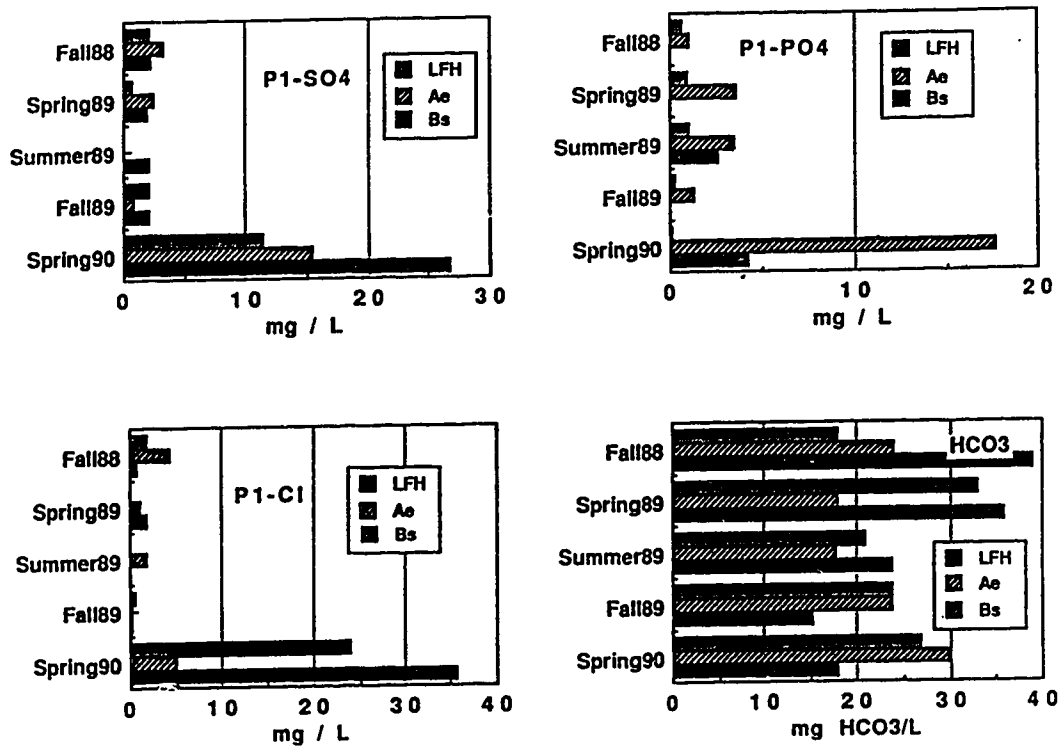


Fig. 4.1-12. Amounts of selected anions in the lysimeter leachates from different horizons of Podzolic soils.

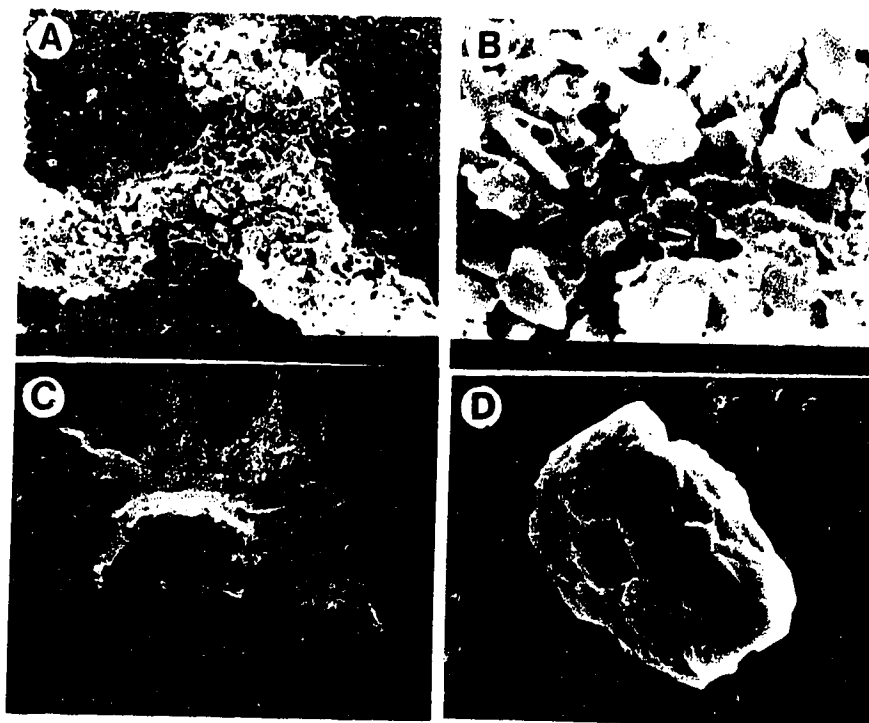


Fig. 4.1-13. Micrographs of the colloidal components of the leachates from the Ae horizon. (A and B) phyllosilicates composed predominantly of hydroxy-interlayered vermiculite (C) globules of ferrihydrite (D) etched sand-size feldspar.

Globules of Fe-rich domains also migrate from Ae horizons (Figs. 4.1-13c) and are probably ferrihydrite because the XRD pattern of air-dried globules shows the absence of crystalline Fe oxides and the heat treatment applied at 750 °C produces XRD reflections around 0.360, 0.268 and 0.256 nm regions indicative of its internal reorganization to form hematite. Similar spheres of ferrihydrite were reported earlier by Eggleton (1987) and Vempati *et al.* (1990). The presence of opaline materials in the colloids is indicated by XRD reflections at 0.312, 0.252, 0.244 and 0.221 nm; these reflections were stable up to 300 °C heat treatment. The strong IR absorption at 1090 cm^{-1} for Si-O-Si stretching vibrations is also diagnostic of their presence. These opaline materials could result from Si concentration brought about by evaporation of soil solution (Shoji *et al.*, 1988) or accumulation of Si from weathering and decomposition of Si-containing organic materials (Kodama and Wang, 1989).

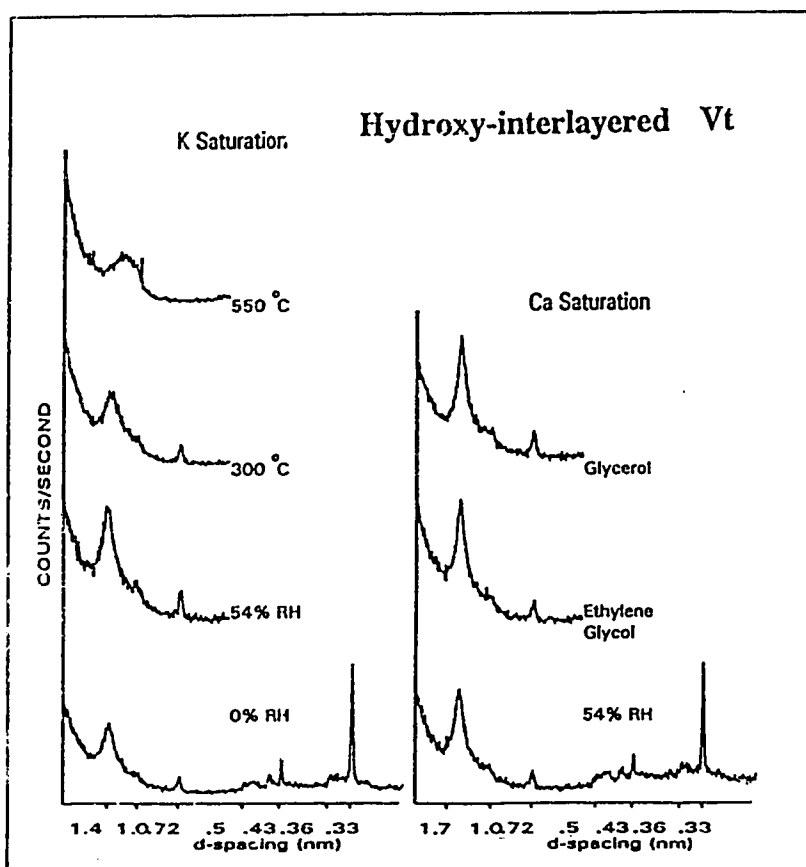


Fig. 4.1-14. X-ray diffractograms of phyllosilicates from the leachates of Ae horizon of Podzolic soils.

Thin layers of whitish sediments in the beaker of the lysimeter from the Ae horizon of pedon 1 are mainly quartz and a component showing IR absorption bands around 340, 425, 580, 970, 1630 and 3470 cm^{-1} indicative of imogolite (Fig. 4.1-15). The material is similar to the white coatings identified earlier on the surfaces of several goethite, feldspar and quartz grains.

4.1.3. *The pedogenesis of microstructures*

Development of microstructures extending from the Ae to the matrix and indurated nodules in the Bf horizon illustrate different stages in the progressive accumulation of the basic soil components in the Bf horizons of the soil sola under study. The observed RDPs of the soil components form the chlamydic sequence described by Pawluk (1983) and Brewer and Sleeman (1988) where the soil fabric evolves from bare coarse-members (orthogranic or monic) to coated coarse-members (matrichlamydic or chitonic) to coarse-members embedded in the fine material (porphyric). Monic and chitonic soil fabrics are attributes of the eluvial Ae horizons while porphyric is characteristic of the matrix and indurated nodules of the illuvial Bf horizons. In coarse textured soils similar to those of the present study, the sequence results from dissolution, migration and accumulation of soil components from eluvial to illuvial horizons (Pawluk, 1983).

The eluvial layers are the organic and Ae horizons where soil fauna produce oxalic, citric and, indirectly, fulvic and other organic acids responsible for the accelerated congruent weathering of chlorite, mica, feldspar and lithogenic Fe nodules (Farmer *et al.*, 1985; Robert and Berthelin, 1986; Tongokonov *et al.*, 1987; Ugolini and Dahlgren, 1987). The functional groups of these acids also contribute to the migration of liberated metals in the form of chelates in the process of podzolization (Ponomareva, 1969; De Coninck, 1980; Duchaufour, 1982; Vance *et al.*, 1985). The dominance of goethite over hematite further points to the presence of organic ligands in the system because the latter favors formation of goethite due to its competitive tendency for extractable Fe. This inhibits the formation of ferrihydrite, and subsequently hematite (Schwertmann, 1985; Cornell *et al.*, 1989a,b). Aluminum present in Fe nodules and as X-ray amorphous Al-rich coatings may have similarly moved together with Fe and organic matter through podzolization. This is shown by the higher amount of Fe in the leachates from Ae horizons where LFH was not removed compared to leachates collected from the Ae after the LFH was scraped off (Fig. 4.1-16). Oxalate and citrate identified in the leachates are examples of these organic ligands responsible for podzolization. Anderson and Bertsch (1988) reported

that the Al-oxalate formation is instantaneous with $k_f = 0.001\text{M}^{-1}\text{s}^{-1}$ and even faster for the citrate so that k_f could not be measured.

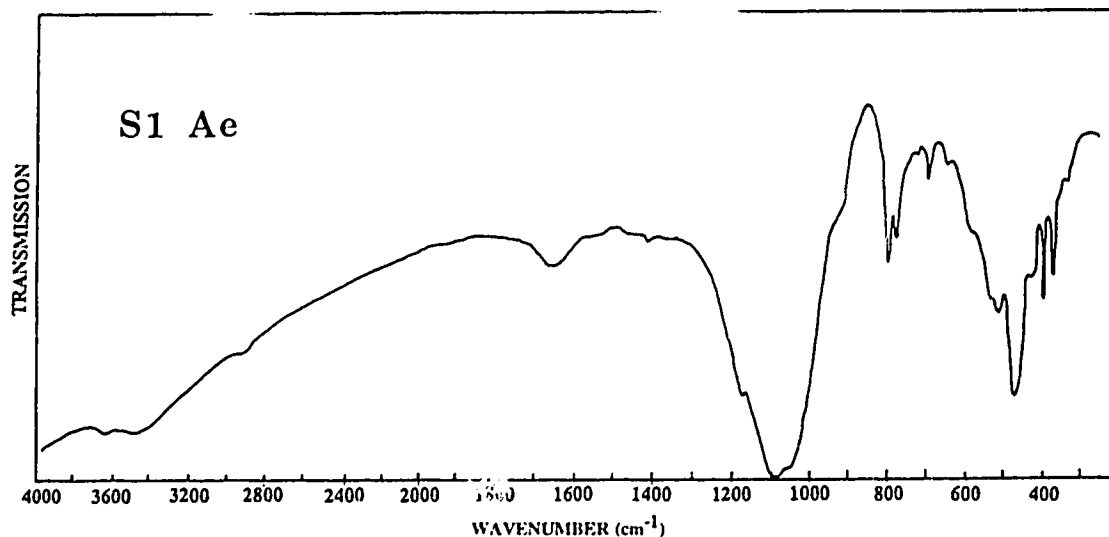


Fig. 4.1-15. Infra red spectrum of whitish sediments in the lysimeter of Ae horizon in pedon 1.

Lessivage is another principal mode of colloidal movement. The ubiquity of fine quartz in the clay coatings, Fe-nodules, and its presence as colloidal components in the leachates probably reflects a physical translocation because peptization of quartz grains is not likely due to its limited number of negative charges. Such physical translocations had been reported earlier as being responsible for the transport of particulate goethite in Podzolic soils (Milnes and Farmer, 1987). The transport of mica and vermiculite are mainly through the process of lessivage, reported as the main soil forming process in Alfisols (Bullock and Thompson, 1985; Howitt and Pawluk, 1985). The high amounts of Fe and Al in the interlayer of HIV merits consideration of the possibility that lessivage can indirectly transport liberated Fe and Al on the assumption that those interlayer oxides are pedogenic in origin. The threshold-controlled subsurface translocation process (Stoner and Ugolini, 1988) is basically a lessivage process that is mediated by episodic high pulses of migrating soil water.

The reorganization of goethite to larger nodules is likely the result of Fe moving as Fe^{+2} . Reduction of lithogenic goethite nodules is possible through intense microbial activity; by polyphenols from leaf litter (Bloomfield, 1957; Coulson *et al.*, 1960) and existence of hydromorphic conditions below the leaf litter during certain times of the year.

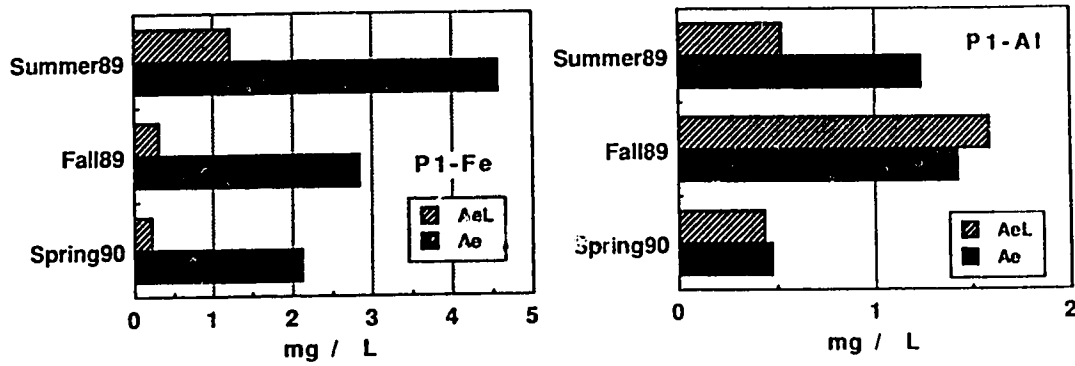


Fig. 4.1-16. Amounts of Fe and Al in the leachates of the Ae horizon before (Ae) and after (AeL) removal of the leaf litter.

The Bf horizon is the accumulation zone. Organic matter and organo-metallic complexes are immobilized wherever they are rendered hydrophobic due to reduction of negative charges through chelation of more metals, higher pH, changes in ionic strength and electrical conductivity (De Coninck, 1980). The higher pH measured in Bf horizon could probably result to this type of accumulation; however, surface reaction is believed to be another dominant mechanism of accumulation as shown by the presence of organics in goethite nodules.

Large areas for surface reaction are provided initially by the detrital goethite nodules that may also serve as seeds for the oxidation of mobile Fe^{+2} to goethite (Schwertmann, 1985). This process is believed to be responsible for the reorganization of Fe to larger goethite nodules. Mobile organic matter and organo-metallic complexes can then be chemisorbed onto the type A OH functional groups of goethite through inner-sphere, metal-carboxylate bonds either by unidentate, bidentate or bridge complexes (Collman *et al.*, 1987; Kung, 1989; Kung and McBride, 1989). Such mechanisms are also responsible for the formation of dispersed goethite and ferrihydrite associated with phyllosilicates in infillings and coatings. The role of Fe-oxides as absorbent media for benzoates, oxalate, salicylate and other organic acids by chelate

formation are well documented in the literature (Parfitt *et al.*, 1977; Cornell and Schindler, 1980; Zeltner *et al.*, 1986; Jensen, 1988; Kung and McBride, 1989). Imogolite is also adsorbed on the surface of goethite nodules and consequently acts as another medium for the precipitation of mobile organo-metallic complexes as originally suggested by Farmer (1982).

The initial formation of argillans is believed to be a physical surface reaction either by electrostatic attraction or by development of van der Waals forces between clays and quartz, feldspar and goethite nodules especially in pits and cracks. Fungal activity through the net-like configuration of hyphae are also presumed to establish initial conditions for accumulation of clays by providing a framework around coarse components. Ensuing layers of argillans are formed when percolating water carrying peptized clays are filtered out and deposited into the soil mass (McKeague, 1983).

4.1.4. Summary

The natural anisotropy and dynamic characteristics of the Podzolic soils of Alberta were investigated with the techniques of micromorphology in combination with lysimeter studies. The different microstructures identified within the profiles of Podzolic soils from Alberta represent the various microenvironments which in turn define the dominant pedogenetic processes when interpretation is based on data for mobile components.

The evolution of microstructure starts from monic or orthogranic RDP (grains are uncoated) in the Ae horizon to chitonic or chlamydic RDP (grains are fully or partially coated) in the matrix of the Bf horizon and to porphyric RDP (grains embedded in fine mass) in the nodule of the Bf horizon. This corresponds to the chlamydic sequence (Pawluk, 1983; Brewer and Sleeman, 1988) and denotes migration and accumulation.

Results from lysimeter studies show that the mobile phases are generally enriched with organic matter, anions and cations including Fe and Al in the LFH and Ae horizons and are greatly impoverished after passing through the Bf horizon. However, Si exhibits an opposite trend where it is enriched in leachates from the Bf horizon. Lignins are arrested preferentially in the Bf horizon when compared to other organic compounds.

The colloidal components of the leachates are clay particles composed of quartz, mica and vermiculite including HIV; stomatocysts of Chrysophycean species of algae; fine sand size quartz and feldspar; and Fe-rich globules of ferrihydrite.

The processes involved in the migration are podzolization which is responsible for the eluviation of organic matter and organo-metallic complexes of Al and Fe; and lessivage which is responsible for the mobilization of phyllosilicates, quartz and feldspar. Colloidal components of the leachates consist of globular Fe-rich domains, opaline materials, imogolite and very fine quartz and feldspar.

The presence of detrital goethite nodules in the C horizons and their reorganization to larger goethite nodules in the Bf horizon serves as the primary adsorbing medium for mobile organic matter and organo-metallic complexes through the highly reactive type A OH-group present on their surfaces. Imogolite can also be adsorbed onto the surfaces of goethite nodules.

Fungal hyphae provide the framework for the accumulation of fine materials around the coarse components. Hydroxy interlayered vermiculite is an important sink for liberated Fe and Al.

4.2. The nature of nodules from Podzolic soils of Alberta

4.2.1. Introduction

A common pedological feature in the soils under study is the presence of indurated nodules in the Bf horizon. These nodules vary in size from less than a centimeter to about 20 cm in diameter. The term nodules as used in this paper refers to pedological features unrelated to voids (Bullock *et al.*, 1985). This definition is similar to the concept of glaebole as proposed by Brewer (1976). Microscopically, a glaebole "exhibits a greater concentration of some constituents and/or a difference in fabric compared to the enclosing material" (Brewer, 1976).

Genetic implications of glaebole formation include accretionary processes occurring *in situ* such as thickening of the fine material coating the coarse materials, the formation of aggregates between coarse materials and void infillings by fine materials. The nature of the fine materials, however, is still subject to discussion. According to the proponents of the fulvate theory (De Coninck, 1980), monomorphic coatings on the quartz grains are made up primarily of organo-metallic complexes. Farmer *et al.* (1980) on the other hand claims that less-ordered allophane and imogolite-like alumino-silicates are the principal constituents of the coatings. Milnes and Farmer (1987) stated that gibbsite can also form coatings on the quartz grain.

This section attempts to determine the nature, origin and formation of indurated nodules in the Bf horizons of Podzolic soils in Alberta. Specifically, the objective of this inquiry is to characterize the nature, spatial arrangement and distribution of the minerals in the nodules and Bf horizon matrix. These characteristics and the role of biological activity will be evaluated to clarify the nature and formation of the nodules.

4.2.2. Results and Discussions

4.2.2.1. Morphological properties of the Bf horizons

Field morphological descriptions of the Bf horizons of the three pedons are summarized in Table 4.2-1. All Bf horizons have bright brown (7.5YR 5/6-8, moist) color, sandy texture, single grain structure, and are very friable. Medium to coarse nodules ranging in colors from reddish brown (5YR 4/6) to bright brown (7.5YR 5/6) are present. The B horizons meet the morphological requirements for Bf as defined in the Canadian System of Soil Classification (Canada Soil Survey Committee, 1978) but the Bf of pedon 1 is too thin to meet the 10 cm depth requirement for a podzolic B; however, they all meet the criteria for spodic B of the International Committee on the Classification of Spodosols (ICOMOD, 1990).

4.2.2.2. Chemical and physical properties of the nodule and Bf matrix

Selected chemical and physical properties of the Bf horizons and nodules are listed in Table 4.2-2. Values for pH and organic carbon show no marked differences between nodules and matrix; they are both mildly acidic and contain 4-6 g organic carbon·(kg soil)⁻¹. Bulk density and clay content are consistently higher in the nodules as compared to the Bf horizons. The frequency distribution for the various sand size fractions are similar for nodules and the soil matrix sampled from within the same soil horizon (Fig. 4.2-1). The 250-100 μm size sand fractions dominate in pedons 1 and 3, while finer fractions (100-53 μm) constitute the major portion of sand in pedon 2. These similarities suggest a common parent material for the nodules and the matrix of the Bf horizons and are evidence for an authigenic origin of the nodules.

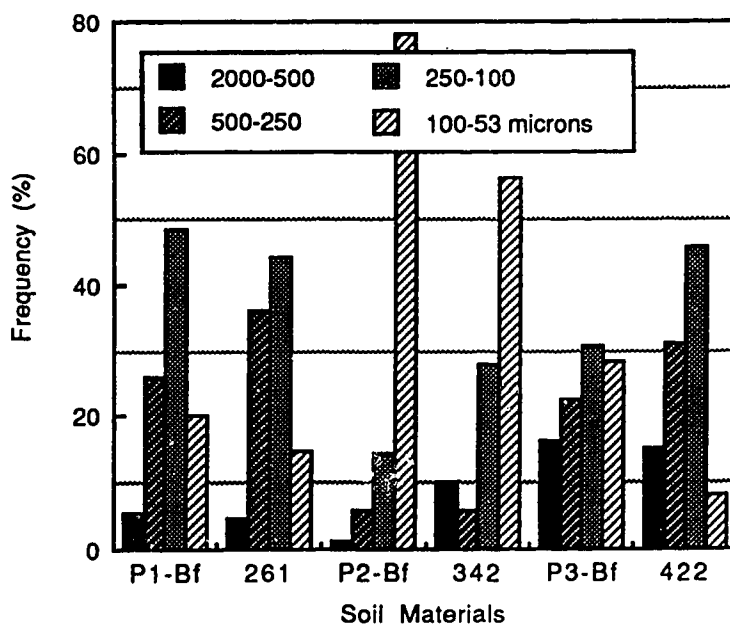


Fig. 4.2-1. Class distribution of the different sand fractions in the Bf matrixes and Bf nodules of Podzolic soils from Alberta.

The nature of the various forms of extractable Fe and Al are reported in Table 4.2-3. Ammonium-oxalate extractable Fe (Fe_o) constitutes a large part (approximately 700 g·(kg free Fe)⁻¹) of the extractable Fe. The Fe_o/Fe_d ratio is about 0.76. The remaining extractable Fe (300 g·(kg free Fe)⁻¹) is organically bound Fe extractable with Na-pyrophosphate (Fe_p) and Fe present as higher ordered Fe oxides extractable with dithionite-citrate-bicarbonate (Fe_d). Extractable Al shows distribution patterns similar to that for Fe; more than 700 g·(kg free Al)⁻¹ is extractable with NH₄-oxalate (Al_o). There is no marked difference in content of extractable Fe and Al between the nodules and the matrix of the Bf horizons. The lower content of pyrophosphate extractable Fe and Al compared to the quantities extractable with NH₄-oxalate suggests only a small fraction of Fe and Al is tied up with the organic fraction relative to that present as less-ordered Fe or Al oxyhydroxides.

Table 4.2-1. Field morphology of the Bf horizon of some Podzolic soils of Alberta.

Horizon	Depth (cm)	Description
<u>Pedon 1. Eluviated Dystric Brunisol</u>		
Bf1	12-20	Bright brown (7.5YR 5/6 m); loamy sand to sand; single grain; very friable to loose; medium nodules (7.5YR 5/6 m) randomly present in the horizon; gradual wavy boundary
<u>Pedon 2. Orthic Humo-Ferric Podzol</u>		
Bf1	9-21	Bright brown (7.5YR 5/8 m); sand; very weak granular to single grain; very friable; nodules (5YR 4/6 m) about 0.5 cm diameter are present in the lower 2 cm of the horizon; gradual wavy boundary
<u>Pedon 3. Orthic Humo-Ferric Podzol</u>		
Bf1	10-20	Bright brown (7.5YR 5/8 m); sand; very weak granular to single grain; very friable; medium and coarse nodules (5YR 4/8 m) in upper 2 cm; gradual wavy boundary

Table 4.2-2. Color, pH, bulk density, total Carbon, and particle size distribution of selected nodules from Podzolic soils of Alberta.

	color (moist)	pH H ₂ O	Db CaCl ₂ (Mg m ⁻³)	Total C (g kg ⁻¹ soil)	Sand	Silt	Clay
<u>Pedon 1: Eluviated Dystric Brunisol</u>							
Bf1	7.5YR 5/6	5.6	4.9	1.28	4	810	166 25
N261	7.5YR 5/6	5.5	4.8	1.38	5	876	81 43
N271	7.5YR 5/6	5.2	4.9	nd	2	917	55 28
<u>Pedon 2: Orthic Humo-Ferric Podzol</u>							
Bf1	7.5YR 5/8	5.7	4.8	1.14	6	681	245 75
N341	5YR 4/6	5.7	4.6	nd	16	665	237 97
N342	5YR 4/6	5.8	5.1	1.47	4	808	120 72
N343	5YR 4/6	5.5	4.9	nd	7	752	144 104
<u>Pedon 3: Orthic Humo-Ferric Podzol</u>							
Bf1	7.5YR 5/8	5.1	4.5	1.26	5	879	61 59
N422	5YR 4/8	4.9	4.3	1.45	6	927	27 46

Table 4.2-3. Na-pyrophosphate (p), NH₄-oxalate (o) and dithionite-citrate-bicarbonate (d) extractable Fe, and Al from nodule and soil matrix (Bf) of Podzolic soils from Alberta.

sample	Fep	Alp	Feo	Alo	Fed	Ald	Feo/d	Alo/d
(g kg ⁻¹ soil)								
<u>Pedon 1: Eluviated Dystric Brunisol</u>								
Bf	2	3	9	4	12	7	0.76	0.64
N261	2	3	4	5	6	5	0.64	0.88
N271	1	1	2	3	5	3	0.32	0.85
<u>Pedon 2: Orthic Humo-Ferric Podzol</u>								
Bf	4	4	11	6	15	7	0.76	0.79
N341	4	4	9	6	11	7	0.82	0.91
N344	3	4	11	6	13	7	0.83	0.83
N3402	5	2	14	3	21	4	0.68	0.86
<u>Pedon 3: Orthic Humo-Ferric Podzol</u>								
Bf	3	3	10	5	14	8	0.67	0.66
N421	4	6	9	8	13	9	0.75	0.90
N422	3	3	5	5	8	6	0.70	0.92

4.2.2.3. Micromorphology

The abridged micromorphological descriptions of the nodules and the matrix of the Bf horizons are tabulated in Tables 4.2-4a and 4b. The nodules and soil matrix have an apedal grain type of microstructure. Grain type covers a range of microstructures in which the composition is almost entirely made up of sand grains and where the fine materials either coat, bridge or are present as aggregates in between the sand grains (Bullock *et al.*, 1985). The soil matrix generally has pellicular (coated) microstructure. Nodules are dominantly bridged grains with minor intergrains micro-aggregate (aggregated) and pellicular microstructures (Fig. 4.2-2a). The porosity is dominated by simple and compound packing voids with minor amounts of vughs and channels.

The coarse/fine (c/f) limit (Stoops and Jongerius, 1975), for the basic components in this study is set at 5 μm which imply materials less than 5 μm are considered as fine and greater than 5 μm as coarse components. This definition of coarse components and fine components is similar to the concept of f-members and f-

matrix, respectively as outlined by Brewer (1976) and Brewer and Sleeman (1988). Qualitatively, the coarse fractions referred to here are the sand, silt and the pseudo-sand fractions while the fine components are basically the fine silt and clay size fractions. The pseudo-sands are composed of fine sand and silt particles aggregated together by dark isotropic material composed of organic matter, Fe, Al, Si and low amounts of K and Ti. The pseudo-sands are present in the entire profile including C horizon indicating their allogenic origin. Figure 4.2-2b shows the typical organization within a pseudo-sand particle.

Table 4.2-4a. Abridged micromorphology of Bf horizon of Podzolic soils from Alberta.

	Pedon 1	Pedon 2	Pedon 3
<u>Microstructure</u>			
type	apedal (pellicular)	apedal (pellicular)	apedal (pellicular)
porosity (%)	30	25-30	30
<u>Basic components</u>			
c/f (ratio)	50 μ m (6:1)	50 μ m (5:2)	50 μ m (5:2)
RDP	chitonic	chitonic with some part enaulic	chitonic
coarse	Qtz(95), Fd(3) Ch+Zr(2)	Qtz(85), Fd(5) Mi(3), Ch+Hb+Zr(2)	Qtz(95), Fd(2)
fine	no fine material (associated to grains as coatings)	brownish, speckled b-fabric	brownish, speckled b-fabric
<u>Pedofeatures</u>	typic clay coatings	typic clay coatings, impregnative nodules	typic clay coatings, impregnative nodules
	polymorphic	polymorphic	polymorphic
<u>Organic</u>			

RDP-related distribution pattern; Qtz-quartz; Fd-feldspars, O-opaques; Ct-chert; We-weathering minerals; PL-plain light; (90) - %

Table 4.2-4b. Abridged micromorphology of nodules from Podzolic soils of Alberta.

	sample #261	sample #341	sample #4231
Microstructure type	apedal (pellicular, bridged grain and intergrain microagg.)	apedal (pellicular, bridged grain and intergrain microagg.)	apedal (pellicular, bridged grain and intergrain microagg.)
porosity (%)	40	20	15
Basic components			
c/f (ratio)	5 μ m (5:1)	5 μ m (5:3)	5 μ m (6:2)
RDP	mainly open porphyric some part chitonic	mainly open porphyric some part chitonic	mainly open porphyric some part chitonic
coarse	Qtz(90), Fd(2) Ct+O(8)	Qtz(95), Fd(2) O+We(3)	Qtz+Ct(90), Fd (2), O(5)
fine	yellowish to reddish brown in PL and mosaic speckled to undiffer. b-fabric	yellowish to reddish brown in PL and mosaic speckled to undiffer. b-fabric	reddish brown in PL with mosaic speckled to undiffer. b-fabric
pedofeatures	typic clay coatings on Qtz/Fd, infillings of clay and Fe- org complexes	typic clay coatings on Qtz/Fd, infillings of clay and Fe- org complexes	typic clay coatings on Qtz/Fd, infillings of clay and Fe- org complexes
organic	polymorphic	polymorphic	polymorphic

Qtz-quartz; Fd-feldspars; O-opaques; Ct-chert; We-weathering minerals; PL-plain light; (90)-%

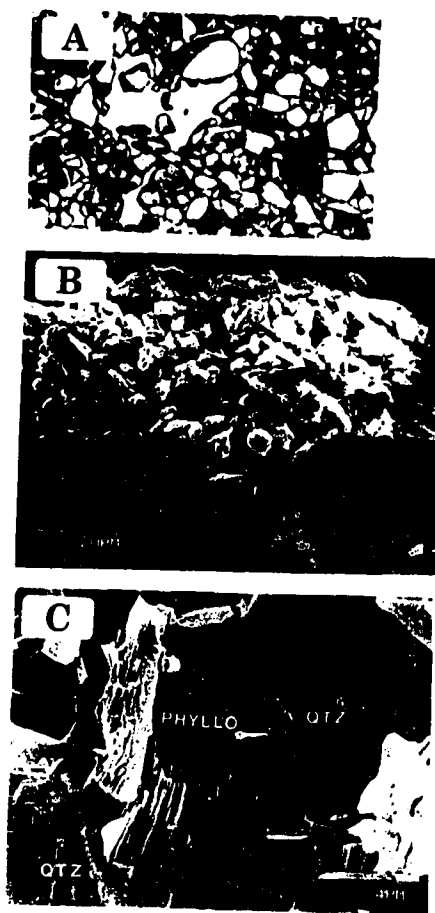


Fig. 4.2-2. Micrographs of (A) pellicular microstructure, 1 cm = 420 μm ; (B) pseudo-sand fraction and (C) phyllosilicate in quartz grains from the Bf nodules.

The related distribution pattern (RDP) of the coarse and fine fractions in the nodules and the soil matrix differ in that nodules have a porphyric RDP while the matrix has mainly chitonic with patches of enaulic RDP. The porphyric RDP is characterized by coarse material embedded in the dense groundmass of fine material while the latter two are best described by the presence of fine materials as thin incomplete coatings on the coarse materials and as aggregates in between the coarse materials, respectively (Bullock *et al.*, 1985). The observed RDPs are members of the chlamydic sequence which reflects the evolution of the soil fabric from the bare f-members (orthogranic or monic) to coated f-members (matrichlamydic or chitonic and enaulic) to f-members embedded in the fine material (porphyric) as proposed by Pawluk (1983) and Brewer and Sleeman (1988).

In coarse textured soils as in the case of the present study, the early stage of bare f-members is characteristic of eluvial horizons and the later stage of zones of porphyric material is characteristic of illuviation (Pawluk, 1983). Porphyric RDP has been reported earlier where the podzolic B exhibits a non-friable consistency (De Coninck and McKeague, 1985; Milnes and Farmer *et al.*, 1987) and is interpreted to reflect the accumulation zone in the podzolization process.

The most common pedological features observed in both the soil matrix and nodules are typic clay coatings on coarse members. Figure 4.2-2c shows an intricate association where the oriented clays fill the cavities in the quartz grains. Infillings of isotropic materials in voids are also observed and are better developed in the nodules than in the soil matrix. Except for nodules, there are no other pedofeatures observed in the soil matrix that are unrelated to voids.

4.2.2.4. Mineralogy of the coarse components in the nodules

Based on optical and XRD analyses, the mineral composition of the sand and silt fractions comprises quartz, feldspar and chlorite. X-ray diffraction patterns of sand and silt fractions have dominant reflections at 0.426 and 0.333 nm spacings indicating the predominance of quartz. Estimated visually from the thin section counts, quartz including chert fragments, constitute about $900 \text{ g} \cdot (\text{kg coarse components})^{-1}$ in the nodules. Their diameters range from 5-600 μm in pedons 1 and 2 and from 5-2000 μm in pedon 3. Feldspar comprise about $20\text{-}50 \text{ g} \cdot (\text{kg coarse components})^{-1}$ with diameter varying from 300-1000 μm . Alteration to highly birefringent secondary minerals such as fine-grained mica is a common feature of the feldspar. Albite is the major feldspar present and XRD reflections for chlorite correspond to the Mg-bearing clinochlore species. Microscopically, the greenish chlorite show anomalous blue interference

colors with distinct alteration most likely to Fe-oxyhydroxides. Minor components of the sand and silt fractions evident from the XRD patterns are anthophyllite, garnet, sillimanite and lithogenic hercynite which represent the main minerals in the heavy mineral suite.

The mineralogy of the fine sand and silt fractions within the pseudo-sand is similar to that of sand and silt fractions in the nodule. Opaque materials are also part of the coarse components. The pseudo-sand and the opaques make up about 30-50 g·(kg coarse components)⁻¹.

4.2.2.5. Mineralogy of the fine components in the nodules

Fine components in this study are primarily clay size particles composed of approximately 900 g kg⁻¹ phyllosilicates and quartz; and the remainder is partitioned between organic matter and various oxyhydroxides of Fe and Al. The latter is a general term encompassing the different oxyhydroxide forms of Fe, Al, Si and their possible combinations excluding layer lattice clays.

The phyllosilicates are dominated by hydroxy interlayered vermiculite (HIV), chlorite with small amounts of vermiculite (Vt), mica, kaolinite and quartz in all the samples investigated. X-ray diffractograms in Fig. 4.2-3 show the behavior of the coarse and fine clays as affected by different cation saturation, organic solvation, heating and relative humidity (RH) treatments. In fine clays, chlorite is indicated by the 1.400 nm reflection at 0 and 54% RH for both K and Ca-saturated clays and lack of expansion with either glycerol or ethylene glycol solvation. The persistence of the 1.400 nm peak upon heating to 550 °C, however, was not observed. After treating the clay samples with 0.33M Na-citrate (C), the mineral partially expanded to 1.6nm upon ethylene glycol solvation but not with glycerol and further-treatment with citrate-dithionite (CD) caused the mineral to completely expand to 1.60 nm upon EG-solvation. (Figs. 4.2-3 and 4.2-4). This suggests that the interstratified 2:1 clay is Vt. Estimates of Vt present after the CD treatment following the method of Alexiades and Jackson (1965) is approximately 160 g·(kg clay)⁻¹. Similar chloritized 2:1 clays are commonly identified in Podzols elsewhere (De Coninck and Righi, 1983; Wada *et al.*, 1987; Cabrera-Martinez *et al.*, 1989; Takahashi *et al.*, 1989).

Measurements of Fe, Al, and Si removed from the interlayer of HIV by six successive CD extractions showed that with time, Fe and Al content generally decreases from about 2.0 g kg⁻¹ and 4.0 g kg⁻¹, respectively to less than 1.0 g kg⁻¹; Si however, remains almost constant at about 4.0 g kg⁻¹ (Table 4.2-5). This suggests that Fe and Al are extracted from the interlayer and that the successive treatments also

attack the Si-tetrahedral sheet (Matsue and Wada, 1988) as reflected in the nearly constant amount of Si removed.

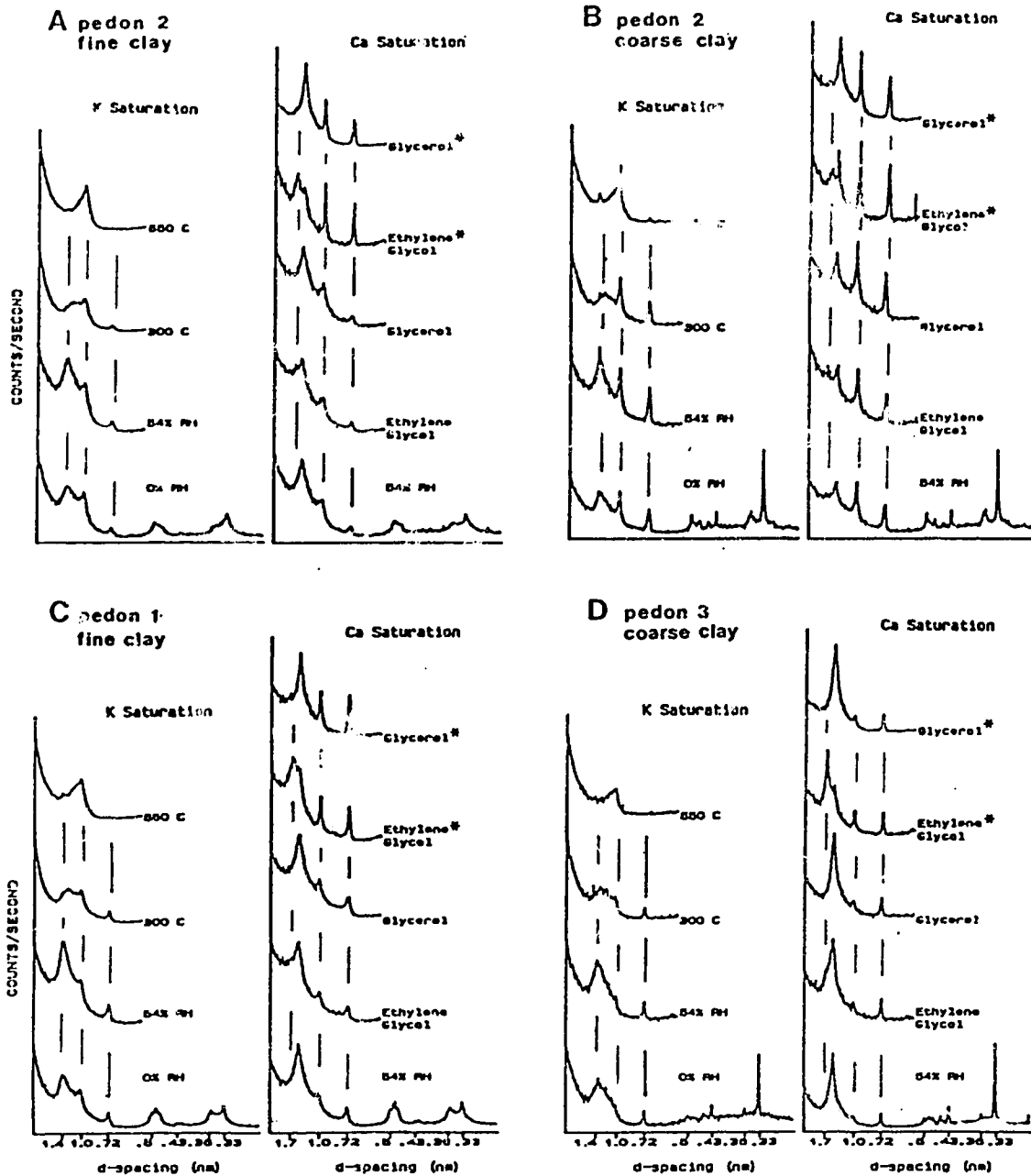


Fig. 4.2-3. X-ray diffractograms of selected clays from nodules of Podzolic soils from Alberta (*-citrate treated)

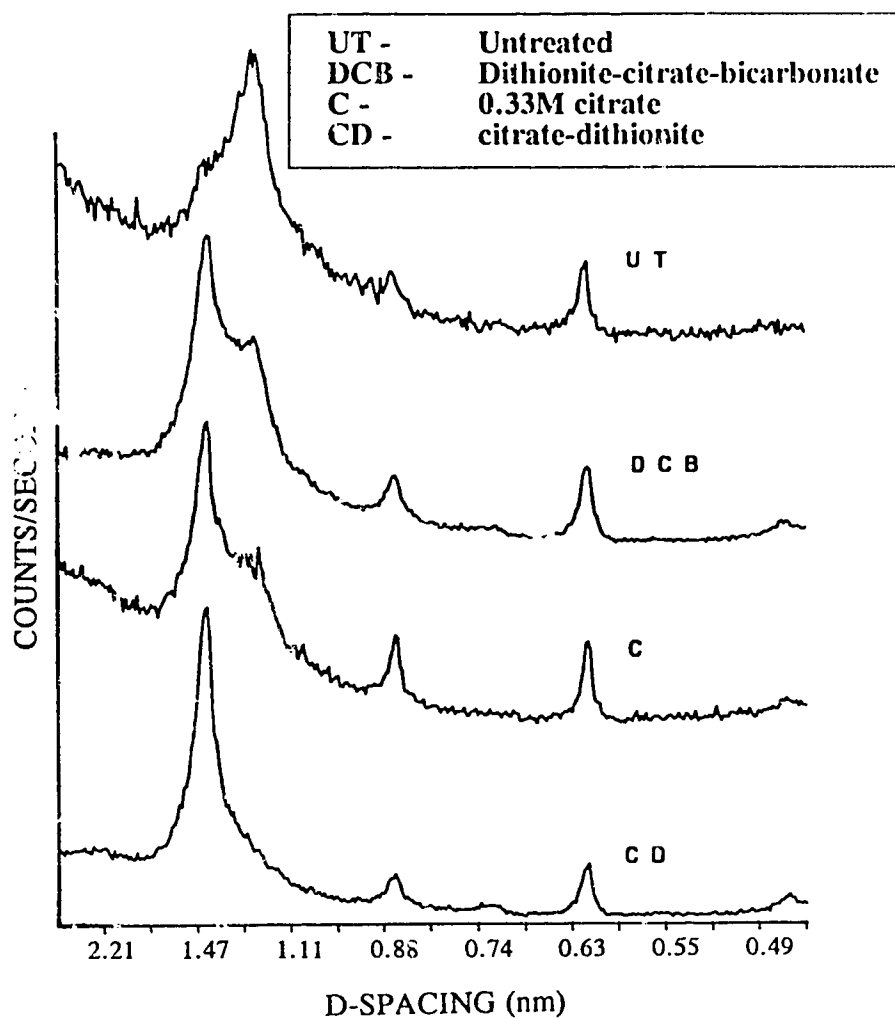


Fig. 4.2-4. X-ray behavior of hydroxy interlayered vermiculite in Podzolic soils of Alberta upon ethylene glycol solvation of untreated (UT) after dithionite-citrate-bicarbonate (DCB), citrate (C) and citrate-dithionite (CD) treatments.

Table 4.2-5. Amounts of Fe, Al, and Si extracted by six successive citrate-dithionite treatments from clay samples of nodules from Podzolic soils of Alberta.

sample #	Extraction #						Total	DCB
	1	2	3	4	5	6		
Fe (g kg ⁻¹ clay)								
N272c2	1.5	2.2	1.1	1.7	1.6	0.6	8.8	68.7
N341c1	2.2	2.4	1.3	1.9	0.2	0.9	8.9	90.3
N343c2	1.2	2.4	1.5	1.8	0.2	0.8	7.9	70.0
N422c2	1.1	1.1	0.7	0.6	0.3	0.7	4.6	76.0
Al (g kg ⁻¹ clay)								
N272c2	4.1	2.5	5.9	2.0	1.4	0.4	16.4	25.9
N341c1	2.5	2.0	2.6	1.2	0.4	0.7	10.3	35.2
N343c2	4.0	1.3	3.6	1.1	0.6	1.0	11.6	26.2
N422c2	2.3	0.8	2.3	0.7	0.3	0.7	7.0	31.4
Si (g kg ⁻¹ clay)								
N272c2	4.8	4.2	2.2	4.3	4.3	3.3	22.9	7.6
N341c1	5.3	3.6	2.7	4.4	2.4	3.4	21.7	12.3
N343c2	4.8	4.2	2.8	3.2	2.3	3.8	21.1	7.2
N422c2	3.1	2.0	1.5	1.6	1.9	2.3	12.5	8.1

c1-fine clay; c2-coarse clay; DCB-dithionite-citrate-bicarbonate

The 2:1 phyllosilicate with variable *ool* spacing as identified in both clay fractions has reflections at 1.400 nm in 54% RH for both Ca and K saturations. This *d*-spacing does not shift upon glycerol solvation but on ethylene glycol treatment shifts to 1.60-1.80 nm. Upon heating to 550 °C, the *ool* spacing reverts to 1.00 nm suggesting that the expanding clay is Vt. The 2:1 phyllosilicate with fixed *ool* spacing at 1.00 nm and a second order peak observed at 0.500 nm is primarily muscovite. Kaolinite and quartz are also identified with the latter present even in the fine clay components. In coarse clays, chlorite with a 1.400 nm peak stable at 550 °C is also present (see Fig. 4.2-3) and is possibly the remnant from physical weathering of inherited chlorite. The presence of less-ordered imogolite is suggested by the observed IR absorption bands around 340, 425, 580, 970, 1630 and 3470 cm⁻¹ and the XRD reflections at 0.762, 0.567, and 0.334 nm measured on Laue photographs of very fine clays (Fig. 4.2-5a).

The Fe oxide mineralogy as determined from XRD patterns mainly comprises goethite, hematite and lepidocrocite. The presence of ferrihydrite is suggested by the high Fe_o/Fe_d ratio of the samples (Table 4.2-1). The high Fe_o/Fe_d ratio is considered a reliable indicator of the presence of ferrihydrite (Schwertmann *et al.*, 1982) provided no Fe carbonate or Fe-phosphate minerals are present (De Geyter *et al.*, 1982); none were present in this study. Goethite is confirmed by reflections at 0.498, 0.416, 0.345, 0.268, 0.255, 0.249 and 0.242 nm measured from *in situ* Laue photographs of a Fe-nodule (Fig. 4.2-5b); the nodule also contains hematite. Lepidocrocite is identified as components of very fine clay (see Fig. 4.2-5a). Campbell and Schwertmann (1984), Milnes and Farmer (1987), Loveland and Clayden (1987) and Shoji *et al.* (1988) also identified the above mentioned Fe oxides in Podzols.

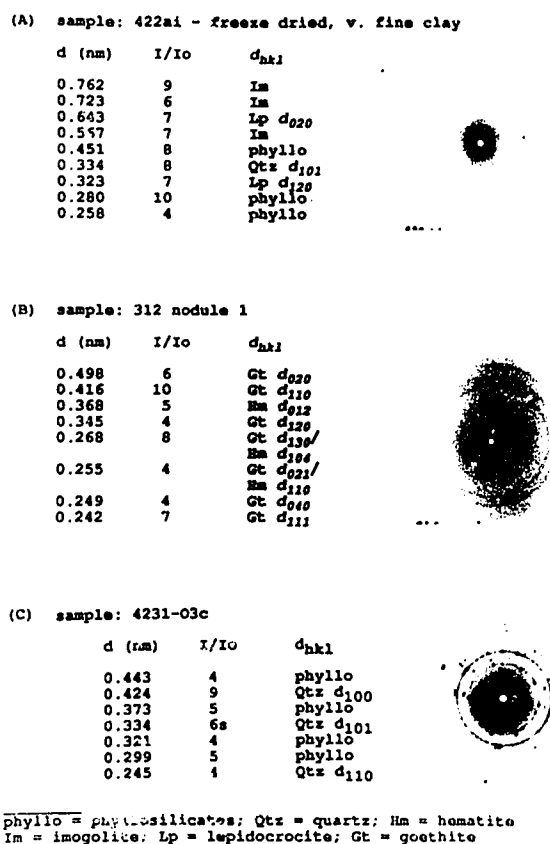


Fig. 4.2-5. Laue photographs of (A) very fine clay (B) Fe-nodule and (C) opaque components in the nodule of Podzolic soils from Alberta.

Figure 4.2-6a shows the presence of coatings of fine material on the quartz grains. Representative *in situ* XRD microcamera reflections taken from the fine materials are shown in Fig. 4.2-6b. The measured *d*-spacings correspond to the reflections at 0.447, 0.257 and 0.245 nm indicating the presence of phyllosilicates; at 0.424 and 0.334 nm indicating the presence of quartz.



B

sample: 312 coating 5

d (nm)	I/I ₀	d _{hkl}
0.447	8	phyllo
0.424	6	Qtz d ₁₀₀
0.334	10	Qtz d ₁₀₁
0.257	6	phyllo
0.245	4	phyllo/ Qtz d ₁₁₀

phyllo = phyllosilicates; Qtz = quartz



Fig. 4.2-6. (A) Micrographs of the coating of quartz grain and (B) its *in situ* Laue photograph.

A representative XRD pattern for opaque f-members (Fig. 4.2-5c) is quite similar to that for the fine material as shown in Fig. 4.2-6b suggesting similarities in mineralogical composition (phyllosilicates and quartz) and indicates that the dark material causing the opacity is compound of poor crystal organization. Semi-quantitative analysis for the opaque f-member using SEM revealed that it contains higher amounts of Si compared to Al, Fe and K. The high amount of Si is attributed to the presence of quartz identified as an integral part of the f-matrix. The presence of chlorine is an impurity from the embedding resin.

4.2.2.6. *Biological activities*

The role of biological materials in the formation of the nodules is evaluated from the results of infra-red, microscopic and sub-microscopic investigations. The presence of fulvic acids in the fine clay fraction is indicated by the IR absorptions at 2920 and 1400 cm^{-1} .

The organic materials in both the soil matrix and nodules are mainly polymorphic (Bullock *et al.*, 1985) consisting of plant roots with some cellular structures. Sub-microscopic analyses with SEM revealed that fungal hyphae provide a frame for network aggregation of the f-members and f-matrix (Fig. 4.2-7a). This network is so stable that dispersion by ultra-sonic treatment failed to bring about disaggregation (Fig. 4.2-7b and 4.2-7c). The absence of "cracked monomorphic coatings" on f-members and the presence of numerous hyphae indicate high turnover of biological products.

4.2.3. *Summary*

Chemical, mineralogical and micromorphological results show the authigenic nature of the nodules with the basic building blocks composed of the following: (a) coarse components - quartz, feldspar mainly albite, sand-size chlorite and traces of heavy minerals like anthophyllite, sillimanite, andalusite and lithogenic hematite; (b) fine components - phyllosilicates mainly chloritized-vermiculite, vermiculite, kaolinite and traces of chlorite, quartz and organic matter. *In situ* mineralogical determinations revealed the omnipresence of quartz in infillings, coatings and even in the opaque f-members within the nodules. The Fe oxides present are ferrihydrite, lepidocrocite, goethite and hematite.

The porphyric RDP of the nodules indicates that its formation is the result of the accumulation of phyllosilicates and in addition quartz, secondary Fe oxyhydroxides, X-ray amorphous organic matter alone or in combination with Fe and Al and less-

ordered aluminosilicates like imogolite. Aluminum, Fe and possibly Si can also be translocated as a component of hydroxy interlayered vermiculite. The role of biological activity in the formation of nodules is clearly suggested through a framework provided by the fungal hyphae in the aggregation of the basic components.

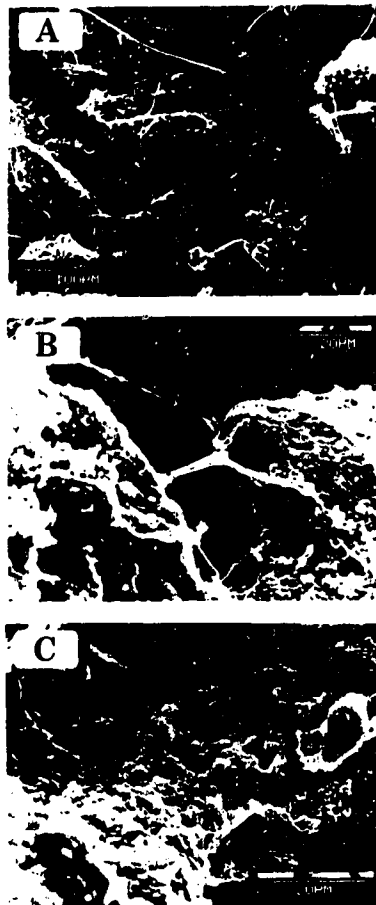


Fig. 4.2-7. Micrographs of the network of fungal hyphae (A) before and (B and C) after ultrasonic dispersion in the nodules of Podzolic soils from Alberta.

4.3. Nature and transformation of minerals in Podzolic soils from Alberta

4.3.1. Introduction

This part of the discussion deals with the mineralogy and *in situ* soil solution composition of the pedons. Its composition will be discussed in conjunction with the stability of selected minerals such as gibbsite and imogolite that readily attain equilibrium with interstitial solutions during 24-48 hours residence time (Turner and Brydon, 1965). Ferrihydrite is another mineral to be evaluated because the calculated ion activity product of Fe and OH in a natural solution of ferrihydrite deposit is reported to equal the K_{sp} of ferrihydrite (Spiers, 1990) and indicates attainment of equilibrium conditions. Other minerals to be studied are the Fe-oxides: goethite, hematite and lepidocrocite. All thermodynamic calculations are based on an environment of 25 °C and 1 atm pressure. Thermodynamic stability calculations for selected phyllosilicates are just approximations at best because of the uncertainty of equilibrium conditions that usually takes 1200 days for kaolinite (May *et al.*, 1986) and about 1-4 years for the 2:1 phyllosilicates (*e.g.*, Kittrick, 1971) to achieve. Moreover, the uncertainty in the chemical composition of the 2:1 phyllosilicates makes it very difficult to choose the appropriate thermodynamic constants. The transformations of phyllosilicates then will be evaluated in terms of empirical mineralogical determinations.

Specifically, the aim of this section is to characterize the nature of minerals with emphasis on phyllosilicates and their transformation within the sola of Podzolic soils from Alberta. Formation and stabilities of gibbsite, imogolite, and Fe-oxides will also be studied in relation to the *in situ* soil solution composition. The properties of goethite, particularly the Al for Fe substitution will also be discussed in relation to mineral weathering.

4.3.2. Results and Discussions

4.3.2.1. Minerals and their distribution within the sola

The classes of minerals identified in the pedons are carbonate, sulfate, oxides and silicates (Table 4.3-1). The carbonate mineral present in pedons 1 and 2 is calcite; it occurs only in the C horizons and mainly in the sand fractions. It is probably inherited from the aeolian material from Brûlé Lake (Dumanski, 1970), from where most of the aeolian deposits in the area originated during the Holocene.

In pedon 3, the presence of gypsum was highly localized in part of the indurated nodules in the Bf horizon. The euhedral crystals are smooth and free of any corrosion or etching thus reflecting its neoformation (Fig. 4.3-1).

Oxides present in the soil are mainly those of Fe and comprise goethite, hematite, lepidocrocite and ferrihydrite. Goethite occurs alone (Fig. 4.3-2a); together with hematite (Fig. 4.3-2b) or in association with phyllosilicates (Fig. 4.3-2c) as ascertained by *in situ* Laue photographs of Fe-rich nodules in thin sections. Lepidocrocite is an indicator of reducing conditions (Campbell and Schwertmann, 1984; Loveland and Clayden, 1987) and is present in the very fine clay fraction of the Bf horizons while the existence of ferrihydrite is apparent from the high Fe_o/Fe_d ratios of the samples (Schulze, 1981; De Geyter *et al.*, 1982) particularly from the Bf horizons (Table 4.3-2).

The silicates constitute the main building blocks of the soil, particularly the tectosilicates which are made up of mainly quartz and feldspar. These two minerals are the main components of the sand and silt fractions which make up about 650-950 g·(kg soil)⁻¹; quartz, however is present even in the clay separates.

Other silicates present are the phyllosilicates which make up the dominant minerals in the clay fractions and minor components in the fine silt fractions throughout the sola. Three classes of sheet silicates are identified: 2:1, 1:1 and 2:1:1. The 2:1 class is divided into groups with fixed and variable basal spacings. The fixed d_{001} spacing at 1.00 nm and the observed d_{002} reflection at 0.500 nm indicate the presence of muscovite. The calculated *b*-dimension from d_{020} of the mineral ranges from 0.888 to 0.896 nm and suggest the presence of dioctahedral mica.

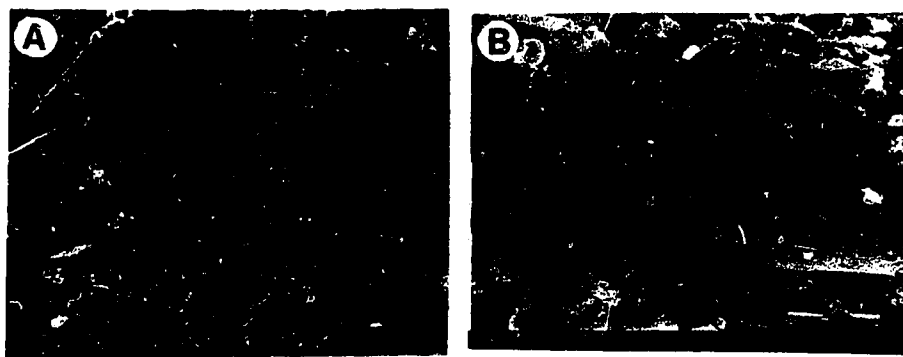


Fig. 4.3-1. Scanning electron micrographs of euhedral gypsum crystals from the indurated nodules in Bf horizon of Podzolic soils from Alberta.

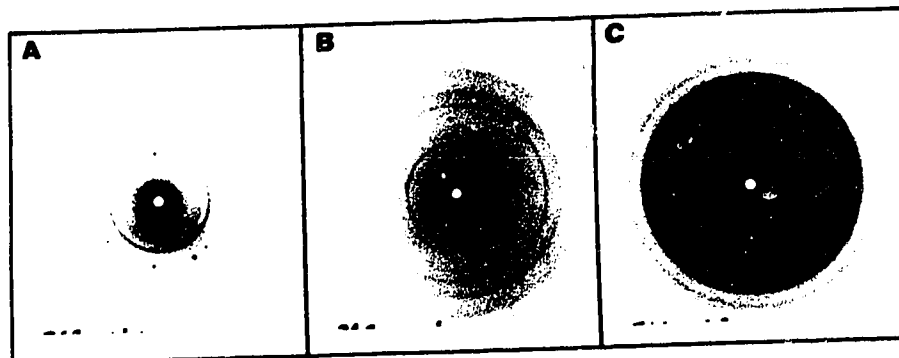


Fig. 4.3-2. *In situ* Laue photographs of (A) goethite alone (B) goethite in association with hematite and (C) goethite in association with phyllosilicates.

Table 4.3-1. Distribution of minerals in Podzolic soils from Alberta.

Minerals	Occurrence
<u>Carbonates</u>	
calcite	C horizons: sand fraction
<u>Sulfate</u>	
gypsum	Bf horizon: indurated nodules
<u>Oxides</u>	
hematite	C horizons: goethite nodules
goethite	Ae, Bf and C horizons: goethite nodules
ferrihydrite	Ae horizons: globules Bf horizons: fine components of matrix
lepidocrocite	Bf horizons: fine components of matrix
<u>Silicates</u>	
<u>tectosilicates</u>	
quartz	Ae, Bf, C horizons: sand, silt and clay
feldspar	Ae, Bf, C horizons: sand and silt fractions
<u>phyllosilicates</u>	
muscovite	Ae, Bf, C horizons: silt and clay fractions
vermiculite	Ae, Bf, C horizons: silt and clay fractions
smectite	C horizons: silt and clay fractions
kaolinite	Ae, Bf, C horizons: silt and clay fractions
proto-imogolite and imogolite	Bf horizons: clay fractions
<u>nesosilicates</u>	
garnets, sillimanite and andalusite	Ae, Bf and C horizons: sand fractions

Table 4.3-2. Allophane content and extractable Fe, Al and Si in clays of Podzolic soil from Alberta.

Hor.	Fep	Alp	Sip	Feo	Alo	Sio	Fed	Ald	Sid	Feo/d	Al/Si ¹	AlI ²
(g kg ⁻¹ clay)												
<u>Pedon 1</u>												
Ae	3.5	5.7	7.2	5.4	8.9	7.6	14.4	13.0	13.9	0.7	0.4	38.0
Bf	15.0	21.9	6.9	34.5	37.7	9.2	58.2	55.4	13.2	0.6	1.7	64.4
C	5.8	5.5	0.0	13.2	9.3	0.8	45.3	15.9	5.0	0.3	4.7	12.8
<u>Pedon 2</u>												
Ae	3.5	3.0	2.3	5.0	5.5	2.9	7.0	6.6	4.4	0.7	0.9	14.5
Bf	10.0	13.9	1.3	19.5	19.6	2.1	8.7	29.5	7.0	0.4	2.7	21.0
C	4.3	1.9	0.3	11.3	4.8	1.5	34.9	8.5	6.5	0.3	1.9	10.5
<u>Pedon 3</u>												
Ae	5.7	4.1	0.9	8.9	6.6	1.9	14.9	11.9	5.8	0.6	1.3	11.4
Bf	23.4	27.3	2.0	100	40.2	5.3	118	54.9	10.6	0.8	2.4	53.0
C	3.0	4.4	2.9	8.0	7.6	3.7	13.3	11.5	8.9	0.2	1.0	18.5

p - pyrophosphate; o = oxalate; d = dithionite-citrate-bicarbonate
 1 - (Alo-Alp)/Sio; 2 - formula of Parfitt (1990)

Three types of phyllosilicates with variable basal spacings were identified in the 2:1 group. The first type is vermiculite (Vt); its XRD patterns are shown under different treatments in Fig. 4.3-3a. Upon intercalation with alkylammonium chloride the XRD shows a straight positive regression line ($r=0.99$) between d_{001} spacings and the number of carbon atoms in the alkylammonium molecules in the interlayer (Fig. 4.3-3b). The measured charge density of this mineral is about 0.71 mole (-) per half cell and confirms a Vt according to the AIPEA classification (Bailey, 1980). Estimates of the quantity of Vt in the coarse clay (Alexiades and Jackson, 1965) ranges from 250-300 g·kg clay⁻¹ in the Ae horizons.

The second type of the 2:1 group with variable basal spacing is smectite (Sm); the XRD patterns for different treatments are shown in Fig. 4.3-4a. Upon intercalation with different chains of alkyl ammonium molecules, this mineral formed a step-wise mono, duo and pseudo-trilayering of alkylammonium molecules (Fig. 4.3-4b); and the measured charge density is about 0.38 mole (-) per half cell. Smectite constitutes a minor component of the clay fraction in the Ae and Bf horizons but is a major part of the clay fraction in the C horizons. Both Vt and Sm are present in the fine silt fraction of the Ae horizon.

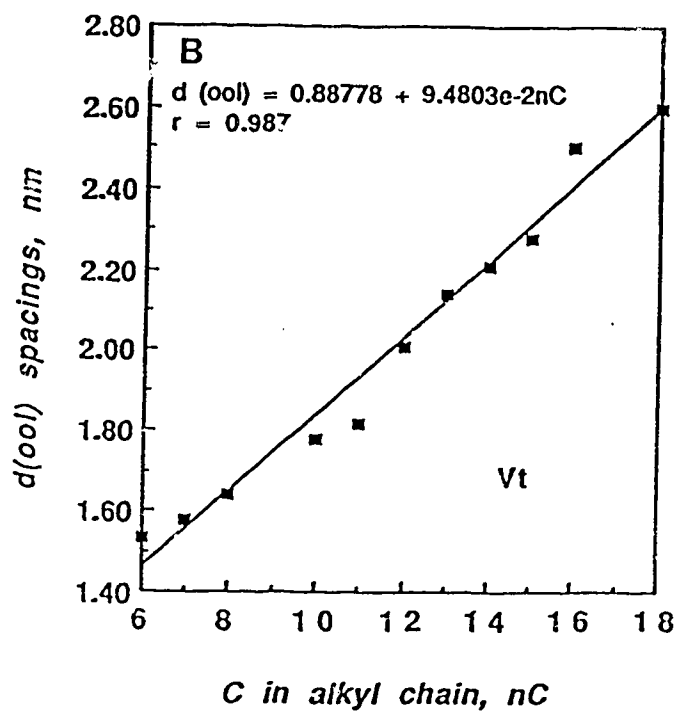
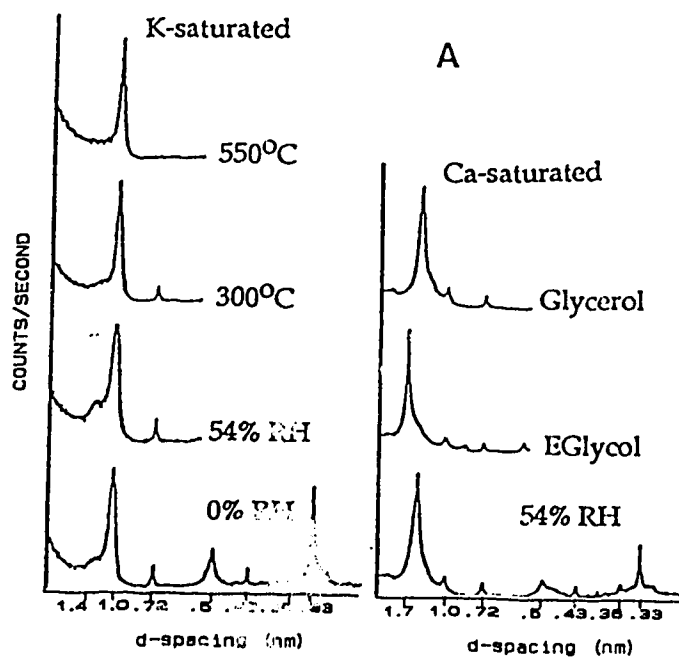


Fig. 4.3-3. The (A) XRD patterns of clay from the Ae horizon under different treatments and (B) relationships between d_{001} spacings and nC in alkylammonium chain.

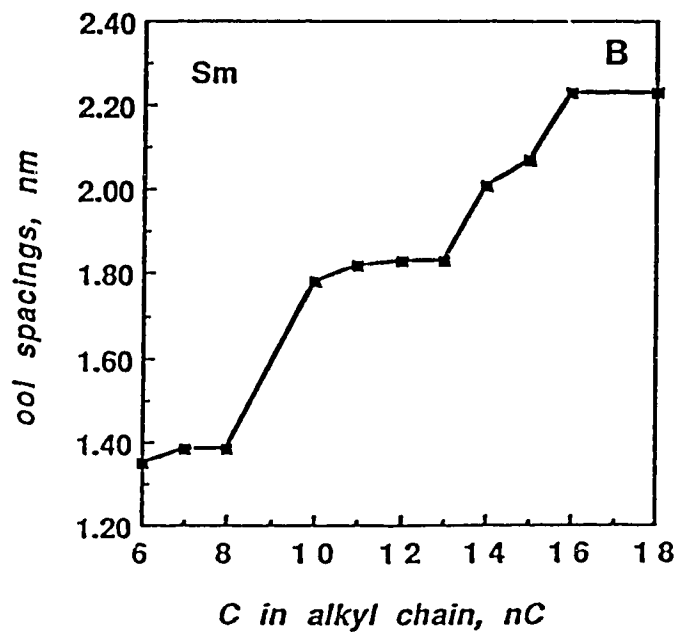
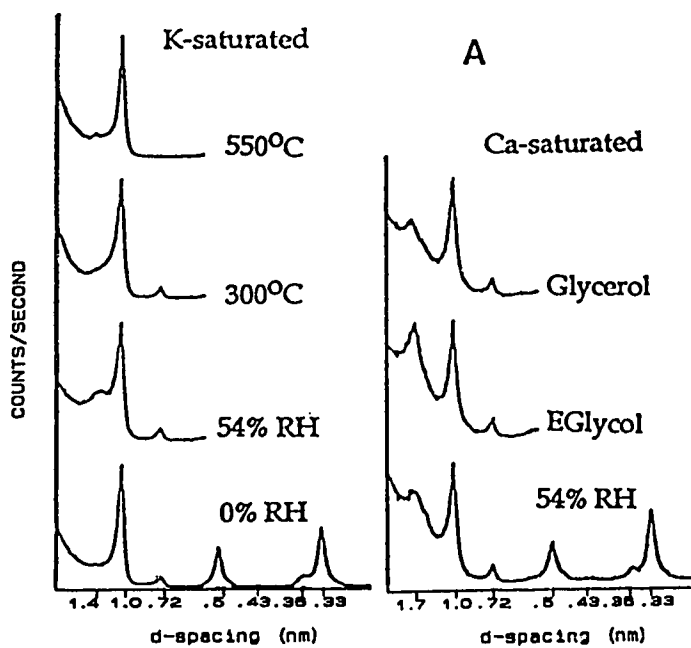


Fig. 4.3-4. The (A) XRD patterns of clay from the C horizon under different treatments and (B) relationships between d_{001} spacings and nC in alkylammonium chain.

The third type of 2:1 clay with variable basal spacing has 1.40 nm d_{001} spacing at 54% RH, fails to expand with either glycerol or EG solvation but gradually collapses to a range of spacings around 1.10-1.30 nm upon 550 °C heat treatment (Fig. 4.3-5). This is considered to be variant of Vt and is referred to as "chloritized" Vt or more recently as hydroxy interlayered Vt (HIV). Removal of interlayered material by citrate dithionite treatments allowed this mineral to expand to 1.60 nm upon EG solvation but not with glycerol solvation (Fig. 4.3-5); this suggests that the interlayered phyllosilicates is Vt. The calculated mean layer charge of this mineral after six citrate dithionite treatments based on d_{001} spacings at $nC=12$ (Olis *et al.*, 1990) is found to be 0.71 mole (-) per half unit-cell and similar to the Vt identified earlier. Hydroxy interlayered Vt is the main component of the clay fractions in the illuvial Bf horizons and has been identified elsewhere in a number of podzols (Farmer *et al.*, 1985; De Coninck *et al.*, 1987).

The species of 2:1:1 class of phyllosilicates identified is clinochlore (Clinochlore-IIb, ferroan) as shown in XRD patterns of magnetic fractions extracted from silt and clay fractions; muscovite and quartz appear as impurities in the separation (Fig. 4.3-6). This chlorite belongs to the trioctahedral subgroup where both the 2:1 layer and interlayer sheet are trioctahedral. It is considered one of the most common forms of chlorite found in soils (Bailey, 1988). Based on the d_{001} reflection, the calculated Al^{IV} is about 1.6 per 4 tetrahedral position or 0.4 for each tetrahedron and is consistent with the modal composition of clinochlore II-b, ferroan given by Rule and Bailey (1987): $(Mg_{2.85}Fe^{+2}_{1.53}Fe^{+3}_{0.22}Al_{1.32}Cr_{0.002}□_{0.08})(Si_{2.62}Al_{1.38})O_{10}(OH)_8$

The species representative of 1:1 class of sheet silicates is kaolinite (Kt). The presence of chlorite poses some problem with the identification of Kt because the d_{001} , d_{002} reflections of Kt coincide with d_{002} , d_{004} reflections of chlorite at 0.715 and 0.355 nm, respectively. Therefore, Kt identification was carried out on samples after chlorite was removed by magnetic separation at 1.7 Tesla. The presence of 0.715 and 0.355 nm reflections in the chlorite free samples and their disappearance after 550 °C heat treatment established the presence of Kt. Kaolinite is present throughout the entire pedon and indicates an allogenic origin for this mineral.

Another group of silicates identified is the less-ordered alumino-silicates. Laue photographs taken from aerogels of very fine clays show consistent Debye-Scherrer rings at 0.762, 0.723 and 0.567 nm regions characteristic for imogolite (Im) (Fig. 4.3-7a) and after heating the aerogel to 550 °C, these X-ray reflections disappeared (Fig. 4.3-7b). X-ray reflections at 1.6, 0.44, 0.33, 0.26 and 0.23 nm from DXRD analyses of the clay from pedon 3 also confirmed its presence (Fig. 4.3-8). The presence of Im

is further suggested by IR absorption band for Si-O vibrations at 348, 425, 980, 1630 and 3620 cm^{-1} . The strands and tubular morphology of the mineral are evident from the transmission electron micrographs shown in Fig. 4.3-9.

Proto-imogolite or allophane was identified from the broad reflections at 0.333 and 0.255 nm of DXRD pattern of clays from the Bf horizons (Fig. 4.3-10). The calculated (Al_o-Al_p)/Si_o values in Bf horizons are greater than 2 (Table 4.3-2) and point to the presence of proto-imogolite (Farmer, 1982). This mineral is considered to be the precursor for the formation of Im (Farmer, 1982) hence, it is called proto-imogolite. Estimates of the amount of this mineral in clay samples based on Si_o (Parfitt, 1990) generally show an enrichment in the Bf horizons compared to other horizons with values from 3.3 to 6.44 $\text{g}\cdot(\text{kg clay})^{-1}$ in the Bf horizons and from 1.24 to 3.8 $\text{g}\cdot(\text{kg clay})^{-1}$ in the Ae and C horizons (Table 4.3-2). A similar type of mineral had been identified in Podzols and Brunisols in eastern Canada (Kodama and Wang, 1989; Wang *et al.*, 1986; Wang and Kodama, 1986).

The remaining group of silicates identified in the soils are the nesosilicates which make up the heavy fractions of the sand; these are garnets, sillimanite and andalusite.

4.3.2.2. Vermiculitization and the fate of mica and chlorite

The formation of vermiculite from chlorite and mica is the major transformation of phyllosilicates observed in the present study. Estimates of the respective amounts of mica and chlorite based on MgO and K₂O contents from total dissolution analyses generally indicate the higher amounts of mica than chlorite in all the pedons (Table 4.3-3). In C horizons, chlorite ranges from 2-15 $\text{g}\cdot(\text{kg soil})^{-1}$ while mica content is from 51-183 $\text{g}\cdot(\text{kg soil})^{-1}$. The distribution of these minerals among different soil separates further shows a relative progressive decrease in their amounts in the sand fraction from C horizons towards the soil surface. For example in case of pedon 3, chlorite in the sand fraction of the C horizon constitutes 79% of total soil chlorite but it decreases to about 67% in the Ae horizon while for mica the decrease is from 45% (C horizon) to 25% (Ae horizon). The Ae horizons have higher chlorite and mica in the clay and silt fractions, compared to Bf horizons probably due to aeolian deposition. This could also result from physical breakdown of sand size chlorite and mica to finer fractions in the Ae horizons mediated by soil-mixing phenomena and chemical weathering (Fanning *et al.*, 1989) or through freezing during the cold winters. The presence of chlorite in the clay fractions of the Ae horizon is inconsistent with the findings of Ross *et al.* (1982) who reported the absence of chlorite in the same fractions of an eluvial horizon of

Podzolic soils in New Brunswick. It should be noted that the chlorite was identified only in magnetically separated fractions and analyses of the bulk clay samples showed an absence to very weak reflections for chlorite (Fig. 4.3-11); furthermore, XRD patterns of the two separates suggest progressively decreasing amounts of chlorite and mica from the C to A the horizons (Fig. 4.3-12 and 4.3-13).

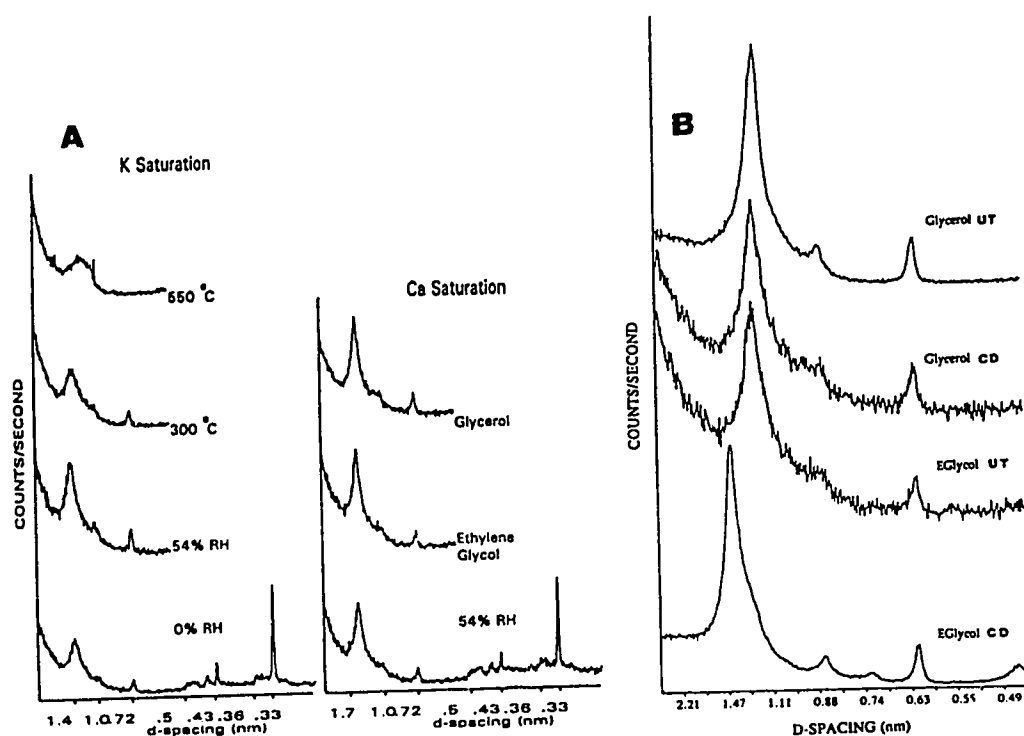


Fig. 4.3-5. The XRD behavior of hydroxy interlayered vermiculite under different treatments (A) before and (B) after citrate-dithionite treatments.

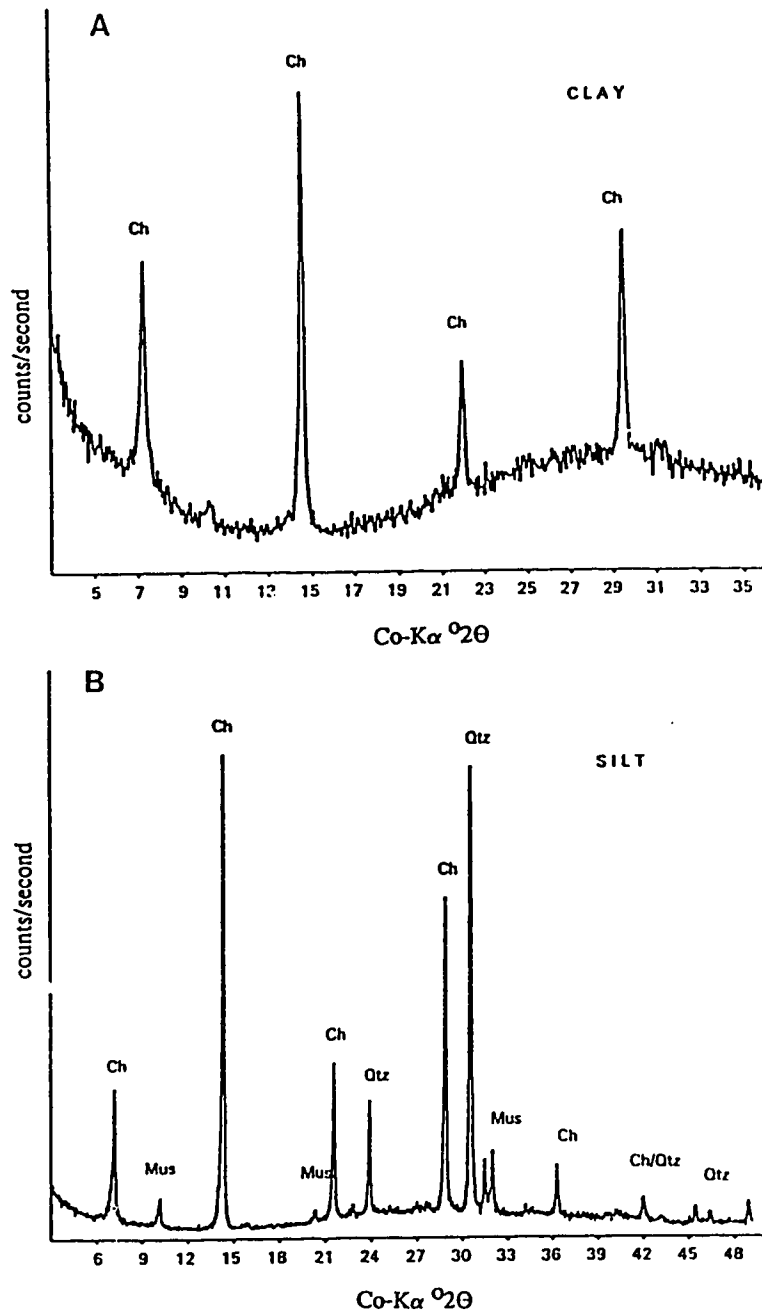


Fig. 4.3-6. XRD diffractograms of chlorite-rich samples from (A) silt and (B) clay fractions of C horizon of Podzolic soils from Alberta.

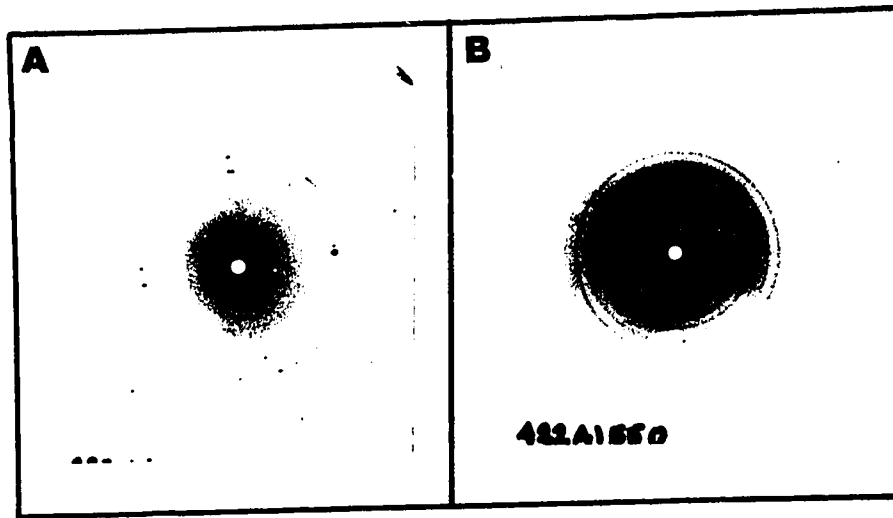


Fig. 4.3-7. Laue photographs of aerogels of very fine clay in the Bf horizon (A) before and (B) after heat treatment at 550 °C .

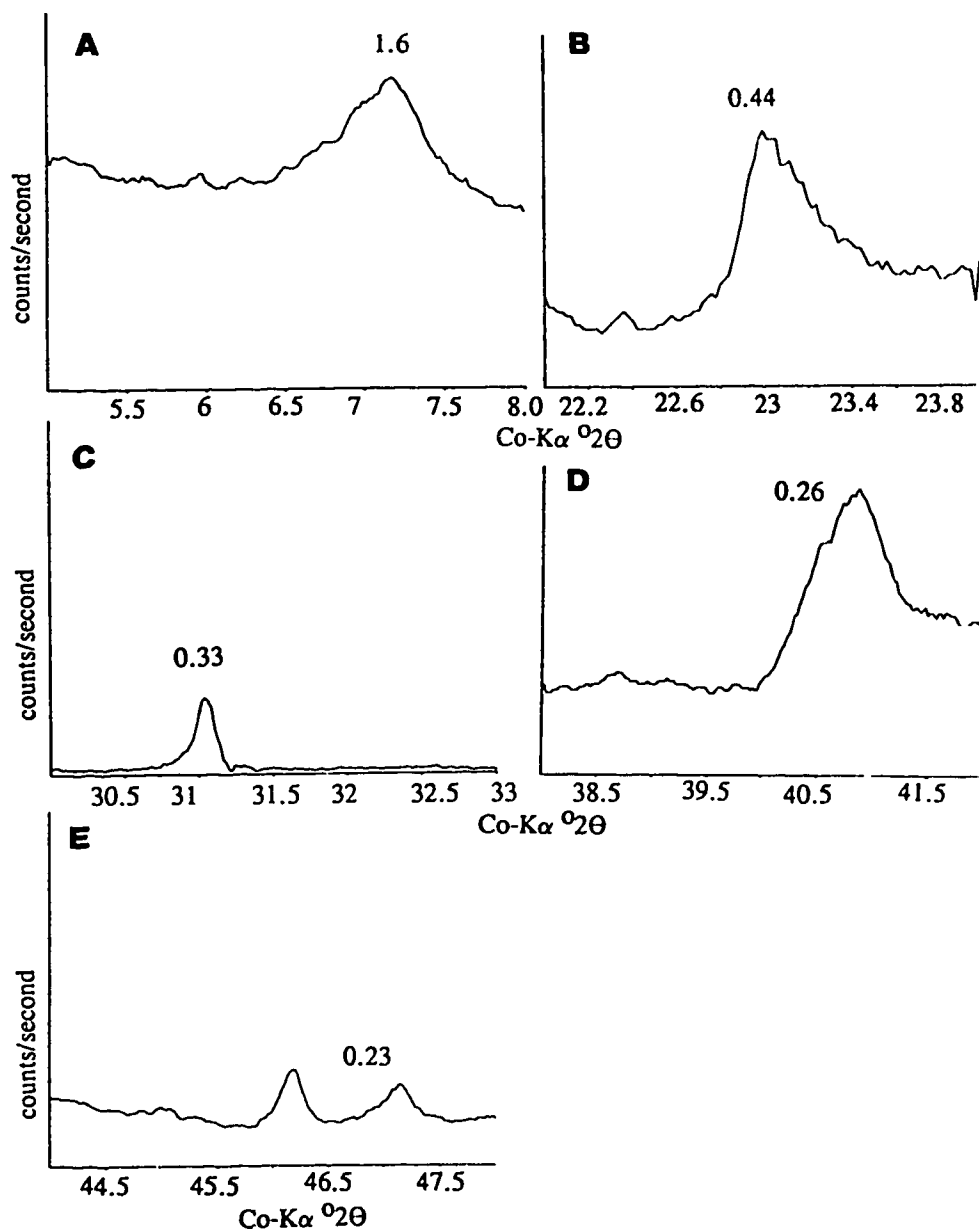


Fig. 4.3-8. Differential XRD of clay fractions from Bf horizons at different regions from (A) 1.6 nm (B) 0.44 nm (C) 0.33 nm (D) 0.26 nm and (E) 0.23 nm.



Fig. 4.3-9. Transmission electron micrograph of imogolite from fine clay fractions of Bf horizon of Podzolic soils from Alberta. magnification = 70,000 X

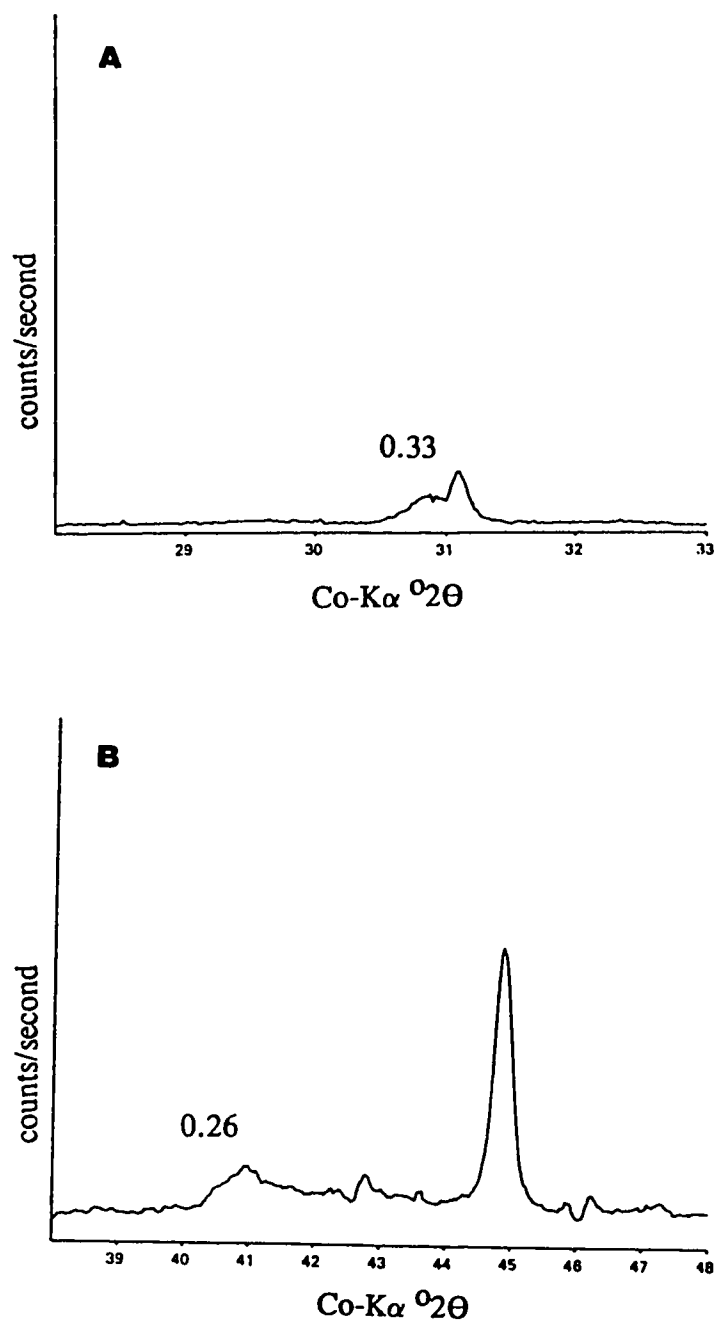


Fig. 4.3-10. Differential XRD patterns of clays from Bf horizon at (A) 0.33 and (B) 0.245 nm regions.

Table 4.3-3. Distribution of chlorite and mica in different soil separates of Podzolic soils from Alberta.

	Total		sand		silt		clay		
	chlo (g kg ⁻¹ soil)	mica soil)	chlo	mica	chlo	mica	chlo ¹	mica	
			(% of total chlorite or mica)						
	<u>Pedon 1</u>								
Ae	3.57	45.6	2.6	45.9	54.9 ¹	44.5	18.8	9.7	
Bf	5.87	82.1	59.3	53.5	32.0	29.0	8.7	7.7	
C	9.82	117.2	63.1	67.3	17.8	67.3	19.0	11.0	
	<u>Pedon 2</u>								
Ae	7.62	76.7	0.0	3.3	91.6 ¹	85.7	8.4	11.0	
Bf	7.61	90.9	67.4	48.8	16.8	23.3	15.8	27.9	
C	14.90	183.1	38.5	21.1	24.4	40.4	37.1	38.5	
	<u>Pedon 3</u>								
Ae	2.12	21.6	67.4	24.7	16.0 ¹	66.2	16.5	9.1	
Bf	7.39	52.8	89.6	67.5	4.9	16.8	5.6	15.8	
C	6.61	50.8	79.0	45.1	9.8	32.9	11.2	21.9	

chlo - chlorite; ¹ - includes other Mg containing 2:1

There is a consistent decrease in the intensities of the 1.4 and 1.0 nm reflections and an increase in the reflection at 1.7 nm after EG solvation, as one proceeds from the C horizon towards the soil surface. The trend is similar to that reported in many studies of transformations of chlorite and mica to vermiculite in Podzolic soils (Ross *et al.*, 1982; Farmer *et al.*, 1985; Righi and Lorphelin, 1986; De Coninck *et al.*, 1987). The weathering involves the removal of K⁺ in mica (Scott and Amonette, 1988) and OH-sheet in chlorite (Bailey, 1988). Such weathering could occur particularly on the edges and along cracks (Barnischel and Bertsch, 1989) where the mineral shows preferential cleavage. The weathering can be initiated by the oxidation of Fe⁺² in chlorite (Ross *et al.*, 1982) or by interlayer opening through edge-weathering in mica (Fanning *et al.*, 1989). The transformation is a degradation process referred to as vermiculitization of chlorite and mica. Moreover, parts of chlorite and mica most likely have undergone complete weathering which accounts for the higher amount of total free Fe, Al and Si in the Bf horizons compared to Ae and C horizons (Table 4.3-2) as suggested earlier by Farmer *et al.* (1985). The disappearance of smectite in the Ae horizon may have also resulted in its congruent dissolution. The production of

organic acids in the organic and eluvial layers is believed to be the driving force in this degradation process (Tongokonov *et al.*, 1987; Ugolini *et al.*, 1987; Kodama and Schnitzer, 1973).

Under conditions of aggressive acid complexing environments typical of Podzolic soils, liberal amounts of Fe and Al are present in soil solution. In this condition, vermiculite is unstable and aggradation processes through the incorporation of Al and Fe as interlayer components is a common phenomenon that leads to the formation of HIV (Farmer *et al.*, 1985; De Coninck *et al.*, 1987; Harris *et al.*, 1988). The incorporation of Al and Fe in the interlayer is evident from the behavior of the HIV after six successive 30-minute citrate-dithionite extractions where the amount of Al removed equals 50% and Fe approximately 10-20% of that removed by dithionite-citrate-bicarbonate (Table 4.3-4). The extracted Al is believed to be an hydroxide in the form of "gibbsite islands" that act similarly to the gibbsite sheet in chlorite (Pawluk and Brewer, 1975). A similar suggestion is proposed for Fe (Carstea *et al.*, 1970; Ghabru *et al.*, 1990) and in addition Fe may also originate from the tetrahedral layer where it may substitute for Si (Cardile, 1989).

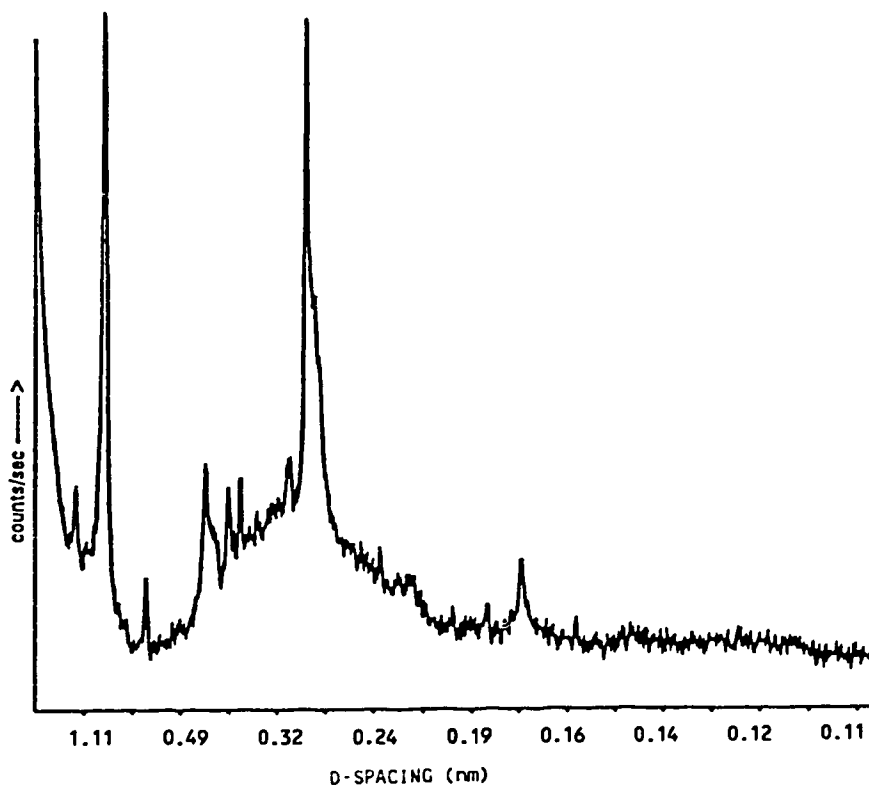


Fig. 4.3-11. X-ray diffractogram of magnetic fraction of clay from the Ae horizon.

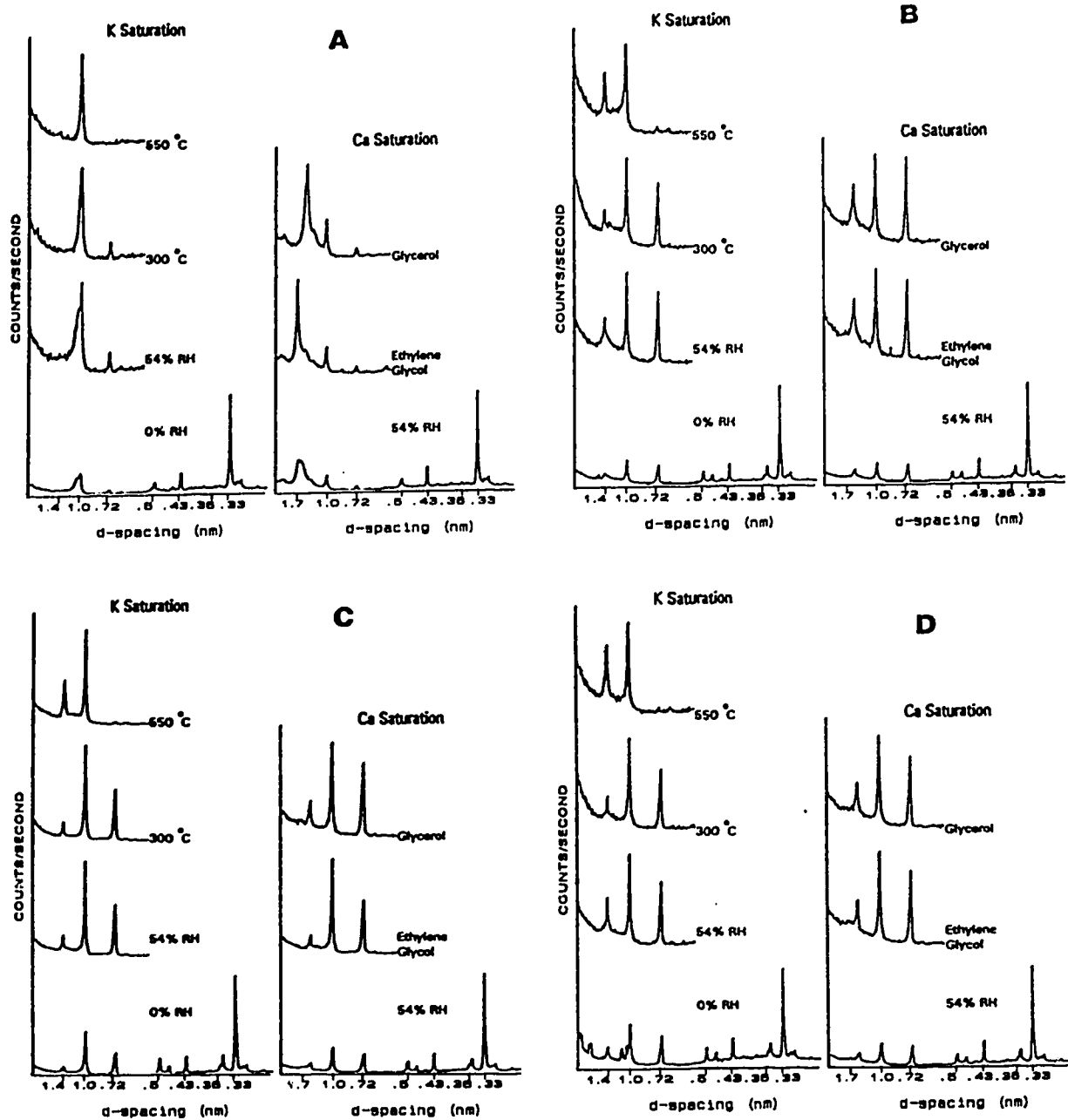


Fig. 4.3.-12. X-ray diffractograms of the silt fractions from the (A) Ae (B) Bf1 (C) Bf2 (D) C horizons.

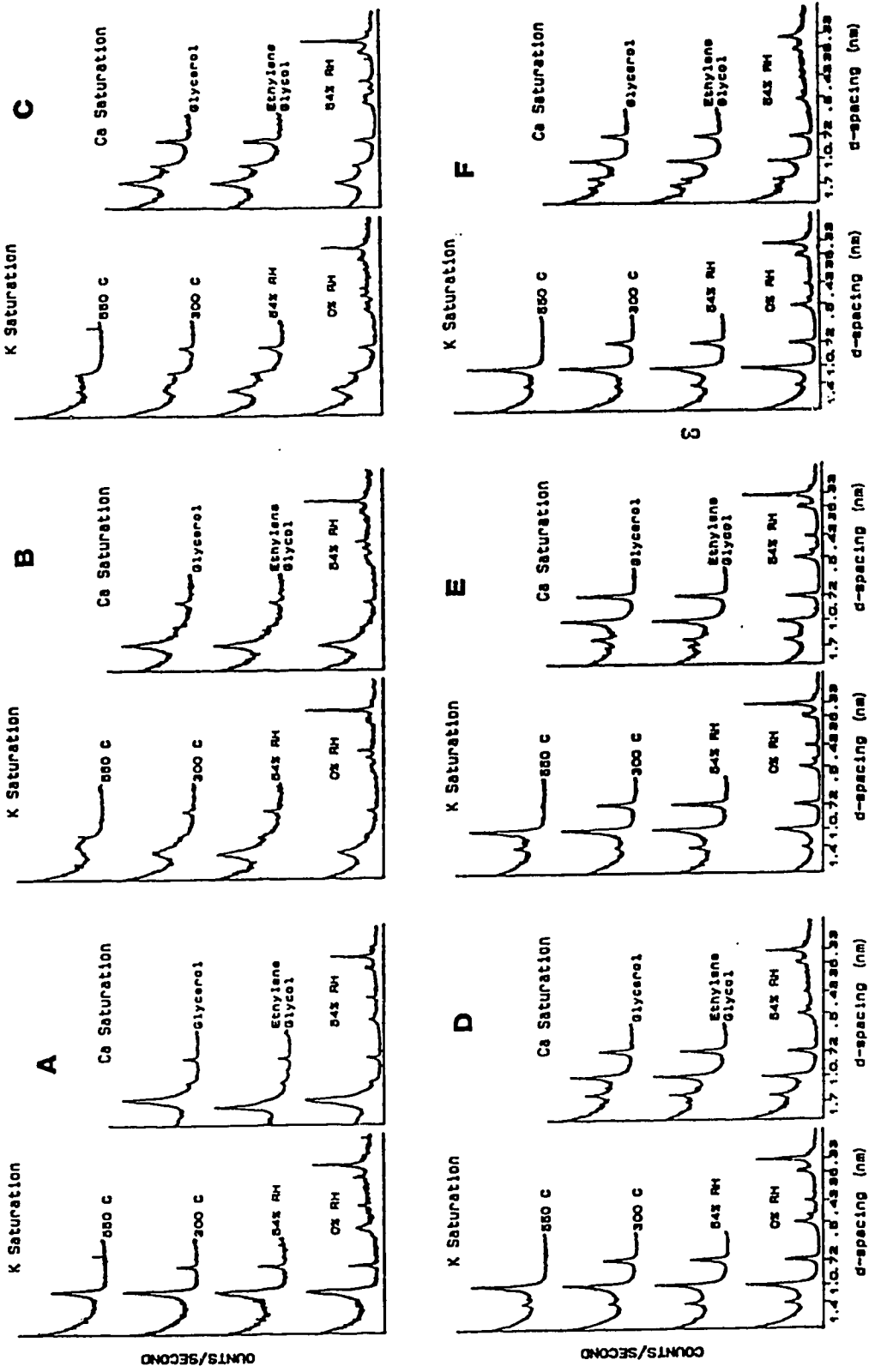


Fig. 4.3-13. X-ray diffractograms of clay fractions from (A) Ae (B) Bf1 (C) Bf2 (D) BC (E) C1 and (F) C2.

Table 4.3-4. Charge density of vermiculite, amounts of Al, Fe and Mg and the ratio of Mg:Fe:Al extracted by citrate-dithionite in clay fraction from Podzolic soils of Alberta.

	charge mole (-) cell ⁻¹	Alcd	Fecd (g kg ⁻¹ clay)	Mgcd	Mg:Fe:Al (molar ratio)
<u>Pedon 1</u>					
Ae	0.71	3.8	1.5	0.29	1: 2.3:11.7
Bfmat	0.71	27.1	12.8	0.37	1:15.3:67.3
Bfnod	nd	16.3	8.7	0.57	1: 6.9:26.5
C	0.71	18.2	8.4	1.51	1: 2.4:11.0
<u>Pedon 2</u>					
Ae	0.71	3.6	1.4	0.31	1: 2.0: 9.5
Bfmat	0.72	15.1	12.1	0.56	1: 9.5:24.3
Bfnod	0.72	10.4	7.9	0.39	1: 8.9:24.2
C	0.72	nd	nd	nd	nd
<u>Pedon 3</u>					
Ae	0.71	4.6	1.2	0.31	1: 1.7:13.4
Bfmat	0.71	30.4	14.7	0.30	1:20.7:91.9
Bfnod	0.71	7.1	4.5	0.22	1: 8.9:29.0
C	0.72	nd	nd	nd	nd

nd - not determined

In the transformation of chlorite, the origin of HIV is not always the aggradation process in Vt but also due to incomplete removal of OH-sheets (Rabenhorst *et al.*, 1982; Adams and Kassim, 1983). In the present study, some of the HIV may have originated by this process as shown by the amount of Mg extracted from the interlayer (Table 4.3-4). The extent of this type of HIV however, is considered lower than the HIV that resulted from the aggradation process because of the large deviation of the calculated Mg:Fe:Al molar ratio from the ideal ratio of 1:0.5:0.8 calculated from the composition of modal clinocllore given in section 4.3.2.1. The amount of excess Fe can be as high as 40 times and for Al as high as 100 times (Bf matrix, pedon 3) after compensation for the amount of Mg extracted from the interlayer based on the ideal molar ratio of Mg:Fe:Al. The excess Fe and Al are believed to be the component of HIV derived from aggradation processes.

A closer examination of the HIV formation revealed that the charge density of basic 2:1 unit (vermiculite) from different horizons throughout the three pedons is

0.71-0.72 mole (-) per half unit cell (Table 4.3-4). The extent or degree of interlayering however, differs between horizons as shown by the behavior of the clays upon intercalation with $nC=12$ alkylammonium molecules before citrate-dithionite treatments (Fig. 4.3-14). An ideal Vt (not interlayered) should have a definite reflection around 2.3 nm that corresponds to a charge density of 0.71 mole (-) per unit cell. The HIV from the Ae horizon is the least interlayered as shown by the hump around 2.3 nm (Fig 4.3-14a) compared to highly interlayered Vt in the matrixes and nodules in the Bf horizon where the reflection is undefined or absent (Fig 4.3-14c,e). Comparing the Bf matrix and the Bf nodule, more Vt in the former is interlayered than in the latter. This is shown by the amounts of Fe and Al extracted from the interlayers which follows the trend Bf matrix > Bf nodule > Ae horizon (Table 4.3-4). The amount of Vt measured after six citrate-dithionite treatments reaches as high as $240 \text{ g} \cdot (\text{kg clay})^{-1}$ from the Bf horizons. The above observations imply that the formation of HIV is a major sink for liberated Fe and Al; the aggradation process can start in the eluvial horizons and when combined with the process of lessivage can result in the transport of a large part of the Fe and Al from the eluvial horizons.

Concerns have been raised about the possibility of artifact formation during the hot citrate-dithionite extractions, but as shown in Fig. 4.3-14a, the charge of 0.71 mole (-) per unit cell is well preserved and the effect is limited to the removal of the interlayer component that caused the intensification of the reflection at 0.23 nm. Similar observations have been reported by Ghabru *et al.* (1990).

4.3.2.3. *Composition of the natural solutions*

Soil solution referred to in this study, is the "stationary" interstitial water extracted by exchange with tetrachloroethylene through centrifugation at 14500 rpm and is different from the "mobile" soil solutions collected from lysimeters. The chemistry of the natural solution in contact with the different horizons show higher acidity in the Ae horizons compared to Bf horizons (Table 4.3-5). In the Ae horizons, the range in pH (3.9-4.6) corresponds to the buffering capacity of most organic acids (Shoji *et al.*, 1988; Ugolini *et al.*, 1988) and justifies the earlier claim of the presence of organics in the eluvial horizons. SOLMINEQ-PC (Kharaka *et al.*, 1988) was used in the calculation of ionic activities. The results showed that the activities of cations are slightly lower in the Ae horizon than the Bf horizons regardless of seasons. Variations in activities of each cation at different times of collection are not evident except for Fe^{+2} which is lower during the Fall of 1989 for both pedons 1 and 2 compared to other seasons. The sum of the calculated activities of the anions is slightly

higher when compared to the total of the activities of the cations. The discrepancy can be attributed to a number of factors like the amount of CO_2 in the solution and the exclusion of the amounts of organic compounds like citrate in the calculation of the activities. Due to the observed cation/anion imbalance, the interpretation of the activities was taken with caution.

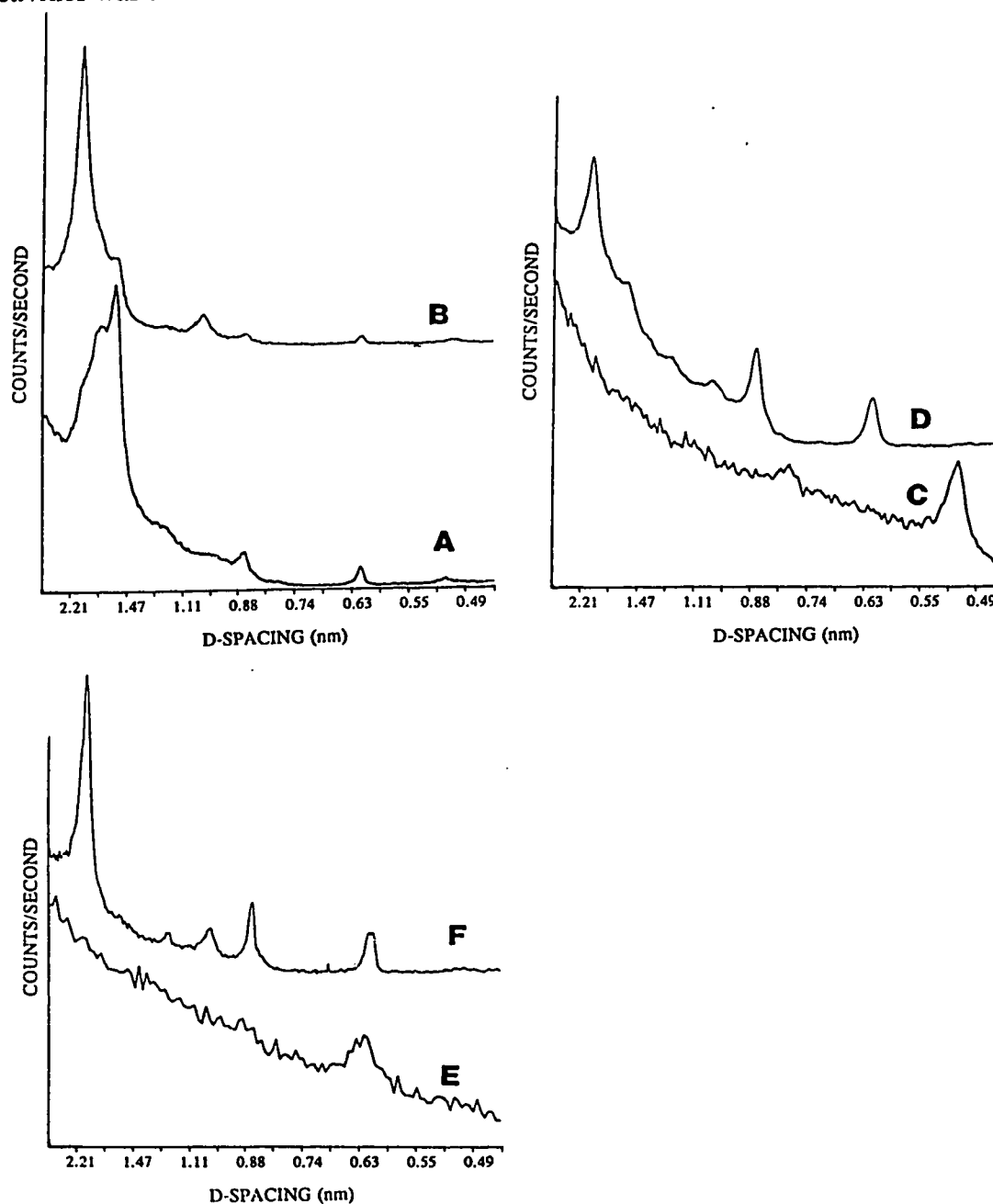


Fig. 4.3-14. X-ray diffractograms of vermiculite from Ae horizons (A) before (B) after; Bf matrix (C) before (D) after and Bf nodule (E) before and (F) after hot citrate-dithionite treatments.

4.3.2.3.1. Thermodynamic formation and stability of selected minerals

Thermodynamic stability calculations for selected minerals were based on the activities of the ionic components given in Table 4.3-5. The saturation index (SI) for each mineral is defined as:

$$\log (IAP/K_{sp})$$

where IAP = ion activity product

K_{sp} = solubility product constant

The SI value of zero denotes equilibrium while of positive and negative values denote saturation and undersaturation, respectively, with respect to the mineral of interest.

Table 4.3-6 shows that the solutions in Ae and Bf horizons are undersaturated with respect to calcite, dolomite, siderite and gypsum and, ideally, indicates their spontaneous dissolution whenever present in the soil. The formation of gypsum observed in the indurated nodules is attributed to the microbial activity in certain microsites of the indurated nodule where higher activity of SO_4^{-2} and Ca^{+2} can exist. Rosanov (1961) has reported earlier on the microbial source of gypsum in serozems of central Asia. Sulfur can be as high as 1.5% of the dry weight of *Aspergillus* (Fitzgerald, 1978) and from 0.4-0.8% of the total microbial dry matter weight (Zinder and Brock, 1978). In the total sulfur content of soils, 90-95% is in organic form which when mineralized can release as much as 60 kg S ha⁻¹ (David *et al.*, 1982).

The formation of Fe oxyhydroxides is particularly important in the study because of their role as adsorbing media particularly in the Bf horizons for mobile organic and inorganic components mentioned in sections 4.1 and 4.2. The equilibrium condition for the less-ordered ferrihydrite was evaluated using the equation provided by Fox (1989) where: $a(\text{Fe}^{+3}) * (a(\text{OH}))^{2.35} = 10^{-31.7}$. Saturation indices calculated for the natural solutions from Ae and Bf horizons are all saturated with respect to ferrihydrite regardless of seasons (Table 4.3-7). Generally, the Ae horizons (SI=2.9-5.6) show greater saturation compared to Bf horizons (SI=0.6-2.0). This finding supports the earlier claim that ferrihydrite can exist in the eluvial horizon. Stabilities of hematite, goethite and lepidocrocite were evaluated using their respective K_{sp} values in the SOLMINEQ-PC (Kharaka *et al.*, 1988). These higher ordered Fe-oxides have negative values for SI in the Ae horizons but not in the Bf horizons (Table 4.3-7) and are consistent with the observed distributions of Fe-oxides in section 4.1

Table 4.3-5. Calculated (-log) activities for the different ionic species of the natural soil solutions based on analytical concentrations. Calculation was done using SOLMINEQ-PC (Kharaka et al., 1988) at 25 °C and 1 atm..

	H ⁺	Ca ⁺²	Mg ⁺²	Na ⁺	K ⁺	Cl ⁻	SO ₄ ⁻²	HCO ₃ ⁻	SiO ₄	Al ⁺³	Fe ⁺²	Fe ⁺³	PO ₄ ⁻³	NO ₃ ⁻
Pedon 1														
Summer 89														
Ae	4.1	3.6	4.0	4.1	3.4	3.1	3.8	3.6	3.3	3.9	4.4	12.0	14.9	5.0
Bf	5.6	4.0	4.3	4.0	3.6	3.0	3.7	3.5	3.4	5.4	4.9	13.4	13.8	5.1
Fall 89														
Ae	4.6	3.1	3.6	4.0	3.1	3.5	4.0	4.7	3.7	4.4	5.4	13.0	14.5	tr
Bf	5.6	3.6	4.2	4.2	4.0	3.6	4.8	3.3	4.2	6.6	5.0	13.6	13.8	tr
Spring 90														
Ae	3.9	3.5	4.0	3.9	4.4	3.4	3.6	4.3	3.4	4.2	4.3	11.9	15.5	4.2
Bf	5.5	3.5	4.0	4.2	4.0	3.5	4.8	3.4	3.6	5.5	4.6	13.1	13.5	4.5
Pedon 2														
Summer 89														
Ae	4.5	3.5	3.9	4.2	3.6	3.1	4.2	3.8	3.1	4.5	4.7	12.3	14.9	5.3
Bf	5.5	3.7	4.0	4.3	4.3	3.1	4.5	3.6	3.5	5.3	4.0	12.3	14.0	5.3
Fall 89														
Ae	4.3	3.3	3.8	4.3	3.5	3.5	4.2	3.7	4.6	4.4	5.5	14.5	15.7	tr
Bf	5.8	3.5	4.0	4.2	4.2	3.8	5.1	3.6	4.6	5.7	5.8	14.1	tr	tr
Spring 90														
Ae	4.1	3.4	3.8	4.3	3.5	3.5	4.2	3.6	3.4	4.3	4.1	13.1	tr	4.2
Bf	5.3	3.7	3.8	4.2	3.6	3.7	5.2	3.9	3.7	4.7	4.9	13.2	14.3	5.8

where Ae horizons have fewer Fe-oxide nodules compared to enrichment in the Bf horizons. Hematite shows higher saturation compared to goethite and lepidocrocite but empirical observations show more goethite than hematite. The presence of organics in the natural solutions caused this discrepancy since the effects of those acids were not taken into account in the calculation of the saturation indices. Schwertmann and Taylor (1989) have suggested the "anti-hematitic" effect of organic compounds occurs because they can tie up available Fe^{3+} as its coordination center and thus lower the quantity of Fe to levels below the K_{sp} of ferrihydrite. This prevents the crystallization of hematite since ferrihydrite is considered the precursor for hematite formation. Reduction of Fe^{3+} following oxidation of ligands also lowers the proportion of Fe^{3+} in the system (Cornell *et al.*, 1989a,b).

Table 4.3-6. Calculated saturation indices of natural solutions with respect to selected carbonates and gypsum in Podzolic soils from Alberta.

	Calcite	Dolomite	Siderite	Gypsum
<u>Pedon 1</u>				
<u>Ae horizon</u>				
summer 89	-4.9	- 9.1	-3.7	-2.7
fall 89	-5.3	-10.1	-5.6	-2.5
spring 90	-5.8	-11.0	-4.5	-2.5
<u>Bf horizon</u>				
summer 89	-3.7	- 6.7	-2.6	-3.1
fall 89	-3.1	- 5.8	-2.6	-3.8
spring 90	-3.3	- 5.9	-2.3	-3.7
<u>Pedon 2</u>				
<u>Ae horizon</u>				
summer 89	-4.6	- 8.4	-3.7	-3.1
fall 89	-4.6	- 8.7	-4.8	-3.0
spring 90	-4.8	- 8.9	-3.4	-3.1
<u>Bf horizon</u>				
summer 89	-3.7	- 6.5	-1.9	-3.6
fall 89	-3.1	- 5.6	-3.4	-4.1
spring 90	-4.2	- 7.3	-3.3	-4.3

Both "amorphous" and crystalline gibbsite have positive SI in the Ae and Bf horizons but XRD observations failed to detect any crystalline gibbsite (Table 4.3-8). This could be attributed to the instability of gibbsite in acid complexing environments (Righi and Lorphelin, 1986) where active formation of HIV in such conditions involved the incorporation of $\text{Al}(\text{OH})_3$ in the interlayers. The amorphous Al coating reported mainly as Al-organo complex in section 4.1, might have some "amorphous" gibbsite in it.

Table 4.3-7. Calculated saturation indices of natural solutions with respect to selected Fe oxides in Podzolic soils from Alberta.

	Ferrihydrite	Goethite	Hematite	Lepidocrocite
<u>Pedon 1</u>				
<u>Ae horizon</u>				
summer 89	3.6	-0.2	0.5	-1.1
fall 89	3.4	-0.6	-0.2	-1.5
spring 90	3.9	-0.7	-0.5	-1.6
<u>Bf horizon</u>				
summer 89	1.4	2.9	6.7	2.0
fall 89	1.6	2.8	6.4	1.9
spring 90	1.4	3.9	6.7	2.00
<u>Pedon 2</u>				
<u>Ae horizon</u>				
summer 89	2.9	0.8	2.4	-0.1
fall 89	5.6	-2.1	-3.2	-3.0
spring 90	4.7	-1.3	-1.6	-1.4
<u>Bf horizon</u>				
summer 89	0.6	3.8	8.5	2.9
fall 89	1.7	2.8	6.6	1.9
spring 90	1.9	2.2	5.4	1.3

The formation and stability of imogolite is evaluated using the equation given by Dahlgren and Ugolini (1989):

$$(a\text{Al}^{+3})^2 * a(\text{H}_4\text{SiO}_4) / (a\text{H}^+)^6 = 10^{12}$$

The calculated SI are consistently positive in both Ae and Bf horizons (Table 4.3-8). Generally, SI values are higher in the Bf horizons (SI=4-7) compared to the

Ae horizons (SI=0.4-3). The saturation of Im in the Ae horizons contradicts the findings of Dahlgren and Ugolini (1989) because the latter used leachates solutions while the present study used solutions which were "stationary" in the horizons at the time of sampling and generally have two to three times more Al and Si compared to lysimeter leachates as presented in section 4.1.

The findings support the initial proposition of Farmer *et al.* (1980), Farmer (1981, 1982) that Im can form in the eluvial horizons. The higher SI values of Im in the Bf horizons connotes additional formation probably from Al and Si released by microbial activity as originally suggested by Buurman and Van Reuwijk (1984).

Kaolinite, muscovite and smectite are all stable in Ae and Bf horizons (Table 4.3-9). Chlorite will undergo dissolution in the Ae and Bf horizons because of the calculated negative values for SI (SI=-48 to -24).

Table 4.3-8. Calculated saturation indices of natural solutions with respect gibbsite and imogolite in Podzolic soils from Alberta.

	Gibbsite _{am}	Gibbsite _{crys}	Imogolite
Pedon 1			
<u>Ae horizon</u>			
summer 89	0.9	1.4	1.5
fall 89	0.9	1.4	3.1
spring 90	-0.1	0.4	-0.4
<u>Bf horizon</u>			
summer 89	3.8	4.3	7.4
fall 89	2.7	3.2	4.2
spring 90	3.4	3.9	6.4
Pedon 2			
<u>Ae horizon</u>			
summer 89	1.4	1.9	2.9
fall 89	1.0	1.5	0.4
spring 90	0.5	1.0	0.6
<u>Bf horizon</u>			
summer 89	3.7	4.2	6.9
fall 89	4.1	4.6	6.8
spring 90	3.6	4.1	6.7

am - amorphous; crys-crystalline

Table 4.3-9. Calculated saturation indices of natural solutions with respect to selected phyllosilicates in Podzolic soils from Alberta.

	Kaolinite	Chlorite	Smectite	Muscovite
<u>Pedon 1</u>				
<u>Ae horizon</u>				
summer 89	4.0	-43.8	2.1	3.1
fall 89	3.4	-41.2	1.0	2.8
spring 90	1.9	-48.4	-0.5	-1.2
<u>Bf horizon</u>				
summer 89	9.7	-24.8	9.0	13.0
fall 89	5.8	-29.0	3.5	6.8
spring 90	8.6	-25.6	7.6	10.7
<u>Pedon 2</u>				
<u>Ae horizon</u>				
summer 89	5.5	-37.6	4.2	5.6
fall 89	1.7	-44.8	-2.1	-0.1
spring 90	3.1	-44.2	1.0	1.7
<u>Bf horizon</u>				
summer 89	9.3	-25.1	8.4	11.6
fall 89	8.0	-24.2	5.7	10.1
spring 90	8.8	-26.7	7.6	11.3

4.3.2.4. Al for Fe substitution in Goethite

Goethite is the dominant Fe-oxide throughout the soil sola of the three pedons. *In situ* Laue photographs taken by Norelco microcamera of this oxide show reflections around 0.498, 0.418, 0.257, 0.244 and 0.23 nm, definitive for goethite (Fig 4.3-15a-d). The smoothness and the continuity of the Debye-Scherrer rings resulted in XRD patterns characteristic of random and rotating powder samples (Wicks and Zussman, 1975). The results indicate that within the resolution of the microcamera (50 μm diameter), the larger (150-300 μm) Fe nodules observed in thin section are actually conglomerate of very fine crystals of goethite in random orientation. The spotty Debye-Scherrer ring around 0.342 nm is the d_{110} spacing of ubiquitous quartz; this reflection was used as an internal standard to correct the sample to specimen distance in the measurement of the unit cell parameters of goethite. The presence of quartz in all the goethite nodule studied points to a certain role provided by quartz in the crystallization of goethite into nodules. The quartz grains are certainly larger than the

goethite as is evident from their spotty reflections and it is proposed that quartz may have attracted together the very fine goethite crystals through van der Waals attraction to the quartz surfaces and initiated the goethite accumulation into nodules.

The allogenic nature of hematite is indicated by its occurrence in association with goethite only in the C horizon (Fig. 4.3-2b).

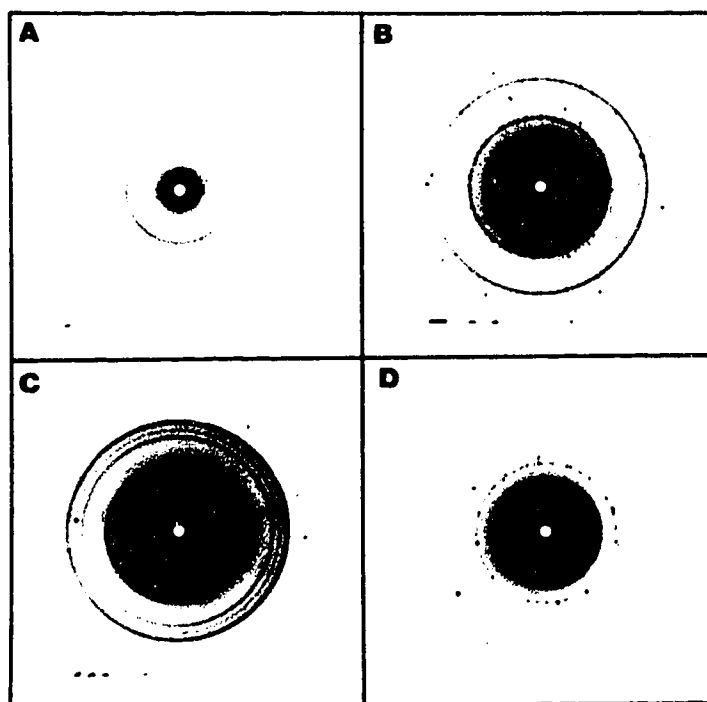


Fig. 4.3-15. *In situ* Laue photographs of goethite from the different horizons (A) Ae (B) Bf matrix (C) Bf nodule (D) C horizon of pedon 3.

Goethite and especially the pedogenic goethite is considered an important indicator of the pedogenic environment (Schwertmann and Taylor, 1989). One of the most common properties of goethite sensitive to conditions of formation is the Al for Fe substitution (*e.g.*, Norrish and Taylor, 1961; Fitzpatrick and Schwertmann, 1981; Schulze, 1984). The smaller radius of Al^{+3} (0.053 nm) compared to Fe^{+3} (0.065 nm) causes a linear decrease of the unit cell parameters (Vegard's rule) and Schulze (1984) indicated that the changes in the *c*-dimension can be used to measure of Al for Fe substitution in goethite. Aluminum in goethite is present as a diaspore component in the solid solution series between the isomorphs goethite and diaspore (Yapp, 1983).

The unit cell parameters of goethite samples isolated from different horizons were calculated using the Appleman and Evans computer program for indexing powder patterns and refining unit cell parameters by least square procedures as adapted to personal computers by Benoit (1986). The *c*-dimension was also calculated from d_{110} and d_{111} spacing as suggested by Schulze (1984). The values from the two methods of calculations are very close to each other.

The degree of Al for Fe substitution (mole% Al) calculated from the *c*-dimension of various goethite nodules was grouped arbitrarily into < 10 ("low"), 10-15 ("medium") and > 15 ("high"). The substitution in the Ae horizon is dominated by the "low" (75%) with 25% "medium" and absence of the "high" goethite while the C horizon has almost equal amounts of the "low" and "medium" and is also devoid of the "high" goethite (Fig. 4.3-16). It is only in the Bf horizon where the "high" goethite was identified with substitution that reached as much as 28 mole% Al.

The low goethite phase (*i.e.*, < 10 mole% Al) is observed to be present in the Ae, Bf matrix, Bf nodule and C horizons. This phase probably represents the original goethite present in the parent material, although medium goethite (*i.e.*, *ca.* 12 mole% Al) is also present in the C horizon. The stability of low over medium or high goethite (*i.e.*, > 20 mole% Al) is suggested by its presence in the Ae and Bf horizons and indicates that not all the original goethite undergoes weathering and reorganization to larger goethite nodules. Reorganization and dissolution occur preferentially in medium goethite which is consistent with the suggestion of Schulze (1984) that higher Al for Fe substitution tends to destabilize the goethite structure. The high goethite phase probably represents the pedogenic goethite that results from the concurrent processes responsible for the formation of the present soil which is characterized by high activity of Al in the present soil solution. In the reorganization of goethite, it is the low goethite that most probably provides the seeding effect for the recrystallization of easily dissolved medium goethite to pedogenic high goethite.

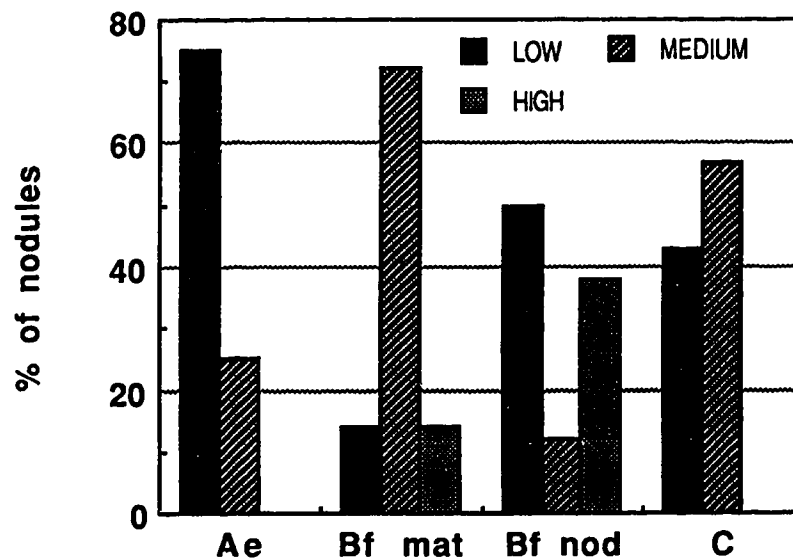


Fig. 4.3-16. Class distribution of the extent of Al for Fe substitution in goethite in pedon 3.

The identification of different degrees of Al for Fe substitution within the same horizon is considered a step further beyond the conventional determination of Al for Fe substitution in bulk sample where the average value is resolved (Schwertmann and Taylor, 1989) and where the heterogeneity within the horizon is often overlooked.

In the Bf horizon for example, the indurated nodules have goethite that has Al for Fe substitution as high as 28 mole% Al compared to the highest value of 15 mole% Al in the matrix. The higher substitution reflects higher Al activity (Campbell and Schwertmann, 1984) and greater amounts of organic ligands in the environment of formation. Moreover, complexing of Al by organic acids decreases the polymerization of hydrous-aluminum species, leaving more Al available for reaction (April and Keller, 1990) such as Al for Fe substitution during goethite formation. This may also be the reason why a higher degree of Vt interlayering was observed in the matrix of the Bf as compared to the indurated nodule.

The higher degree of microbial activity in the indurated nodules has been suggested in section 4.2 and claimed to be the principal reason for the formation of the nodule as well as the euhedral gypsum crystals in certain microsites of those nodules mentioned in section 4.3.2.1. Ergosterol assay (Johnson, 1989) for total fungal activity generally suggest higher fungal populations in the indurated nodule compared to the matrix of the Bf horizon.

4.3.3. Summary

Vermiculitization of chlorite and mica is the major transformation process observed for the phyllosilicates in this study. The transformation leads to the formation of hydroxy interlayered vermiculite through aggradation of Al and Fe hydroxides in the interlayers although some of the HIV probably resulted from the incomplete removal of the OH-sheets from clinocllore. The formation of HIV starts in the eluvial horizons with the following order of intensity throughout the pedon: Bf matrix > Bf nodule > Ae horizons.

In situ natural soil solutions from the Ae and the Bf horizons are saturated with respect to gibbsite, ferrihydrite and imogolite. The higher ordered Fe-oxides (goethite, hematite and lepidocrocite) are undersaturated in the Ae horizons but not in the Bf horizons.

The use of the X-ray microcamera enabled the identification of different goethite phases throughout the sola through the measurement of the *c*-dimensions to estimate the Al for Fe substitution. The lowest substitution (< 10 mole% Al) probably represents the allogenic goethite while the highest substitution (> 20 mole%) represents the pedogenic goethite.

The higher microbial activity in the indurated nodule is considered responsible, in part, for the higher Al for Fe substitution in goethite, differences in the degree of vermiculite interlayering between Bf matrix and the Bf nodule and the formation of euhedral gypsum crystals.

Chapter 5

SYNTHESIS: Genesis and Taxonomy of the pedons

5.1. Introduction

The state of soil classification (or any type of classification), reflects the "state-of-the art" of the soil science (or the discipline). The classification changes as the fundamental knowledge about the pedon accumulates and is updated. Historically, efforts have been made to reconcile "utilitarian" and "genetic" biases of soil classification. For pedologists, the obvious choice has always been the emphasis on the genetic processes involved in the soil formation. They argue that utility of the soil can be easily and soundly harnessed if one has a grasp of the various soil forming events in the pedon. The pedon should not be mistaken for the soil materials one shakes in test tubes nor the dirt with which one fills the flower pot with. The soil has its characteristic anatomy and physiology (Joffe, 1949) which, incidentally are the main concerns of pedologists.

The investigation of the microstructure of Alberta Podzols in this thesis amplifies its anatomy and provides an understanding of its physiology or "its behavior and responses to the forces responsible for its creation" (Joffe, 1949). The synthesis of the knowledge of the genesis of the pedons will culminate in the discussion of their classification in the Canadian System of Soil Classification (Canada Soil Survey Committee, 1978), Soil Taxonomy (Soil Survey Staff, 1975) and the FAO-UNESCO Soil Map of the World (FAO-UNESCO, 1988).

5.2. Genesis of the Alberta Podzols

5.2.1 Microstructures

The Bf horizon of Alberta Podzols are generally redder and of finer texture than the overlying bleached eluvial Ae horizon. One important pedological feature of the Bf horizon is the presence of indurated nodules with diameter from less than 1 cm to about 20 cm. The nodules occur in different parts of the Bf horizons: in pedon 1, the nodules are random; in pedon 2, the nodules are near the lower boundary and in pedon 3, the indurated nodules are prominent in the upper boundary.

Under the microscope, the related distribution patterns (RDP) from the eluvial Ae to the Bf matrix to the Bf nodule demonstrate the chlamydic sequence of microstructural evolution (Pawluk, 1983). The sequence is typical for soils where eluviation/illuviation processes are dominant. The Ae horizons are characterized by monic RDP (*i.e.*, coarse materials are uncoated with fine materials); the Bf matrix by

chitonic RDP (*i.e.*, coarse materials are coated with fine materials) and the Bf nodule by porphyric RDP (*i.e.*, coarse materials are embedded in a matrix of fine materials). This set of soil anatomical features, shows that the Bf horizon is the result of the accumulation of materials leached out from the Ae horizon. Often at this point, investigators are forced to end with such generalizations because the information obtained is limited to the characterization of the chemistry, physics and mineralogy of each *horizon*. A closer examination will show that within the Bf horizon, accumulation processes are not homogeneous.

The RDP of the Bf nodule is at a more advanced stage than the RDP of Bf matrix, as reflected from the porphyric arrangement in the nodule compared to chitonic arrangement in the Bf matrix. Fine materials fill up most of the voids in the former and are responsible for porosity as low as 15% compared to the more porous Bf matrix with porosity as high as 30%. This observation reflects the various environments of accumulations within the Bf horizon and demonstrates that the natural anisotropy of the soil is an important characteristic of the pedon and must be seriously considered in any investigation. In other words, (micro)structural variation in soils is as important as chemical or physical attributes.

5.2.2. *Mobile components*

The soil is not only anisotropic, but also dynamic in that genetic investigations are incomplete should one limit investigation to static pedology (or soil anatomy - *i.e.*, chemical, physical, micromorphological and mineralogical observations). Genetic studies should also answer questions such as: what are the mobile components?, how do these mobile constituents accumulate? or how do they move?. Results from lysimeter studies are indispensable to such enquiries.

Leachates from LFH layers can have as high as 1.0 mg Fe and Al L⁻¹ believed to come mainly from the decomposition of the leaf and other plant litter. Additional amounts are mobilized from the congruent transformations of the minerals in the Ae horizon and contribute as high as 3.0 mg Fe L⁻¹ and 2.0 mg Al L⁻¹ to the leachates. Mineral dissolution is claimed to result mainly from action of the organic acids on the minerals. Among those acids are oxalic and citric which were identified with the use of ion-chromatography in the leachates from LFH and Ae horizons. The more general group of acids, the humic and fulvic acids, were identified in the leachates with the use of IR spectroscopy.

The relationship between organic acids and the mode of Fe and Al transport is one of the main concerns of this thesis. The amount of Fe leached from the Ae horizon

is highly reduced after the LFH layers above the horizon were removed. The decrease reaches as high as 2.0 mg Fe L^{-1} solution or about 50% of mobile Fe from the LFH and Ae horizons. The decrease is accompanied by a lower amount of oxalic acid in the leachate from the Ae horizons where LFH layers were removed as compared to the leachates from Ae where LFH layers are intact. Data for Al do not clearly show the trend observed for Fe. This finding supports one of the earliest concepts that Fe migrates as a chelate during the process of "podzolization" (*e.g.*, Rode, 1936; De Coninck, 1980; Duchaufour, 1982).

Other mobile components present in the leachates are the colloidal components which consists of phyllosilicates, Fe globules, quartz and feldspars. Globules of Fe are mainly ferrihydrite that can be transformed to hematite upon heat treatment to $750 \text{ }^\circ\text{C}$ for 2 hours. Mobilization of Fe in this form is believed to be the result of oxidation and reduction processes. The occurrence of reducing conditions is supported by the presence of lepidocrocite, a natural indicator of reducing condition.

The mobile phyllosilicates are mainly mica and vermiculite. Some of the vermiculite is interlayered and contains significant amounts of Fe and Al in their interlayer that can be as high as 20% of Fe and as high as 50% of the Al as extracted by dithionite-citrate-bicarbonate. The data suggest two things: (1) liberated Fe and Al can migrate as a component of the interlayered vermiculite and (2) dithionite-citrate-bicarbonate is inaccurate as a measure of total free Fe and Al in the pedons under study.

The translocated sand-size quartz and feldspar of about $100 \text{ }\mu\text{m}$ diameter are strongly etched. This reflects the aggressive mineral attack by organic acids in the Ae horizons. The movement of these larger fractions is through lessivage attributed to the episodic high pulses of migrating solutions during heavy rainstorms (Stoner and Ugolini, 1988).

Another mobile constituent is imogolite. Imogolite together with fine quartz accumulates as a whitish sediments at the bottom of the lysimeter collection beaker beneath the Ae horizon. The presence of imogolite in the leachates supports the proposition by Farmer (1982) that Al can migrate in the form of proto-imogolite, the precursor for imogolite formation. This and the earlier finding that Fe moves as an organo-metal complex, suggest the presence of both the inorganic and organic complexes in the genesis of Alberta Podzols. This is not surprising in view of the natural anisotropy of the pedons.

5.2.3. Processes of accumulation

Lysimeter results in chapter 4.1 show that the typical "podzolic signature" (Ugolini, 1988) is composed of two compartments: (1) leachates from the eluvial horizons enriched with metals and (2) leachates from Bf horizons impoverished with metals. The Bf horizon is the zone of immobilization which is consistent with an earlier generalizations based on microstructures.

Mobile organics and organo-metallic complexes are immobilized after they are rendered hydrophobic due to a change in pH or chelation of more metals in the Bf horizons. Adsorption into goethite nodules through chemisorption by the type A OH functional group is another mode of immobilization (*e.g.*, Collman *et al.*, 1987; Kung and McBride, 1989). The large goethite nodules occupy about 50% of the total area in the Bf1 horizon and are believed to play the major role in the immobilization of mobile components. Evidence for imogolite and phyllosilicates adsorbed onto the goethite nodules also suggests they served as the adsorbent for the mobile proto-imogolite complexes and the phyllosilicates.

5.2.4. Transformation of minerals

Vermiculitization of chlorite and mica is the major transformation of phyllosilicates observed in the study. The transformation leads to the formation of hydroxy interlayered vermiculite through aggradation of Al and Fe hydroxides in the interlayers although some of the HIV resulted from incomplete removal of the OH-sheets from clinocllore. The formation of HIV probably resulted is initiated in the eluvial horizons; while the following is the order of extent of vermiculite interlayering: Bf matrix > Bf nodule > Ae horizons.

In situ natural soil solutions from Ae and Bf horizons are saturated with respect to gibbsite, ferrihydrite and imogolite. The higher ordered Fe-oxides (goethite, hematite and lepidocrocite) are undersaturated in the Ae horizons but not in the Bf horizons.

The use of X-ray microdiffraction techniques enabled the identification of different goethite phases throughout the sola and through the measurement of *c*-dimension to evaluate Al for Fe substitution within each horizon. The lowest substitution (< 10 mole % Al) probably represents the allogenic goethite while the highest substitution (> 20 mole %) probably represents the pedogenic goethite. The higher Al activity due to aggressive mineral transformation may have resulted in the higher Al for Fe substitution in the pedogenic goethite.

Moreover, a higher microbial activity in the indurated nodules is implicated in contributing to the higher Al for Fe substitution of goethite, to the difference in the degree of vermiculite interlayering between Bf matrix and Bf nodule and to the formation of euhedral gypsum crystals. The higher microbial activity produces complexing organic ligands that prevent formation of alumino-silicates such as imogolite, and cause the higher Al activity available for Fe substitution in goethite and aggradation into hydroxides in the interlayers of vermiculite. Microbial activity can also mineralize a high amount of sulfur for crystallization to euhedral gypsum crystals.

5.3. Taxonomy of the pedons

The genetic bias of most classification systems can be easily seen in the use of diagnostic horizons or layer(s) as expressions of the dominant processes in the development of pedons and in placement of pedons in specific taxa in the classification system. Podzolic soils are no exception.

5.3.1. Diagnostic surface horizon

All the pedons have layers of fresh and decomposing leaf litter on the surface, admixed with few varieties of mosses and mineral matter deposited by aeolian activity. The layer(s) are not saturated with water during most of the year but may act as good reservoirs of water in the wet season. The diagnostic surface horizon of these pedons is the *ochric* epipedon, or a surface horizon with no special characteristics to affect the placement of the pedons in specific taxa (Soil Survey Staff, 1975; FAO-UNESCO, 1988). This horizon includes the LF layer and the Ae horizon. The diagnostic ochric epipedon is not recognized in the Canadian System of Classification.

5.3.2. Diagnostic subsurface horizons

The eluvial layer (Ae horizon) is a diagnostic *albic* horizon that is a from layer where phyllosilicates and iron oxides have been removed and the color is mainly due to the primary minerals in the silt and sand fractions (Soil Survey Staff, 1975; FAO, 1988). Albic horizons are not defined in the Canadian System of Soil Classification.

All the reddish Bf horizons are diagnostic *spodic* horizon following the latest criteria of the International Commission on Spodosols (ICOMOD, 1990) and is given in Appendix No. 7.5. The FAO-UNESCO system is expected to adopt the new definition of spodic horizon and in this thesis, classification of the pedons in the FAO system is based on the diagnostic horizons and properties as used in Soil Taxonomy (Soil Survey Staff, 1975).

In the Canadian system, the Bf horizons of pedons 2 and 3 meet the morphological and chemical requirements for *podzolic B*. The Bf horizon of pedon 1 meets the color and chemical requirements but not the minimum thickness of 10 cm.

5.3.3. Other diagnostic properties

Most of these properties are needed for the placement of the pedons in the family level of classification. The soil temperature regime of the pedons based on the climatological data given in chapter 3 and actual measurements of soil temperature at 30 cm depth during summer, is *cryic*; the mean annual soil temperature is > 0 °C but less than 8 °C and the mean annual summer soil temperature is < 8 °C. The measured summer temperature is 7 °C at 30 cm depth. In the Canadian system, the regime is classified as *cool*.

The soil moisture regime based on the moisture distribution is *udic*. It implies that in most years, the soil moisture control section is not dry for as long as 90 days (cumulative). This is equivalent to the humid regime of the Canadian system.

The particle size class for the three systems of soil classification is *sandy*. The mineralogical class is *mixed* and indicates that there is no particular mineral other than feldspar and quartz that makes up more than 40% of the mineral suite.

5.3.4. Classification of the pedons

The Order of the pedons studied are all Podzolic except for pedon 1 which does not meet the criteria for thickness requirements of podzolic B in the Canadian system. It is however, classified as a Brunisolic integrate to Podzols. The classification of the pedons up to family level is given below:

The Canadian System of Soil Classification (Canada Soil Survey Committee, 1978)

- Pedon 1: *Eluviated Dystric Brunisol, sandy, mixed, neutral, cool, humid*
- Pedon 2: *Orthic Humo-Ferric Podzol, sandy, mixed, neutral, cool, humid*
- Pedon 3: *Orthic Humo-Ferric Podzol, sandy, mixed, neutral, cool, humid*

Soil Taxonomy (Soil Survey Staff, 1975)

- Pedon 1: *sandy, mixed Entic Cryorthod*
- Pedon 2: *sandy, mixed Entic Cryorthod*
- Pedon 3: *sandy, mixed Entic Cryorthod*

FAO-UNESCO Soil Map of the World (FAO, 1990)

- Pedon 1: *Albi-Orthi-Haplic Podzol*
- Pedon 2: *Albi-Orthi-Haplic Podzol*
- Pedon 3: *Albi-Orthi-Haplic Podzol*

BIBLIOGRAPHY

- Adams, W. A. and J. K. Kassim. 1983. The origin of vermiculite in soils developed from lower Paleozoic sedimentary rocks in mid-Wales. *Soil Sci. Soc. Am. J.* 47:316-320.
- Alexiades, C. A. and M. L. Jackson. 1965. Quantitative determination of vermiculite in soils. *Soil Sci. Soc. Am. Proc.* 29: 522-527.
- Anderson, M. and P. M. Bertsch. 1988. Aluminum complexation in multiple ligand system. *Soil Sci. Soc. Am. J.* 52:1597-1602.
- Anderson, H. A., M. L. Berrow, V. C. Farmer, A. Hepburn, J. D. Russel and A. D. Walker. 1982. A reassessment of podzol formation processes. *J. Soil Sci.* 33:125-136.
- April, R. and D. Keller. 1990. Mineralogy of the rhizosphere in forest soils of the eastern United States. *Biogeochemistry* 9: 1-18.
- Arp, P. A. and R. Ouimet. 1986. Aluminum speciation in soil solution: equilibrium calculations. *Water, Air and Soil Poll.* 31:131-154.
- Aurousseau, P. 1983. Diagnostic properties and microfabrics of acid B horizon comparison with podzolic Bs, cambic Bw and acid eluvial horizon. p. 459-465. *In* P. Bullock and C.P. Murphy (ed). *Soil Micromorphology*. AB Academic Press, Oxford.
- Babel, U. 1985. Basic organic components. p. 74-87. *In* P. Bullock, N. Fedoroff, A. Jongerijs, G. Stoops and T. Tursina. 1985. *Handbook for soil thin section description*. Waine Research Publ. U.K. 152 pp.
- Bailey, S. W. 1980. Summary of the recommendation of AIPEA nomenclature committee. *Clays and Clay Miner.* 28: 73-78.
- Bailey, S. W. 1988. Chlorites: Structures and crystal chemistry. p. 347-398. *In* S. W. Bailey (ed) *Hydrous phyllosilicates. Reviews in Mineralogy # 19*. Bookcrafters, Inc. Chelsea, Michigan. 725 pp.
- Barnischel, R. I. and P. M. Bertsch. 1989. Chlorite and hydroxy interlayered vermiculite and smectite. p. 729-788. *In* J. B. Dixon and S. B. Weed (ed) *Minerals in Soil Environments*. 2nd ed. SSSA Book Series # 1.
- Beke, G. J. and S. Pawluk. 1971. The pedogenic significance of volcanic ash layers in the soils of an east slopes (Alberta) watershed basin. *Can. J. Earth Sci.* 8:664-675.
- Benoit, P. H. 1986. A computer package for indexing and least square refinements of powder diffraction data written by D.E. Appleman and H.T. Evans: Microcomputer version. Lehigh University, Bethlehem, Pa.
- Bergvist, B. 1987. Soil solution chemistry and metal budgets of spruce forest ecosystems in S. Sweden. *Water, Air and Soil Poll.* 33:131-154.

- Bloomfield, C. 1957. The possible significance of polyphenols in soil formation. *J. Soil Food and Agric.* 6:389-392.
- Brewer, R. 1976. Fabric and mineral analysis of soils. 2nd ed. R.E. Krieger Publishing Co. Huntington, New York. 482 pp.
- Brewer, R. and J. Sleeman. 1988. Soil structure and fabric. CSIRO Australia. 173 pp.
- Brewer, R. and S. Pawluk. 1975. Investigation of some soils developed in hummocks of the Canadian sub-Arctic and southern Arctic regions. I. Morphology and micromorphology. *Can. J. Soil Sci.* 55:301-319.
- Bullock, P. and M. L. Thompson. 1985. Micromorphology of Alfisols. p. 17-48. *In* L.A. Douglas and M.L. Thompson (ed) Soil Micromorphology and Soil Classification. SSSA Spec Publ # 15.
- Bullock, P., N. Fedoroff, A. Jongerius, G. Stoops and T. Tursina. 1985. Handbook for soil thin section description. Waine Research Publ. U.K. 152 pp.
- Buurman, P. and L. P. Van Reeuwijk. 1984. Proto-imogolite and the process of podzol formation: a critical note. *J. Soil Sci.* 35:447-452.
- Cabrera-Martinez, F., W. G. Harris, V. W. Carlisle and M. E. Collins. 1989. Partitioning of clay-size minerals in the coastal plain soils with sandy/loamy boundary. *Soil Sci. Soc. Am. J.* 53:1584-1587.
- Campbell, A. S. and U. Schwertmann. 1984. Iron-oxide mineralogy of placic horizons. *J. Soil Sci.* 35:569-582.
- Canada Soil Survey Committee. 1978. The Canadian system of soil classification. Can. Dep. Agric. Publ. # 1646. Supply and Services Canada, Ottawa, Ont. 164 pp.
- Cardile, C. M. 1989. Tetrahedral iron in smectite: A critical comment. *Clays and Clay Miner.* 37:156-158.
- Carney, H. J. and C. P. Sandgren. 1983. Chrysophycean cysts: Indicators of eutrophication in recent sediments of Frains Lake, Michigan, U.S.A.. *Hydrobiologia* 101:195-202.
- Carstea, D. D., M. E. Harward and E. G. Knox. 1970. Comparison of iron and aluminum hydroxy interlayers in montmorillonite and vermiculite. II. Dissolution. *Soil Sci. Soc. Am. Proc.* 34:522-526.
- Chesworth, W. and F. Macias-Vasques. 1985. pe, pH and podzolization. *Amer. J. of Sci.* 285:128-146.
- Coen, G. M. and R. W. Arnold. 1972. Clay mineral genesis of some New York Spodosols. *Soil Sci. Soc. Am. Proc.* 36:342-350.
- Collman, J. P., L. S. Hegedus, J. R. Norton and R. G. Finke. 1987. Principles and Application of Organotransition Chemistry. Univ. Sci. Books, Mill Valley, California.

- Cornell, R. M. and P. W. Schindler. 1980. Infra red study of the adsorption of hydroxy carboxylic acids on FeOOH and amorphous Fe(III) hydroxides. *Colloid and Polymer Sci.* 258:1171-1175.
- Cornell, R.M., W. Schneider and R. Giovanalli. 1989a. The transformation of ferrihydrite to lepidocrocite. *Clays and Clay Miner.* 24:549-553.
- Cornell, R. M., W. Schneider and R. Giovanalli. 1989b. Phase transition in the ferrihydrite/cysteine system. *Polyhedron* 8:2829-2836.
- Coulson, C. B., R. I. Davis, and P. A. Lewis. 1960. Polyphenols in plant, humus and soils. I. Polyphenols of leaves, litter and surficial humus from mull and mor sites. *J. Soil Sci.* 11:20-29.
- Dahlgren, R. A. and F. C. Ugolini. 1989. Formation and stability of imogolite in a tephritic Spodosol, Cascade Range, Washington, U.S.A. *Geochim. Cosmochim. Acta.* 53:1897-1904.
- David, M. B. and C. T. Driscoll. 1983. Aluminum speciation and equilibria in soil solutions of a Haplorthod in the Adirondack mountains (New York, U.S.A.). *Geoderma* 33:297-318.
- David, M. B., J. M. Mitchell and J. P. Nakas. 1982. Organic and inorganic sulfur constituents of a forest soil and their relationships to microbial activity. *Soil Sci. Soc. Am. J.* 46:847-857.
- De Coninck, F. 1980. Major mechanisms in the formation of spodic horizon. *Geoderma* 24:101-128.
- De Coninck, F., F. W. Jensen and C. De Kimpe. 1987. Evolution of silicates, especially phyllosilicates during podzolization. p. 147-161. *In* D. Righi and A. Chauvel (ed) *Podzol and Podzolization*, AFES, INRA, Paris.
- De Coninck, F. R. Langhor, J. Embrechts and E. Van Ranst. 1986. The Belgian soil classification system under the microscope. *Pedologie* 36:235-261.
- De Coninck, F. and J. A. McKeague. 1985. Micromorphology of spodosols. p. 121-144. *In* L.A. Douglas and M.L. Thompson (ed) *Soil Micromorphology and soil classification*. SSSA Spec. Publ. # 15.
- De Coninck, F. and D. Righi. 1983. Podzolization and the spodic horizon. p. 389-417. *In* P. Bullock and C.P. Murphy (ed). *Soil Micromorphology*. AB Academic Press, Oxford.
- De Geyter, G., S. Hoste, G. Stoops, R. Vandenberghe and L. Verdonck. 1982. Mineralogy of the ferriferous soil materials in the source area of Blanchimont (Province of Liege), Belgium. *Pedologie* 32:349-366.
- Driscoll, C. T., N. van Breemen, and J. Mulder. 1985. Aluminum chemistry in a forested Spodosol. *Soil Sci. Soc. Am. J.* 49:437-444.
- Duchaufour, P. 1982. *Pedology*. T.R. Paton (trans.), Allen and Unwin, London.

- Duff, K. E. and J. P. Smol. 1988. Chrysophycean stomatocysts from the post glacial sediments of the high Arctic lake. *Can. J. Bot.* 66:1117-1128.
- Dufresne, A. and W. H. Hendershot. 1986. Comparison of Al speciation in soil solutions extracted by batch and column methods. *Can. J. Soil Sci.* 66:367-371.
- Dumanski, J., T. M. Macyk, C. F. Veavy and J. D. Lindsay. 1972. Soil Survey and Land Evaluation of the Hinton-Edson Area, Alberta. Alberta Institute of Pedology Report # s-72-31. 119 pp.
- Dumanski, J. 1970. A micromorphological investigation of the genesis of soils developed on calcareous aeolian material. Ph D Thesis. University of Alberta. 143 pp.
- Eggleton, R. A. 1987. Noncrystalline Fe-Si-Al oxyhydroxides. *Clays and Clay Miner.* 35:29-37.
- Evans, L. J.. 1980. Podzol development north of Lake Huron in relation to geology and vegetation. *Can. J. Soil Sci.* 60:527-539.
- Fanning, D. S., V. S. Keramidas and M. A. El-Desoky. 1989. Micas. p. 551-634. *In* J.B. Dixon and S.B. Weed (ed) *Minerals in Soil Environments*. 2nd ed. SSSA Book Series # 1.
- FAO-UNESCO. 1988. FAO-UNESCO Soil Map of the World. FAO-UNESCO World Soil Resources Report. 56 pp.
- Farmer, V. C. 1981. Possible roles of mobile hydroxyaluminium orthosilicate complex (proto-imogolite) in podzolization. p. 275-279. *In* Migration organominérales dans les sols tempérés. Coll. Int. du CNRS, No. 3. , Nancy, France.
- Farmer, V. C. 1982. Significance of the presence of allophane and imogolite in Podzol Bs horizon for podzolization mechanisms: A review. *Soil Sci. Plt. Nutr.* 28:571-578.
- Farmer, V. C. 1984. Distribution of allophane and organic matter in podzol B horizons: reply to Buurman and Van Reeuwijk. *J. Soil Sci.* 35:453-458.
- Farmer, V. C. and A. R. Fraser. 1982. Chemical and colloidal stability of sols in the Al_2O_3 - Fe_2O_3 - SiO_2 - H_2O system: their role in podzolization. *J. Soil Sci.* 33:737-742.
- Farmer, V. C., J. D. Russel and M. L. Berrow. 1980. Imogolite and proto-imogolite allophane in spodic horizon: evidence for mobile aluminum silicate complex in podzol formation. *J. Soil Sci.* 31:673-684.
- Farmer, V. C., W. J. McHardy, L. Robertson, A. Walker and M.J. Wilson. 1985. Micromorphology and sub-microscopy of allophane in a podzol Bs horizon: evidence for translocation and origin. *J. Soil Sci.* 36:87-95.

- Fernandez-Marcos, M. L., F. Macias-Vasquez and F. Guitian-Ojea. 1979. Contribution to the study of the stability of clay minerals from soil solution composition at different pF values. *Clay Miner.* 14:29-38.
- Fitzgerald, J. W. 1978. Naturally-occurring organo-sulfur compound in soils. p. 391-440. *In* J.O. Nriagu (ed) *Sulfur in the Environment. Part II. Ecological Importance.* John Wiley and Sons, Toronto.
- Fitzpatrick, P. W. and U. Schwertmann. 1981. Al-substituted goethite-an indicator of pedogenic and other weathering environments in South Africa. *Geoderma* 27:335-347.
- Flach, K. W., C. S. Holshey, F. De Coninck and R. J. Bartlett. 1980. Genesis and classification of Andepts and Spodosols. p. 411-426. *In* B.K.G.Theng (ed) *Soils with variable charge.* New Zealand Society of Soil Science. Soils Bureau. Dept of Science and Industrial Research, Lower Hutt, New Zealand.
- Fordham, A. W., R. H. Merry and K. Norrish. 1984. Occurrence of microcrystalline goethite in an unusual fibrous form. *Geoderma* 135-148.
- Foster, N. W. and J. A. Nicholson. 1986. Trace elements in the hydrologic cycle of a tolerant hardwood forest ecosystem. *Water, Air and Soil Pollution.* 31:501-508.
- Fox, L. E. 1988. Solubility of colloidal ferric hydroxide. *Nature* 333:442-444.
- Friesleben, N. E. V. and L. Rasmussen. 1986. Effects of acid rain on ion leaching in a Danish forest soil. *Water, Air and Soil Poll.* 31:965-968.
- Ghabru, S. K., A. R. Mermut and R. J. St. Arnaud. 1990. Isolation and characterization of iron-rich chlorite-like minerals from soil clays. *Soil Sci. Soc. Am. J.* 54: 281-287.
- Guthrie, R. L. and J. E. Witty. 1982. New designations for soil horizons and layers and the new soil survey manual. *Soil Sci. Soc. Am. J.* 46:443-444.
- Hallmark, C. T., L. P. Wilding and N. E. Smeck. 1982. Silicon. p. 263-271. *In* Page *et al.* (ed) *Methods of soil analysis, Part 2: Chemical and microbiological properties.* 2nd ed, ASA, SSSA, Madison, WI.
- Hantschel, R., M. Kaupenjohann, R. Horn and W. Zech. 1986. Kationen Konzentrationen in der Gleichgewichts-und perkolation bodenlosung (GBL und PBL)-ein methodenvergleich. *Z. Pflanzehernähr., Dung. Bodenkunde* 144:136-139.
- Harris, W. G., K. A. Hollien, T. L. Yuan, S. R. Bates and W. A. Acree. 1988. Non-exchangeable potassium associated with hydroxy interlayered minerals from coastal plain soils. *Soil Sci. Soc. Am. J.* 52:1486-1492.
- Hendershot, W. H., H. Lalonde and A. Dufresne. 1984. Aluminum speciation and movement in three small watersheds in the southern Laurentians. *Water Poll. Res. J. Can.* 19:11-26.

- Hornung, M., P. A. Stevens and B. Reynolds. 1986. The impact of pasture improvement on the soil solution chemistry of some stagnopodzols in Mid-Wales. *Soil Use Mgt.* 2:18-26.
- Howitt, R. and S. Pawluk. 1985. The genesis of Gray Luvisols within the boreal forest. II. Dynamic pedology. *Can. J. Soil Sci.* 65:9-19.
- ICOMOD. 1984. A brief review of spodosol taxonomic placement as influenced by morphology and chemical criteria. Circular #1. April 1984.
- ICOMOD. 1990. International Committee on the Classification of Spodosols, Circular Letter #9, 23 March 1990.
- Jensen, F. A. 1988. Molecular weight fractionation of Fe and Al species in Podzols and phenolic acid retention by amorphous Fe hydroxides. M. Sc. Thesis. University of Guelph. 277 pp.
- Joffe, J. S. 1949. *Pedology*. 2nd ed. Pedology Publ., Somerset Press, Inc. Somerville, New Jersey. 662 pp.
- Johnson, B. N. 1989. Ergosterol content and activities of polyamine biosynthesis enzymes to characterize mycorrhizal root:soil system. Ph. D. Thesis. University of Alberta.
- Kassim, J. K., S. N. Gafoor and W. A. Adams. 1984. Ferrihydrite in pyrophosphate extract of podzol B horizon. *Clay Min.* 19:99-106.
- Kharaka, Y. K., W. D. Gunter, P. K. Aggarawall, E. H. Perkins, and J. D. De Bral. 1988. SOLMINEQ-88: A computer program code for geochemical modelling of water-rock interactions. US Geological Water Investigation Report # 88, Washington, D.C. U.S.A.
- Kittrick, J. 1980. Gibbsite and kaolinite solubilities by immiscible displacement of equilibrium solution. *Soil Sci. Soc. Am. J.* 44:139-142.
- Kittrick, J. A. 1971. Montmorillonite equilibrium and weathering environments. *Soil Sci. Soc. Am. Proc.* 35:815-820.
- Kodama, H. and C. Wang. 1989. Distribution of characterization of non-crystalline inorganic components in Spodosols and Spodosol-like soils. *Soil Sci. Soc. Am. J.* 53:526-534.
- Kodama, H. and M. Schnitzer. 1973. Dissolution of chlorite minerals by fulvic acids. *Can. J. Soil Sci.* 53:240-243.
- Kooistra, M. J. 1990. The future of soil micromorphology. p.1-8. *In* L.A. Douglas (ed). *Soil Micromorphology: A basic and applied science*. Elsevier, Amsterdam. 716 pp.
- Kung, K. H. 1989. Surface reactions of low molecular weight phenols and benzoic acids with manganese and iron oxides. Ph. D. Thesis. Cornell University. 98 pp.

- Kung, K. H. and M. McBride. 1989. Adsorption of para-substituted benzoates on iron oxides. *Soil Sci. Soc. Am. J.* 53:1673-1678.
- Lagaly, G. and A. Weiss. 1969. Determination of the layer charge in mica-type layer silicates. p. 61-80. *In* L. Heller (ed) *Proc. Int. Clay Conf.*, Tokyo. Israel Univ. Press, Jerusalem.
- Lietzke, D. A. and G. A. McGuire. 1987. Characterization and classification of soils with spodic morphology in southern Appalachian. *Soil Sci. Soc. Am. J.* 51:165-170.
- Loveland, P. J. and B. Clayden. 1987. A hardpan podzol of Yarnewood, Devon. *J. Soil Sci.* 38:357-367.
- Manley, E. P., W. Chesworth and L. J. Evans. 1987. The solution chemistry of podzolic soils from the eastern Canadian shield: a thermodynamic interpretation of the mineral phases controlling soluble Al^{+3} and H_4SiO_4 . *J. Soil Sci.* 38:39-51.
- Matsue, N. and K. Wada. 1988. Interlayer materials of partially interlayered vermiculite in Dystrochrepts derived from Tertiary sediments. *J. Soil Sci.* 39:155-162.
- May, H. M., D. G. Kinniburgh, P. A. Helmke and M. L. Jackson. 1986. Aqueous dissolution, solubilities and thermodynamic stabilities of common aluminosilicate clay minerals: kaolinite and smectite. *Geochim. Cosmochim. Acta.* 50:1667-1677.
- McDowell, W. H. and T. Wood. 1984. Podzolization: soil processes control dissolved organic carbon concentrations in stream water. *Soil Sci.* 137:23-32.
- McGill, W. B. and J. R. Spence. 1985. Soil fauna and soil architecture: Feedback between size and architecture. *Questiones Entom.* 21:695-634.
- McGill, W. B. and R. J. K. Myers. 1987. Controls on dynamics of soil and fertilizer nitrogen. p. 73-99. *In* *Soil Fertility and Organic Matter as Critical Components of the Production System.* SSSA Spec Publ # 19.
- McIntosh, P. D., W. G. Lee and T. Backs. 1983. Soil development and vegetation trend along a rainfall gradient in the east of Otago upland. *New Zealand J. Sci.* 26:379-401.
- McKeague, J. A. (ed) 1981. *Manual on soil sampling and methods of analysis.* Canadian Soil Survey Committee, Can. Soil Survey.
- McKeague, J. A. 1967. An evaluation of 0.1M pyrophosphate and pyrphosphate-dithionite in comparison with oxalate as extractants of the accumulation products in podzols and some other soils. *Can. J. Soil Sci.* 47: 95-99.
- McKeague, J. A. 1983. Clay skins and the argillic horizons. p.367-387. *In* P. Bullock and C.P. Murphy (ed) *Soil Micromorphology.* AB Academic Press, Oxford. 706 pp.

- McKeague, J. A., F. De Coninck and D. P. Franzmeier. 1983. Spodosols. In L.P. Wilding, N.E. Smeck and C.F. Hall (ed) *Pedogenesis and soil taxonomy: II. The soil orders*. Elsevier Publishing, Amsterdam.
- Mehra, O. P. and M. L. Jackson. 1960. Iron removal from soils and clays by dithionite-citrate system buffered with sodium bicarbonate. p. 317-327. In A. Swineford (ed) *Proc. 7th Nat. Conf. Clays and Clay Miner. Monograph 5*. Pergamon Press, New York.
- Milnes, A. R. and V. C. Farmer. 1987. Micromorphological and analytical studies of the fine matrix of an Australian humus iron Podzol. *J. Soil Sci.* 38:593-606.
- Mizota, C. 1982. Clay mineralogy of spodic horizons from Cryorthods in Japan. *Soil Sci. Plt. Nutr.* 28:257-268.
- Nilsson, S. I. and B. Bergvist. 1983. Aluminum chemistry and acidification processes in a shallow podzol on the Swedish west coast. *Water, Air and Soil Poll.* 20:311-329.
- Nordstrom, D. K. 1982. The effect of sulfate on aluminum concentration in natural waters: some stability relation in the system $Al_2O_3-SO_3-H_2O$ at 298 °K. *Geochim. Cosmochim. Acta.* 46:681-692.
- Nordstrom, D. K. and J. W. Ball. 1986. The geochemical behavior of aluminum in acidified waters. *Science* 2:54-56.
- Norrish, K. and R. M. Taylor. 1961. The isomorphous replacement of iron by aluminum in soil goethites. *J. Soil Sci.* 12:294-306.
- Olis, A. C., P. B. Malla and L. A. Douglas. 1990. The rapid estimation of the layer charges in 2:1 expanding clays from single alkylammonium ion expansion. *Clay Miner.* 25:39-50.
- Parfitt, R. L. 1990. Allophane in New Zealand - A Review. *Aust. J. Soil Sci.* 28:343-60.
- Page, A. L., R. H. Miller and D. R. Keeney. 1982. *Methods of soil analysis, Part 2: Chemical and microbiological properties*. 2nd ed. ASA, SSSA, Madison .
- Parfitt, R. L., V. C. Farmer and J. D. Russel. 1977. Adsorption of hydrous oxides. 1. Oxalate and benzoate on goethite. *J. Soil Sci.* 28:29-39.
- Pawluk, S. 1983. Fabric sequences as related to genetic processes in two Alberta soils. *Geoderma* 30:233-242.
- Pawluk, S. 1985. Soil micromorphology and soil fauna: Problems and importance. *Questiones Entom.* 21:473-496.
- Pawluk, S. and R. Brewer. 1975. Micromorphological, mineralogical and chemical characteristics of some Alpine soils and their genetic implications. *Can. J. Soil Sci.* 55:415-437.
- Pettapiece, W. W. 1970. *Pedological investigations in the front ranges of the Rocky mountains along the north Saskatchewan River Valley*. Ph D Thesis. University of Alberta. 185 pp.

- Ponomareva, V. V.. 1969. Theory of Podzolization. IPST Press, Jerusalem. 309 pp.
- Rabenhorst, M. D., D. S. Fanning, and J. E. Foss. 1982. Regularly interstratified chlorite/vermicuited in soils over meta-igneous mafic rocks in Maryland. *Clays and Clay Miner.* 36:156-158.
- Rasmussen, L.. 1986. Potential leaching of elements in three Danish Spruce forest soils. *Water, Air and Soil Poll.* 31:377-383.
- Righi, D. and F. De Coninck. 1977. Mineralogic evolution in hydromorphic sandy soils and podzols in "Landes du Medoc", France. *Geoderma* 19:339-359.
- Righi, D. and J. P. Borot. 1985. Occurrence of Podzolic soils with reversed Bh and Bs horizons on the Plateau de Millevaches (Massif Central, France). *Sci. du Sol.* 3:129-138.
- Righi, D. and L. Lorphelin. 1986. Weathering of silt and clay in soils of a toposequence in the Himalayas, Nepal. *Geoderma* 39:741-755.
- Righi, D., E. Van Ranst, F. De Coninck and B. Guillet. 1982. Microprobe study of a plachomod in the Antwerp campine (North Belgium). *Pedologie* 32:117-134.
- Robert, M. and J. Berthelin. 1986. Role of biological and biochemical factors in soil mineral weathering. SSSA spec. publ. #17.
- Rode, A. A. 1936. The problem of the degree of podzolization. *Trans. Dockuchaev Soils Institute.* 13:113-161.
- Roed, M. A. 1968. Surficial geology of the Edson-Hinton Area, Alberta. Ph. D. Thesis. University of Alberta.
- Rosanov, A. N. 1961. Serozems of central Asia. Israel Program for Scientific Translation. Jerusalem.
- Ross, G. J. and H. Kodama. 1977. Experimental transformation of chlorite into vermiculite. *Clays and Clay Miner.* 22:205-211.
- Ross, G. J., C. Wang, A. I. Ozkan and H. W. Rees. 1982. Weathering of chlorite and mica in New Brunswick Podzol on till derived from chlorite-mica schist. *Geoderma* 27:255-267.
- Ross, G. J., N. M. Miles and H. Kodama. 1979. Occurrence and determination of lepidocrocite in Canadian soils. *Can. J. Soil Sci.* 59:155-162.
- Rourke, R. V., B. R. Brasher, R. D. Yeck and F. T. Miller. 1988. Characteristic morphology of U.S. Spodosols. *Soil Sci. Soc. Am. J.* 52:445-449.
- Rule, A. C. and S. W. Bailey. 1987. Refinement of the crystal structure of a monoclinic ferroan clinichlore. *Clays and Clay Miner.* 35:129-138.
- Samoilova, E. M. 1986. Concept of elementary pedogenetic process. *Pochvovedenie* 41:7-12.

- Schulze, D. G. 1981. Identification of soil iron oxide minerals by differential X-ray diffraction. *Soil Sci. Soc. Am. J.* 45: 437-440.
- Schulze, D. G. 1984. The influence of aluminum on iron oxides. VIII. Unit cell dimensions of Al-substituted goethites and estimation of Al from them. *Clays and Clay Miner.* 32:36-44.
- Schwertmann, U.: 1964. Differenzierung der Eisenoxide des Bodens durch Extraktion mit Ammoniumoxalat Lösung. *Z. Pflanzehernähr., Dung. Bodenkunde* 105:194-202.
- Schwertmann, U. 1985. Occurrence and formation of Fe oxides in various pedoenvironments. *In Iron in soils and Clay minerals. A NATO advanced study institute on Fe. Bad Windsheim, FRG.1-13 July,1985.*
- Schwertmann, U., D. Schulze and E. Murad.1982. Identification of ferrihydrite in soils by dissolution kinetics, differential X-ray diffraction and Mössbauer spectroscopy. *Soil Sci. Soc. Am. J.* 46:869-875.
- Schwertmann, U. and R. M. Taylor. 1989. Iron oxides. p.379-427. *In J.B. Dixon and S.B. Weed (ed) Minerals in Soil Environments. 2nd ed. SSSA Book Series # 1.*
- Scott, A. D. and J. Amonette. 1988. Role of mica in weathering. p. 537-623. *In J.W. Stucki, B.A. Goodman and U. Schwertmann (ed) Iron in soils and clay minerals. D. Reidel Publishing Co.*
- Shoji, S. T., Y. Fujiwara, I. Yamada and M. Saigusa.1982. Chemistry and mineralogy of ando soils, brown forest earth, and podzolic soils formed from recent Towada ashes, northeastern Japan. *Soil Sci.* 133:69-86.
- Shoji, S. T., Y. Takahashi, M. Saigusa, I. Yamada and F. C. Ugolini. 1988. Properties of Spodosols and Andisols showing climosequential and biosequential relations in southern Hokkaido, northeastern Japan. *Soil Sci.* 145:135-150.
- Simmard, R. R., L. J. Evans and T. E. Bates.1988. The effects of CaCO₃ and P on the soil solution chemistry of a podzolic soil. *Can. J. Soil Sci.* 68:41-52.
- Singer, M., F. C. Ugolini and J. Zachara. 1978. *In situ* study of podzolization of tephra and bedrock. *Soil Sci. Soc. Am. J.* 42:105-111.
- Smith, C. A. S., G. M. Coen and D. J. Pluth. 1981. Podzolic soils with Luvisolic-like morphologies in the upper subalpine subzone of the Canadian Rockies. I: Stratigraphy and mineralogy. *Can. J. Soil Sci.* 61: 325-335.
- Smol, J. P. 1988. Chrysophycean microfossils in paleolimnological studies. *Paleoeco. Paleoclim. Paleoeco.* 62:287-297.
- Soil Survey Staff. 1960. Soil classification, a comprehensive system, 7th approximation. Soil Conserv. Service, USDA. US Govt. Printing Office, Washington, D.C. 503 pp.

- Soil Survey Staff. 1975. Soil Taxonomy. Agricultural Handbook 436. Soil Conservation Service, USDA, Washington, D.C.
- Spiers, G. A. 1990. Mineral transformation and authigenesis in selected Alberta soils. Ph. D. Thesis. University of Alberta. 173 pp.
- Stanjek, H. 1987. The formation of maghemite and hematite from lepidocrocite and goethite in Cambisol in Corsica, France. *Z. Pflanzenernähr., Dung. Bodenkunde* 150:314-318.
- Stoner, M. G. and F. C. Ugolini. 1988. Arctic Pedogenesis: 2. Threshold-controlled leaching episodes. *Soil Sci.* 145:46-51.
- Stoops, G. and A. Jongerius. 1975. Proposal for the micromorphological classification of soil materials: I. A classification of the related distributions of the fine and coarse particles. *Geoderma* 23: 189-199.
- Sullivan, L. A. and J. A. Koppi. 1987. *In situ* organic matter studies using scanning electron microscopy and low-temperature ashing. *Geoderma* 40:317-332.
- Tait, J. M., N. Yoshinaga and B. D. Mitchell. 1978. The occurrence of imogolite in some Scottish soils. *Soil Sci. Plt. Nutr.* 24:145-151.
- Takahashi, T., S. Shoji and A. Sato. 1989. Clayey spodosols and andisols showing bisequential relation from the Shinokita peninsula, northeastern, Japan. *Soil Sci.* 148:204-218.
- Tongokonov, V. D., B. P. Gradusov, N. Ye. Rubilina, V. O. Targul'yan and N. P. Chizhikova. 1987. Differentiation of the mineral and chemical composition in sod-podsolic and podzolic soils. *Soviet Soil Sci.* 19:23-36.
- Turner, R. V. and J. E. Brydon. 1965. Effect of length of time of reaction on some properties of suspensions of Arizona bentonite, illite and kaolinite in which aluminum hydroxide is precipitated. *Soil Sci.* 103:111-117.
- Twardy, A. G. and I. G. W. Corns. 1980. Soil Survey and Interpretations of the Wapiti Map Area, Alberta. Alberta Institute of Pedology Bull. # 39. 134 pp.
- Ugolini, F. C. and R. A. Dahlgren. 1987. The mechanism of podzolization as revealed by soil solution studies. p. 195-203. *In* D. Righi and A. Chauvel (ed) *Podzol and Podzolization*. AFES, INRA, Paris, France.
- Ugolini, F. C., H. Dawson and J. Zachara. 1977. Direct evidence of particle migration in the soil solution of a Podzol. *Science* 198: 603-650.
- Ugolini, F. C., M. G. Stoner and D. J. Marrett. 1987. Arctic pedogenesis: 1. Evidence for contemporary podzolization. *Soil Sci.* 144:90-100.
- Ugolini, F. C., R. Dahlgren, S. Shoji and T. Ito. 1988. An example of andosolization and podzolization as revealed by soil solution studies, southern Hokkaido, northeastern Japan. *Soil Sci.* 145:111-125.

- van der Marel, H. W. and H. Beutelspacher. 1976. Atlas of Infrared Spectroscopy of Clay Minerals and their Admixtures. Elsevier Sci. Publ. Co. Amsterdam. 396 pp.
- Van Ranst, E., D. Righi, F. De Coninck, A. M. Robin and M. Jamagne. 1980. Morphology, composition and genesis of argillans and organans in soils. *J. Microscopy* 120:353-361.
- Vance, G. F., S. A. Boyd, and D. L. Mokma. 1985. Extraction of phenolic compounds from a Spodosol profile: an evaluation of three methods. *Soil Sci.* 140:412-420.
- Vance, G. F., D. L. Mokma and S. A. Boyd. 1986. Phenolic compounds in soils of hydrosequences and development sequences of Spodosols. *Soil Sci. Soc. Am. J.* 50:992-996.
- Vempati, R. K., R. H. Loeppert, H. Sittertz-Bhatkar and R. C. Burghardt. 1990. Infra red vibrations of hematite formed from aqueous- and dry-incubation of Si-containing ferrihydrite. *Clays and Clay Miner.* 38:294-298.
- Wada, K., Y. Kakuto and K. Fukuhara. 1987. "Chloritized" vermiculite and smectite in some Inceptisols and Spodosols. *Soil Sci. Plt. Nutr.* 33:317-326.
- Wang, C. and H. Kodama. 1986. Pedogenetic imogolite in sandy Brunisols of eastern Ontario. *Can. J. Soil Sci.* 66: 135-142.
- Wang, C. and J. A. McKeague. 1982. Illuviated clay in sandy podzolic soils of New Brunswick. *Can. J. Soil Sci.* 62:79-89.
- Wang, C., J. A. McKeague and H. Kodama. 1986. Pedogenetic imogolite and soil environments: case study of Spodosols in Quebec, Canada. *Soil Sci. Soc. Am. J.* 50:711-718.
- Warren, C. J., B. Xing and M. J. Dudas. 1990. Procedure for microwave digestion and total dissolution of inorganic soil and clay minerals. *Can. J. Soil Sci.* 70:617-720.
- Whitehead, D. C., H. Dibb, and R. D. Hartley. 1983. Bound phenolic compounds in water extracts of soil, plant and leaf litter. *Soil Biol. Biochem.* 15:133-136.
- Wicks, F. J. and J. Zussman. 1975. Microbeam X-ray diffraction patterns of the serpentine minerals. *Can. Miner.* 13:244-258.
- Wilding, L. P. Preface. p. vii-x. *In* L.A. Douglas (ed). *Soil Micromorphology: A basic and applied science.* Elsevier, Amsterdam. 716 pp.
- Yapp, C. 1983. Effects of $AlOOH.FeOOH$ solid solution on Gt-Hm equilibrium. *Clays and Clay Miner.* 31:239-240.

- Zeltner, W. A., E. C. Yost, M. L. Machesky, M. I. Tejedor-Tejedor and M. A. Anderson. 1986. Characterization of anion binding on goethite using titration calorimetry and cylindrical internal reflection-fourier transform infrared spectroscopy. p.142-161. *In* J.A. Davis and K. F. Hayes (ed) *Geochemical Processes at Mineral Surfaces*. Amer. Chem. Soc. Symp. Series # 323.
- Zinder, S. H. and T. D. Brock. 1978. Mineral transformation of sulfur in the environment. p.445-466. *In* J.O. Nriagu (ed) *Sulfur in the Environment*. Part II. Ecological Importance. John Wiley and Sons, Toronto.

Appendix 7.1. Distribution of different sand fractions in Podzolic soils from Alberta.

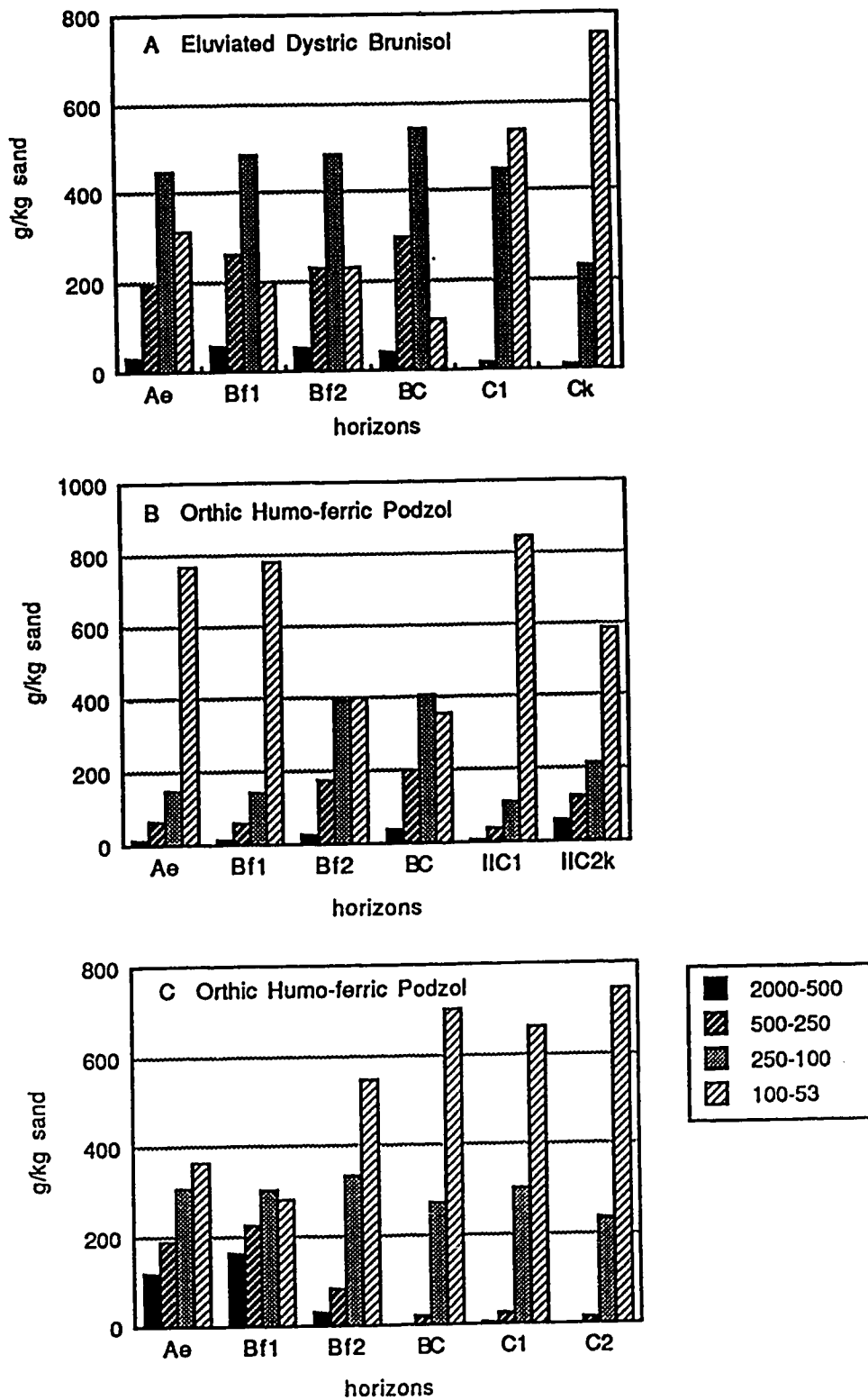


Fig. 7.1.1. Distribution of different sand fractions in Podzolic soils from Alberta.

Appendix 7.2. X-ray diffractograms of clay fractions of Podzolic soils from Alberta.

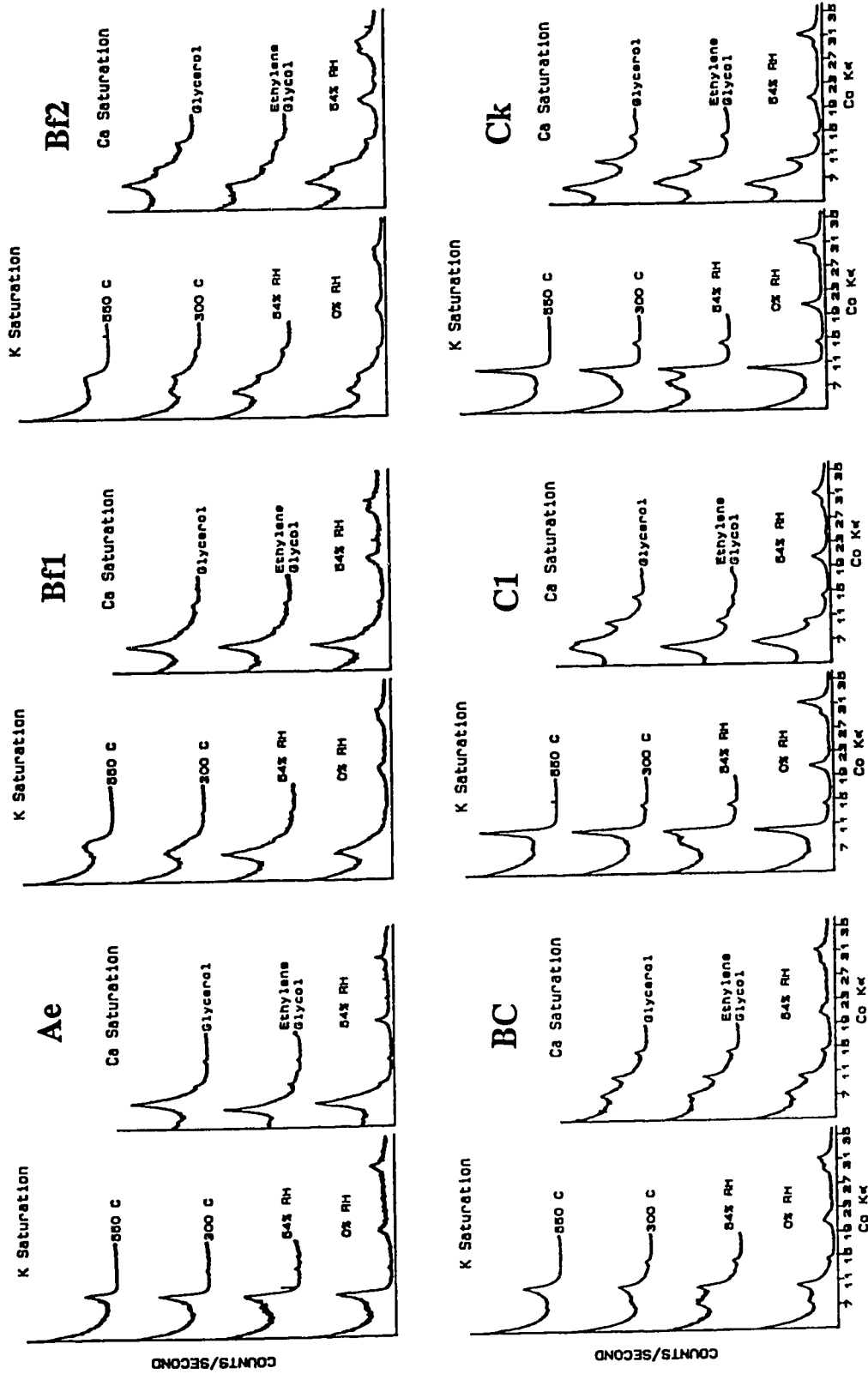


Fig. 7.2.1. X-ray diffractograms of fine clays in pedon 1.

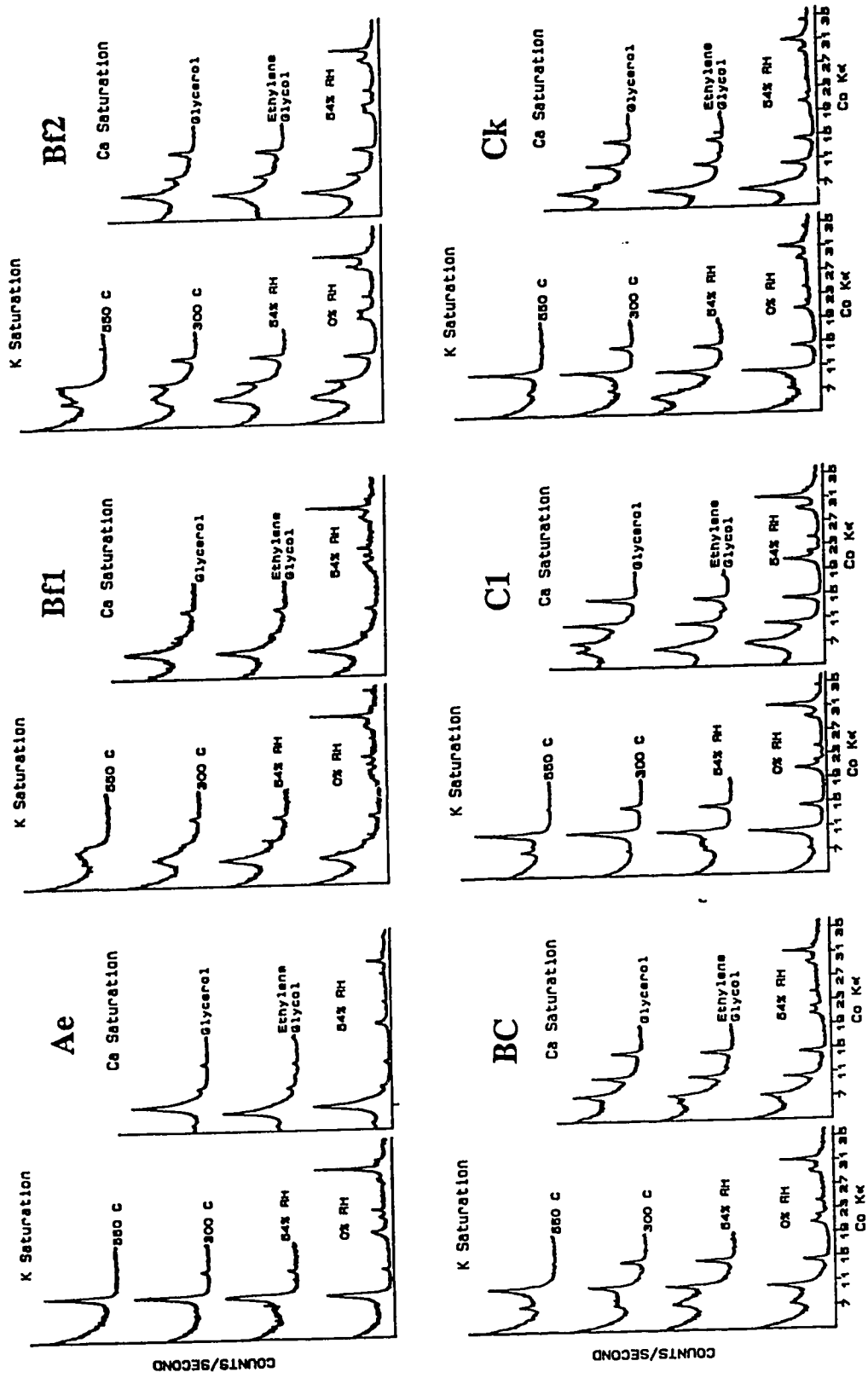


Fig. 7.2.2. X-ray diffractograms of coarse clays in pedon 1.

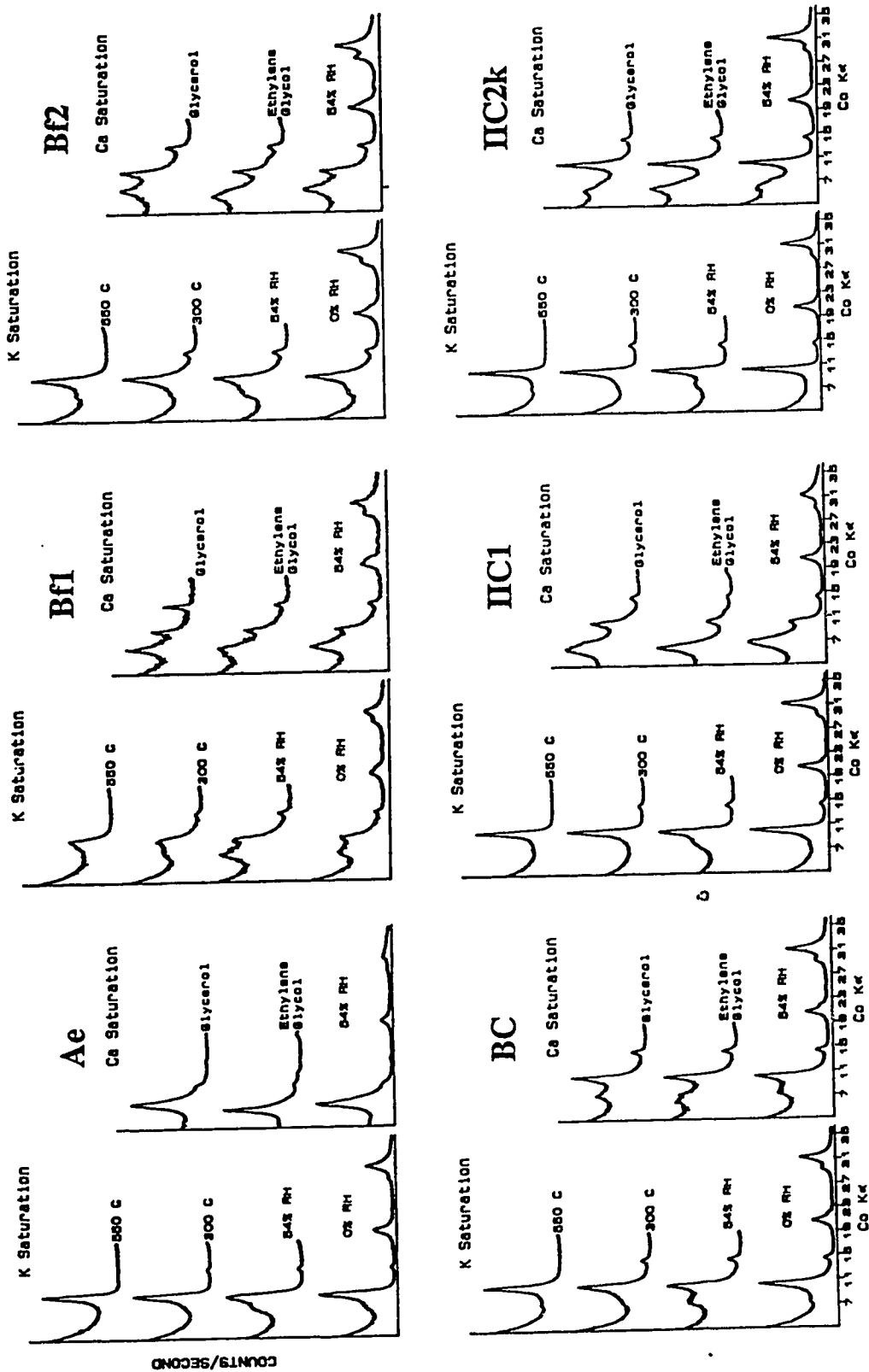


Fig. 7.2.3. X-ray diffractograms of fine clays in pedon 2.

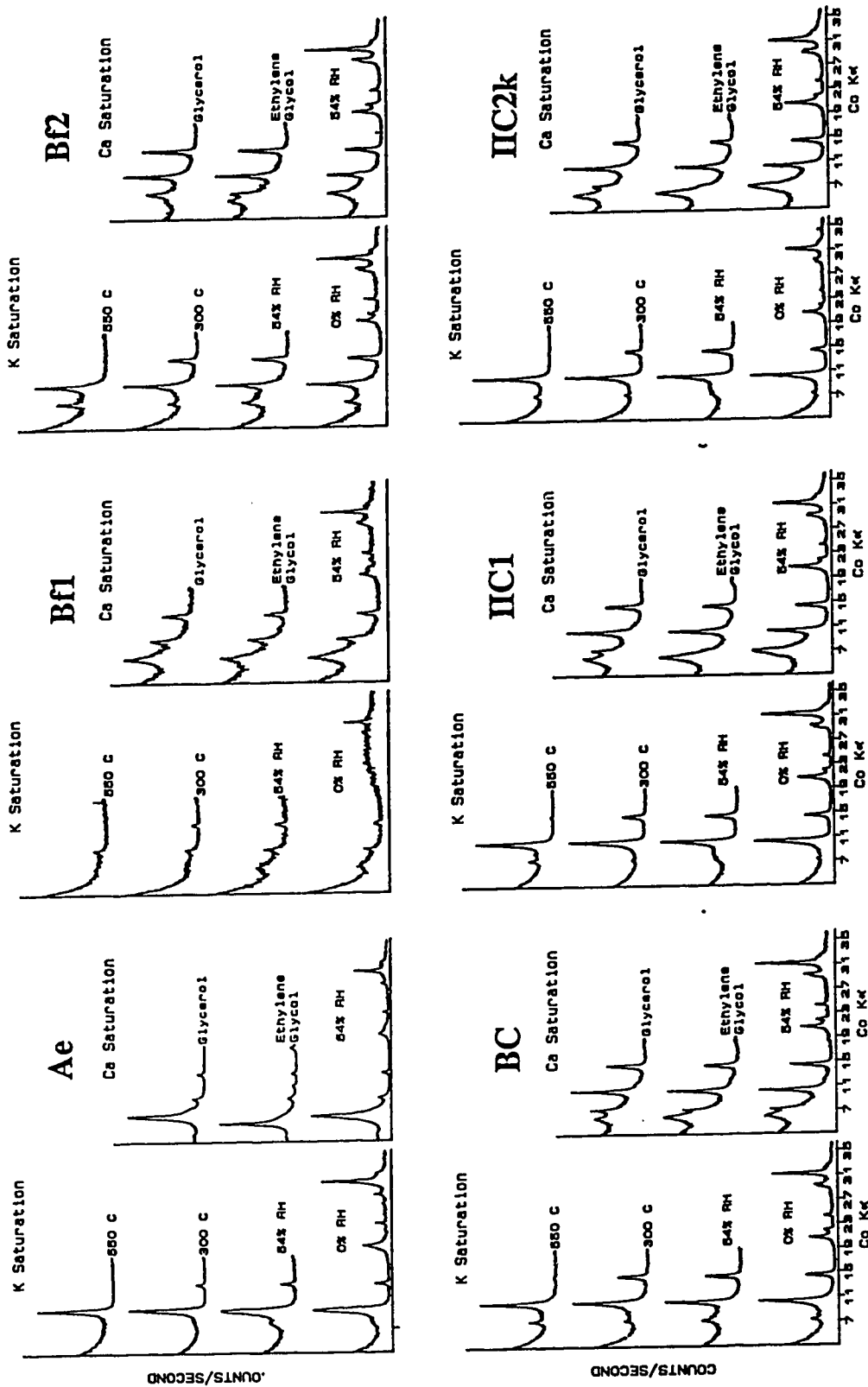


Fig. 7.2.4. X-ray diffractograms of coarse clays in pedon 2.

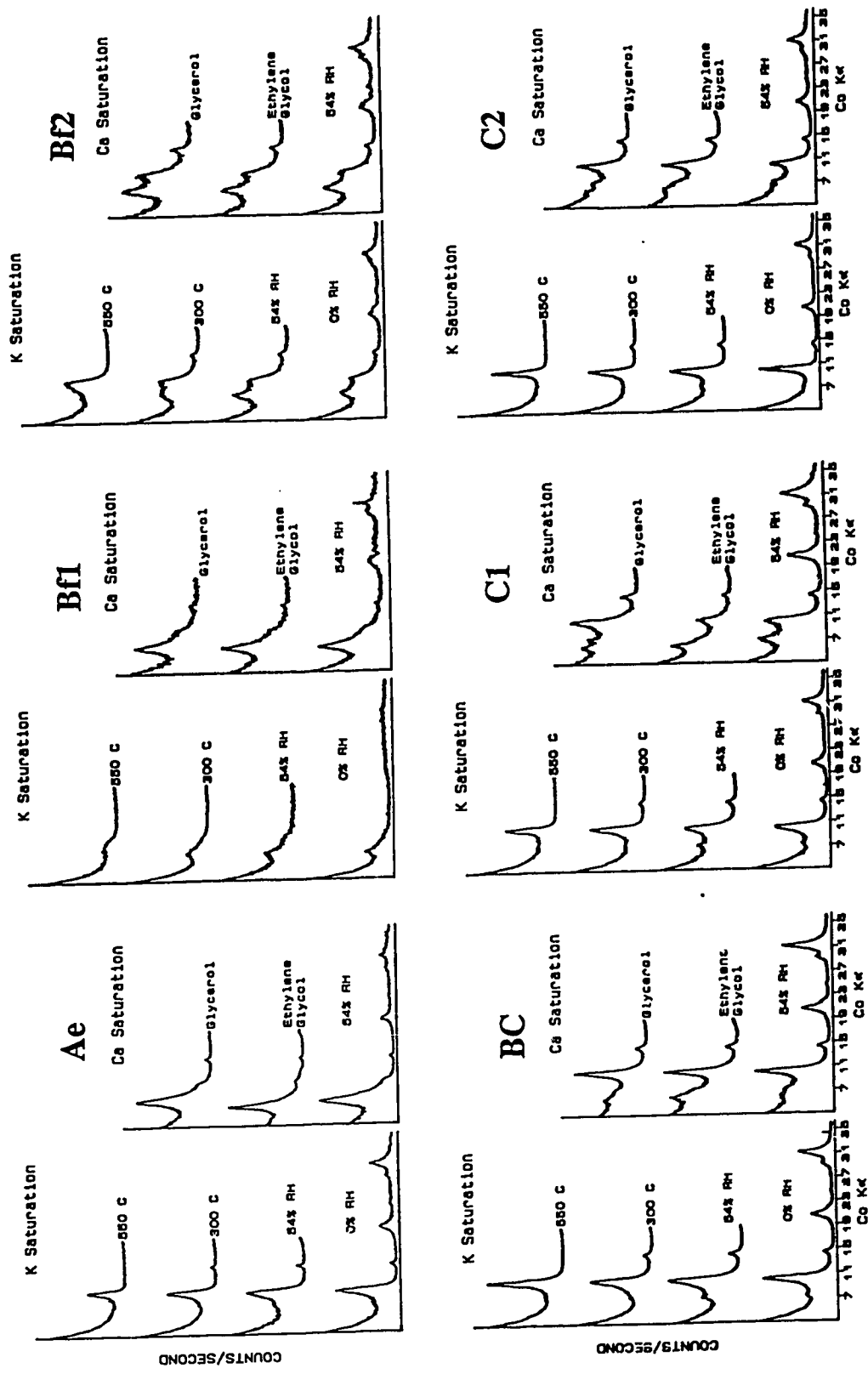


Fig. 7.2.5. X-ray diffractograms of fine clays in pedon 3.

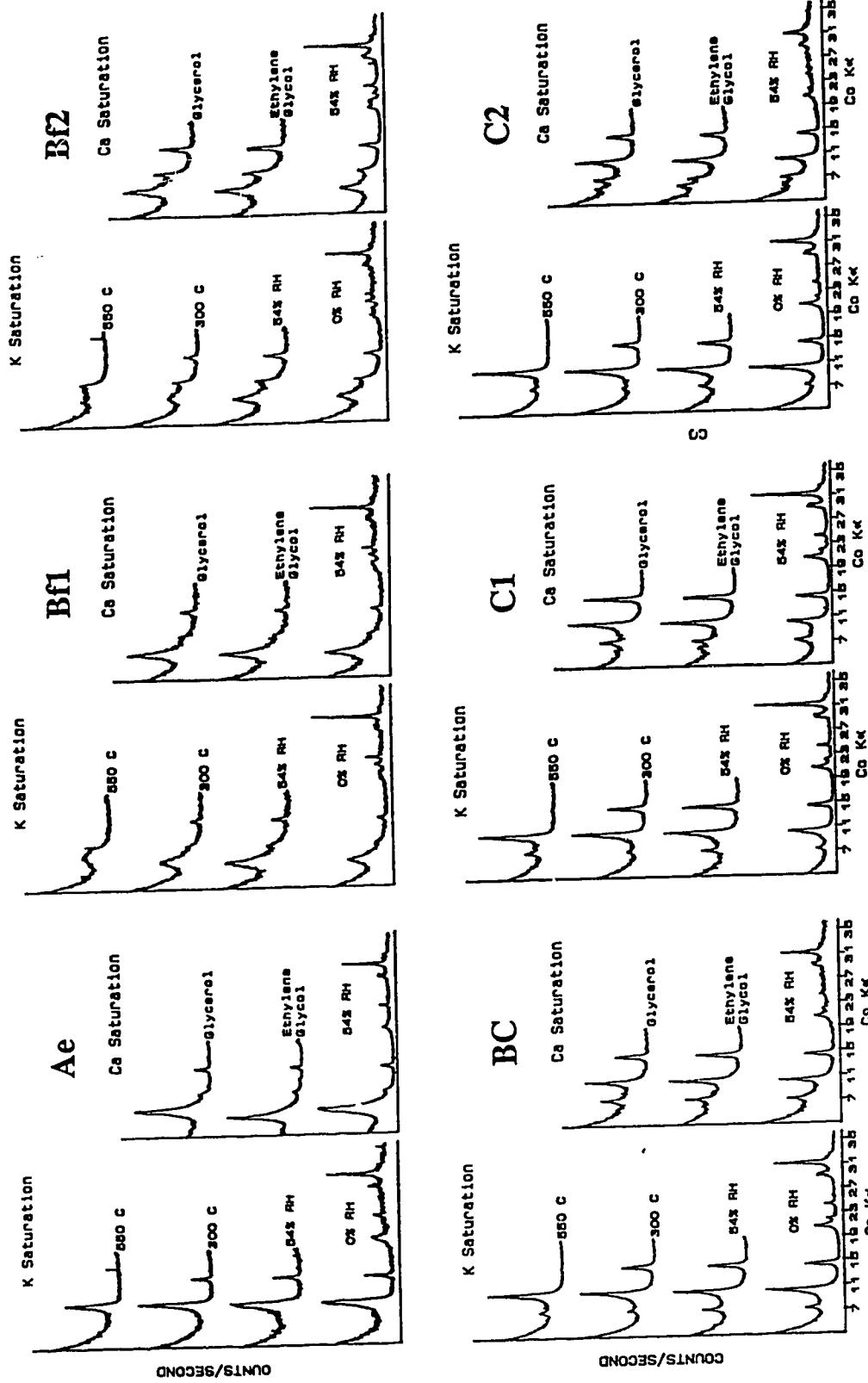


Fig. 7.2.1. X-ray diffractograms of coarse clays in pedon 3.

Appendix 7.3. X-ray diffractograms of silt fraction of Podzolic soils from Alberta.

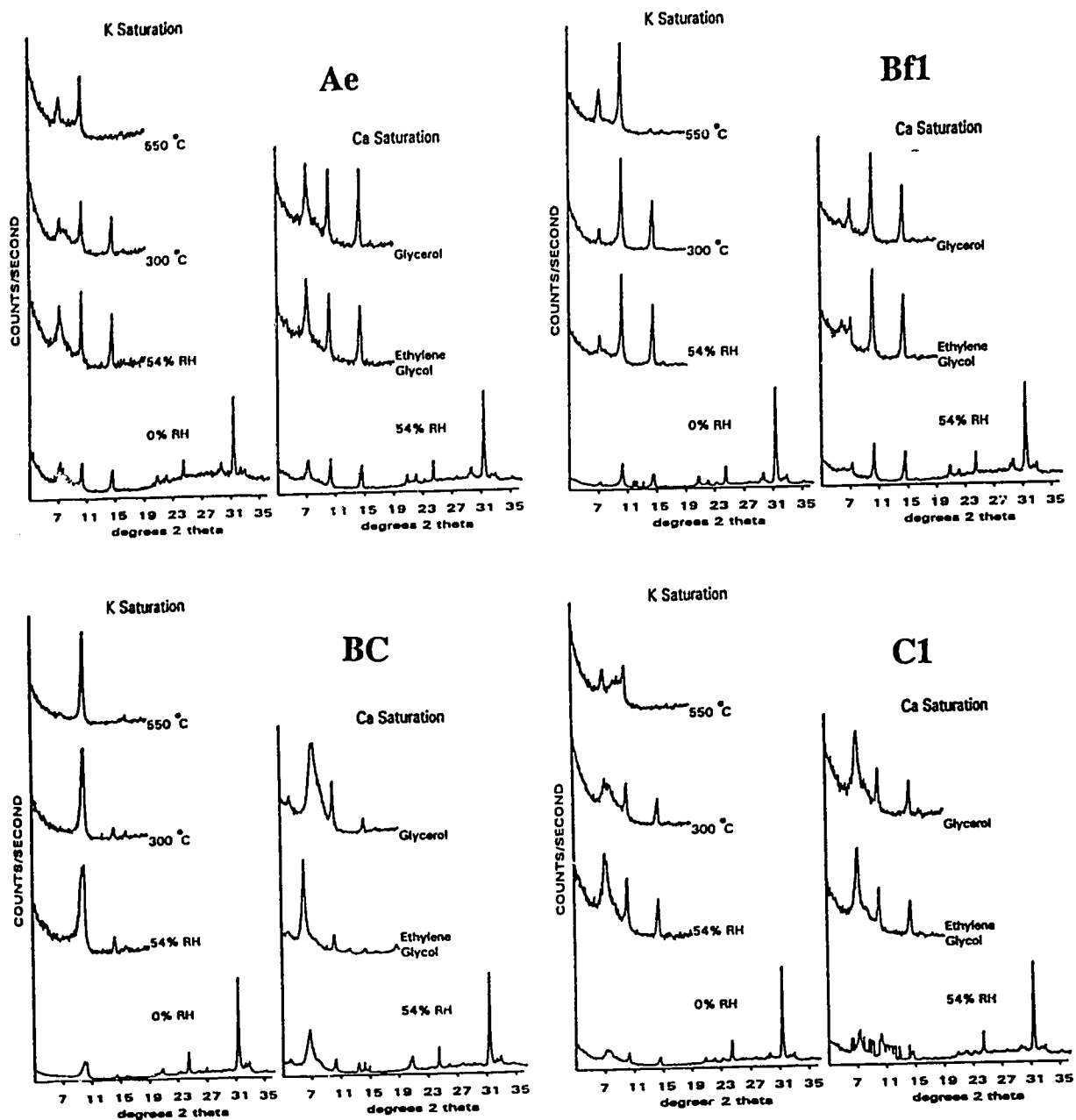


Fig. 7.3.1. X-ray diffractograms of silt fraction in pedon 1.

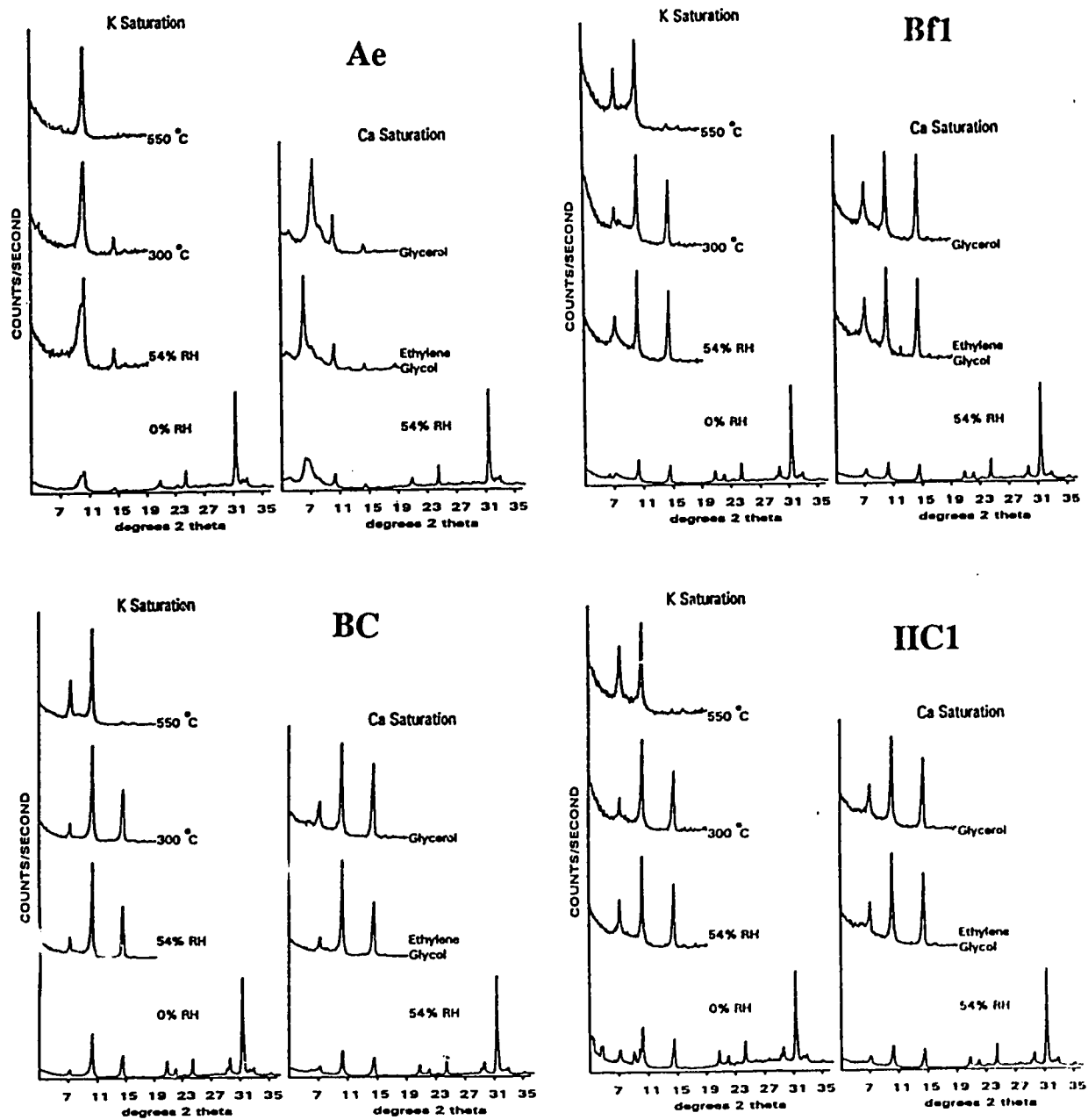


Fig. 7.3.2. X-ray diffractograms of silt fraction in pedon 2.

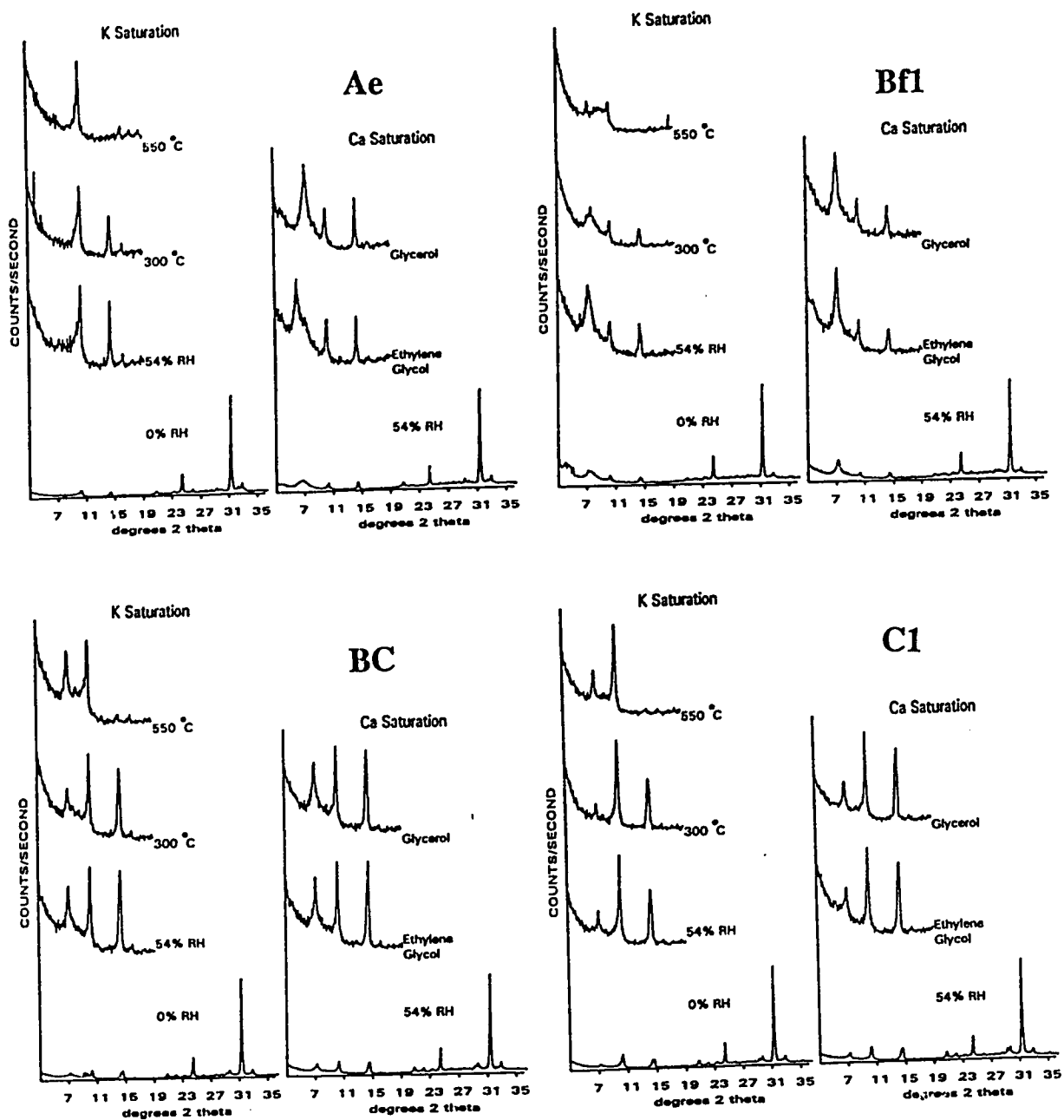


Fig. 7.3.3. X-ray diffractograms of silt fraction in pedon 3.

Appendix 7.4. X-ray diffractograms of sand fraction of Podzolic soils from Alberta.

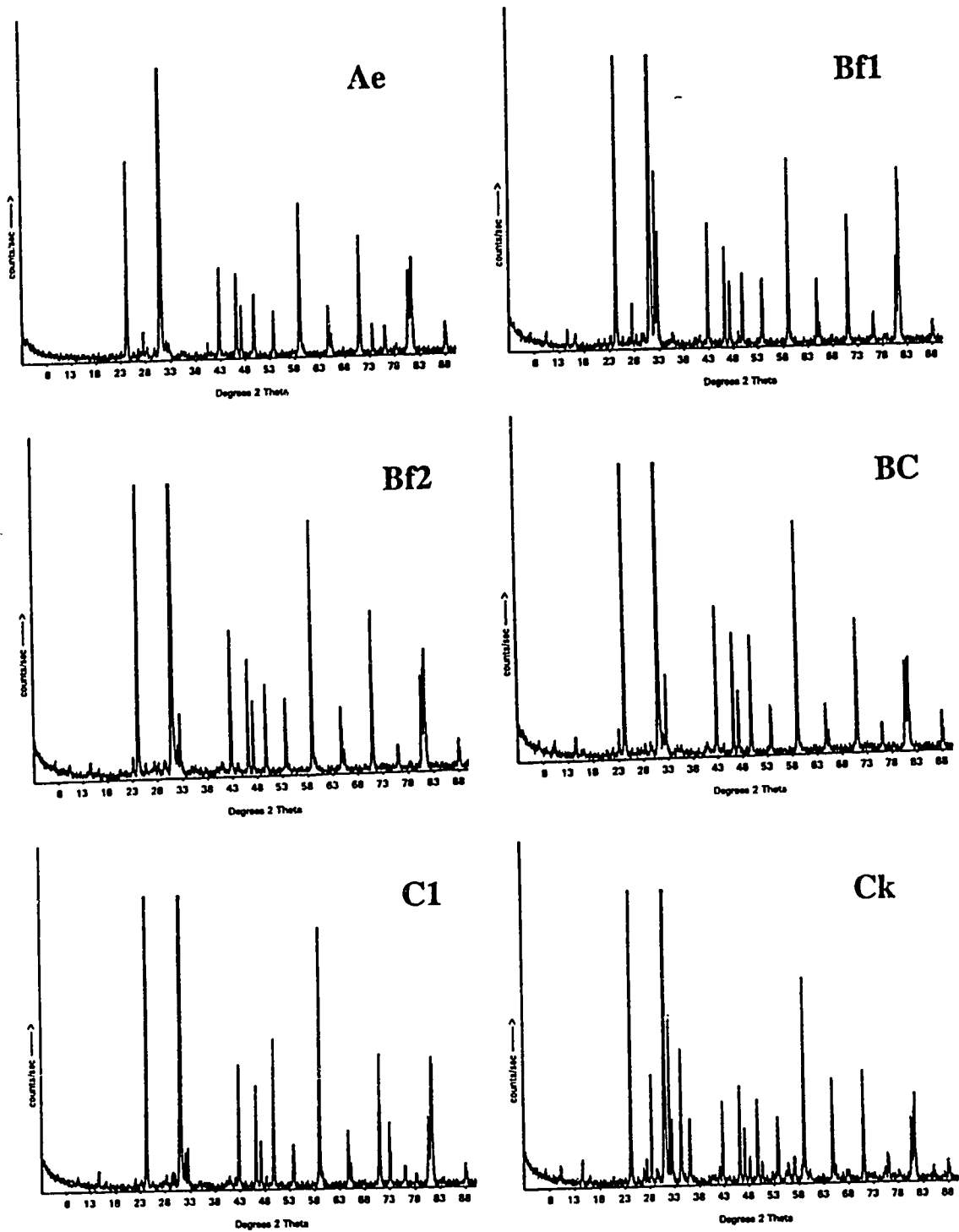


Fig. 7.4.1. X-ray diffractograms of sand fraction in pedon 1.

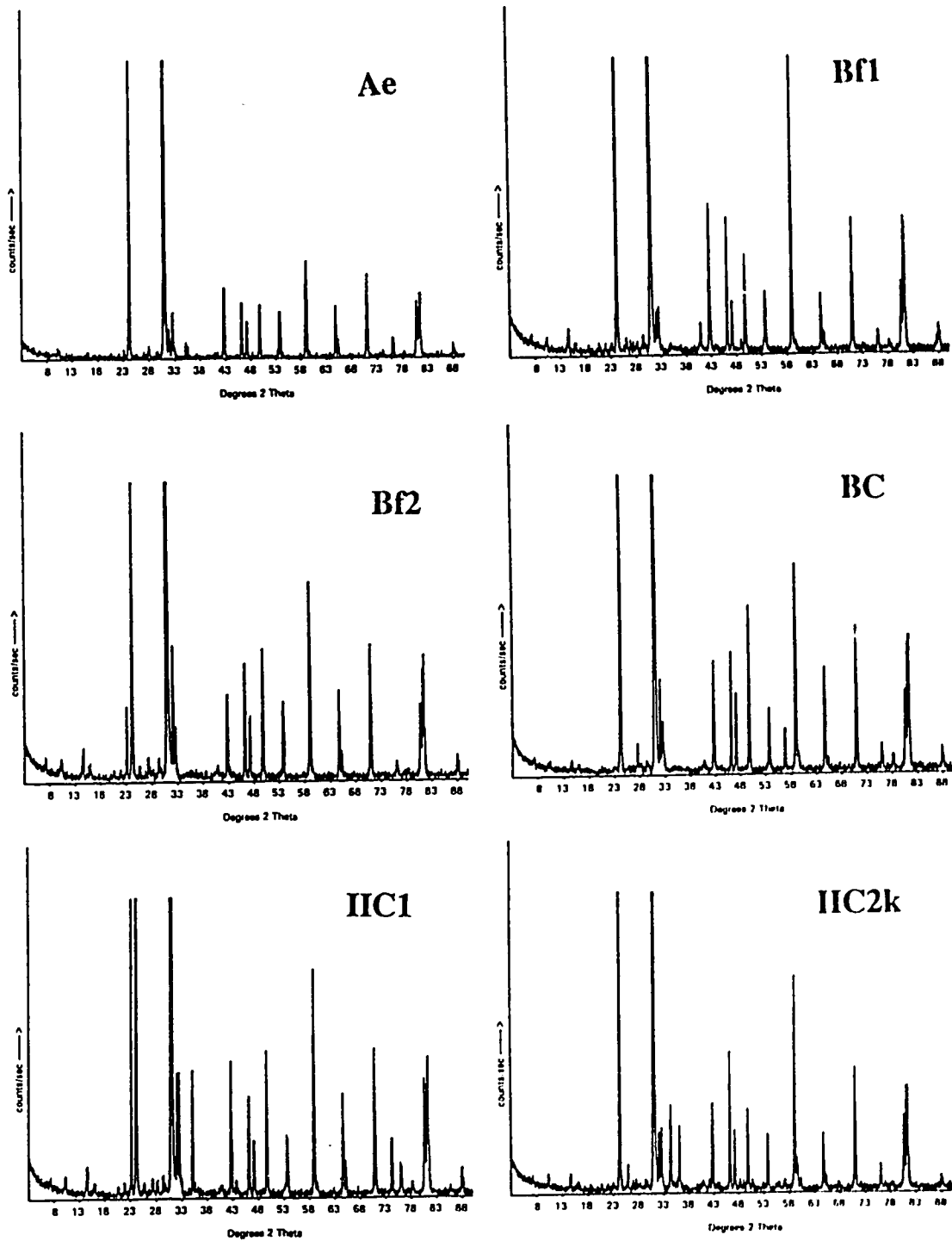


Fig. 7.4.2. X-ray diffractograms of sand fraction in pedon 2.

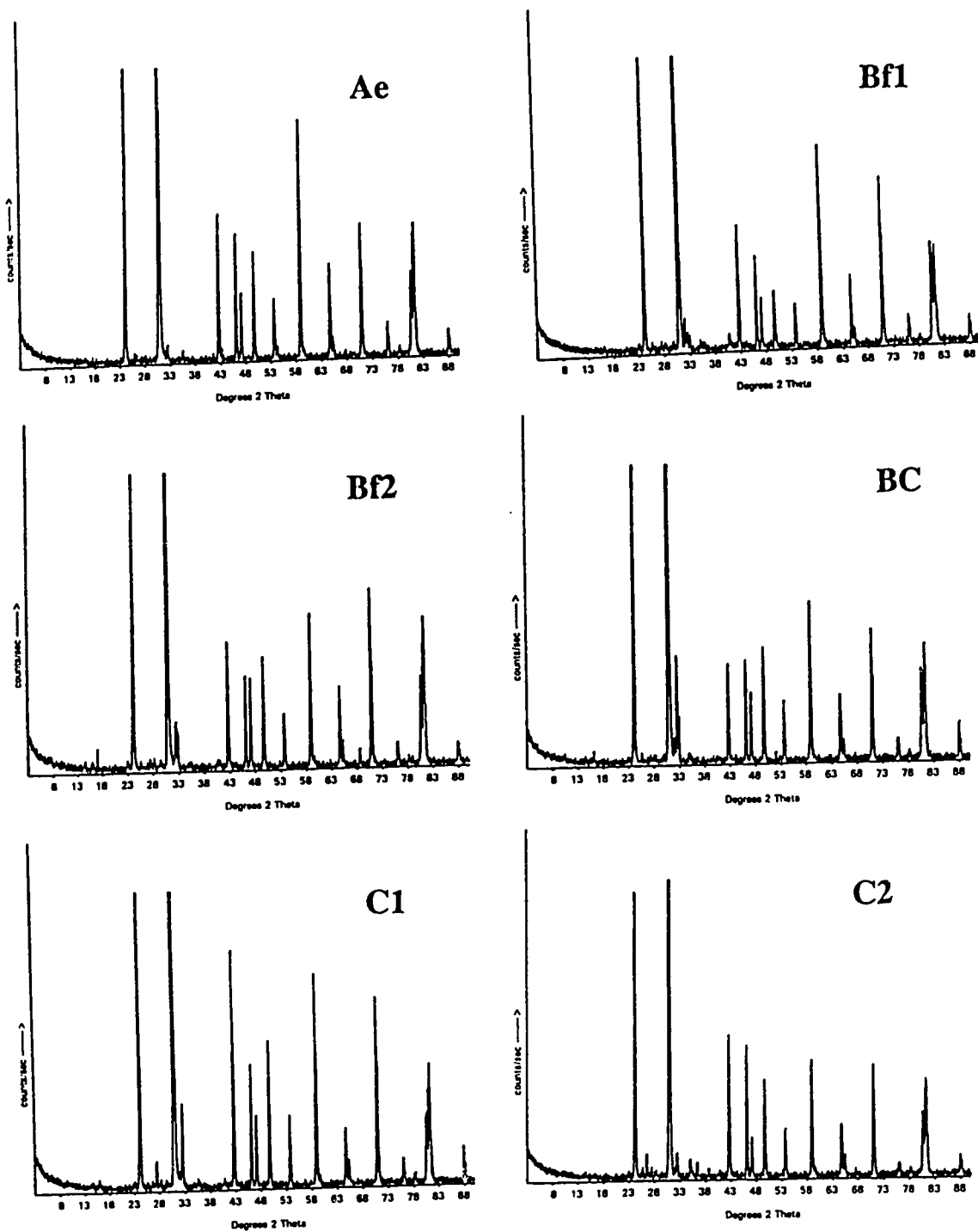


Fig. 7.4.3. X-ray diffractograms of sand fraction in pedon 3.

Appendix 7.5. Definition of Spodic materials (ICOMOD, 1990).

PROPOSED SPODIC MATERIALS DEFINITION

Spodic soil materials must:

1. Meet the following in an illuvial horizon:

a. Have one of the following color requirements:

1. Have a dominant hue in a B subhorizon that is 7.5YR or redder, a value ≤ 5.5 and a chroma ≤ 6.5 in the matrix;

OR,

2. Hue is 10YR with a value and chroma ≤ 2.5 , or a color of 10YR 3/1.

OR,

b. Have an horizon ≥ 2.5 cm thick laterally continuous in 50% of each pedon cemented by organic matter with some combination of either Fe or Al, or both, that has a color value < 3.5 and a chroma < 2.5 .

AND,

c. Meet at least one of the following morphologic or chemical requirements in the illuvial horizons:

1. Have in some B subhorizon beneath an albic horizon a value and chroma ≤ 3.5 in materials ≥ 20 cm thick and have a pH ≤ 5.5 ;

OR,

2. Have some sand grains with cracked coatings;

OR,

3. Have in some B subhorizon \geq two times Fe_{ox} than in the overlying E, A, or Ap horizon;

4. Have in some B subhorizon \geq two times more Al_{ox} plus $Fe_{ox}/2$ than in the overlying E, A, Ap horizon;

5. Have in some B subhorizon an ODOE value ≥ 0.25 and at least two times more ODOE than in the overlying E, A, or Ap horizon.

OR,

2. Have an Ap horizon ≥ 20 cm thick, or when mixed to that thickness, that has some subhorizon that meets or exceeds both of the following chemical requirements:

a. $Al_{ox} + (Fe_{ox}/2) \geq 0.9$

AND

b. ODOE ≥ 0.15

INTERNATIONAL COMMITTEE ON THE
CLASSIFICATION OF SPODOSOLS

CIRCULAR LETTER NUMBER 9
MARCH 23, 1990